AD

USAAVLABS TECHNICAL REPORT 67-71

A METHOD FOR PREDICTING THE TRIM CONSTANTS AND THE ROTOR-BLADE LOADINGS AND RESPONSES OF A SINGLE-ROTOR HELICOPTER

By

T. T. Chang

November 1967

U. S. ARMY AVIATION MATERIEL LABORATORIES
FORT EUSTIS, VIRGINIA

CONTRACT DA 44-177-AMC-384(T)

CORNELL AERONAUTICAL LABORATORY, INC.
BUFFALO, NEW YORK

Disclaimers

The findings in this report are not to be construed as an official Department of the Army position unless so designated by other authorized documents.

When Government drawings, specifications, or other data are used for any purpose other than in connection with a definitely related Government procurement operation, the United States Government thereby incurs no responsibility nor any obligation whatsoever; and the fact that the Government may have formulated, furnished, or in any way supplied the said drawings, specifications, or other data is not to be regarded by implication or otherwise as in any manner licensing the holder or any other person or corporation, or conveying any rights or permission, to manufacture, use, or sell any patented invention that may in any way be related thereto.

Disposition Instructions

Destroy this report when no longer needed. Do not return it to originator.

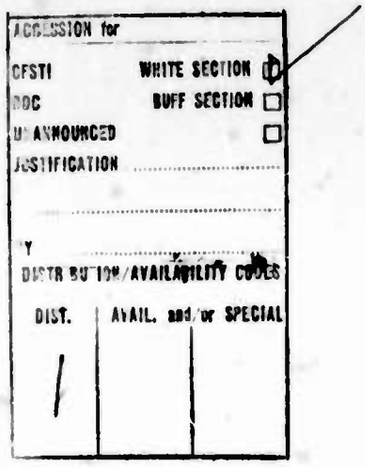

DEPARTMENT OF THE ARMY
U. S. ARMY AVIATION MATERIEL LABORATORIES
FORT EUSTIS, VIRGINIA 23604

This report has been reviewed by the U. S. Army Aviation Materiel Laboratories and is considered to be technically sound. It is published for the exchange of information and the stimulation of further ideas and understanding in rotary-wing aerodynamics.

Task 1F125901A14604
Contract DA 44-177-AMC-384(T)
USAAVLABS Technical Report 67-71
November 1967

A METHOD FOR PREDICTING THE TRIM CONSTANTS AND THE ROTOR-BLADE LOADINGS AND RESPONSES OF A SINGLE-ROTOR HELICOPTER

Final Report

CAL Report No. BB-2205-S-1

by

T. T. Chang

Prepared by

Cornell Aeronautical Laboratory, Inc.
Buffalo, New York

for

U. S. ARMY AVIATION MATERIEL LABORATORIES
FORT EUSTIS, VIRGINIA

SUMMARY

During a previous program, Cornell Aeronautical Laboratory, Inc., developed a method of computing rotor-blade loads and motions of a single-rotor helicopter in steady forward flight by assuming that the blade pitch-control settings (collective, longitudinal cyclic, and lateral cyclic) and the rotor-shaft tilt angle are known and that the blade motions are restricted to flapping and flapwise bending. The present effort was undertaken to extend the previously developed method by (1) including the blade inplane and torsional motions and (2) treating the four trim constants (namely, the blade pitch-control settings and the rotor-shaft tilt angle) as unknowns.

The trim constants are different for different flight conditions and are determined through the use of four appropriate, average equilibrium conditions of the helicopter. These equilibrium conditions are called the trim equations and are derived in this report, taking into account the inertial forces of the blades due to elastic deformations.

Lagrange's equations for the blade motions are given. The generalized coordinates employed in these equations to represent blade bending are those which have deflection components in two mutually perpendicular directions. Orthogonality relations of vibration modes of twisted, rotating blades are derived and are used in simplifying the equations of blade motions.

A successive approximation procedure was developed which, upon incorporation with the previously developed iterative procedure, yields the aerodynamic loads, the blade responses, and the required trim constants.

Computed results are obtained for the UH-1A rotor at advance ratios of 0.26 and 0.08 and for the H-34 rotor at advance ratios of 0.29 and 0.18. Comparisons of these results with available measured results are presented.

FOREWORD

This investigation of helicopter rotor-blade loading was performed by the Cornell Aeronautical Laboratory, Inc. (CAL), Buffalo, New York, for the U.S. Army Aviation Materiel Laboratories (USAAVLABS), Fort Eustis, Virginia, during the period February 1966 through July 1967. Mr. J. E. Yeates monitored the program for USAAVLABS.

Mr. T. T. Chang was project engineer and author of this report. Mr. J. C. Balcerak conducted the computer program and was author of the section entitled "Computer Program". Many helpful discussions with Messrs. R. P. White, Jr., F. A. DuWaldt, and R. A. Piziali of CAL are appreciated by the author.

TABLE OF CONTENTS

LIST OF ILLUSTRATIONS

LIST OF SYMBOLS

b	semichord.
C_{d_p}	profile drag coefficient.
C_{l_α}	slope of lift coefficient versus angle-of-attack plot.
C_{q_i}	generalized force in q_i when the blade is rotating in vacuum with all h_j and θ_j held zero.
$2C_{q_i q_j}$	generalized Coriolis force coefficient; it yields the generalized Coriolis force in q_i proportional to $\Omega\dot{q}_j$ when multiplied by $\Omega\dot{q}_j$.
D_x and D_z	distances from the center of gravity of helicopter to the origin of the x, y, z system in the x- and z-directions, respectively.
d_p	profile drag per unit span.
EI_B	flatwise flexural rigidity.
EI_C	chordwise flexural rigidity.
e	chordwise distance from midchord point to elastic axis. (All positive chordwise distances measure forward.)
e_1	chordwise distance from midchord point to the pitching axis.
e_D	chordwise offset of lead-lag hinge with respect to blade reference line, positive forward.
e_P	chordwise offset of pitching axis with respect to lead-lag hinge, positive forward.
f_{c_j}	radial variation of inplane deflection of elastic axis describing the j^{th} bending mode.
f_{h_j}	radial variation of flapwise deflection of elastic axis describing the j^{th} bending mode.
f_{θ_j}	radial variation of torsional deflection describing the j^{th} torsional mode.

GJ	conventional torsional rigidity.
G_{q_i}	generalized aerodynamic force in q_i.
h_j	generalized coordinate representing j^{th} bending mode ($j = 1 \rightarrow s$).
I_α	mass moment of inertia, about elastic axis, per unit span.
$K_{q_i q_j}$	generalized restraining force coefficient; it yields the generalized spring force in q_i due to the presence of q_j when multiplied by $(-q_j)$.
k_A	radius of gyration of cross-sectional area effective in taking centrifugal force.
ℓ	lift per unit span.
M	total pitching moment (about the negative y-axis) acting on one blade.
M_F	aerodynamic pitching moment acting on fuselage (which includes horizontal tail surface), about helicopter center of gravity, positive nose down.
$M_{q_i q_j}$	generalized mass coefficient; it yields the generalized inertia force in q_i due to the presence of q_j when multiplied by $(-\ddot{q}_j)$.
m	mass per unit span.
$\mathcal{M}$	aerodynamic pitching moment (about elastic axis, positive nose up) per unit span.
N	half of the total number of blade azimuth positions (equally spaced in the rotor disc) used in the computer program.
n_B	number of rotor blades.
Q	total torque (i.e., moment about the negative z-axis) acting on one blade.
q_j	j^{th} generalized coordinate representing either a bending or a torsional mode $[j = 1 \rightarrow (s + \gamma)]$.
R	blade radius (equal to r of blade tip section).

R_t	tail length (i. e., the distance from the yz-plane to the tail rotor shaft).
r	radial distance from rotor shaft, it defines a blade section.
r_c	coning offset radius (i. e., $\beta_c = 0$ for $r < r_c$).
r_D	lead-lag hinge radial offset.
r_F	flapping hinge radial offset.
r_o	radius of blade root section.
s	total number of bending modes used for describing blade bending deflection.
$T_{q_i q_j}$	generalized centrifugal force coefficient; it yields the generalized centrifugal force in q_i due to the presence of q_j when multiplied by $\Omega^2 q_j$.
$\bar{T}$	$\bar{T} \equiv \bar{T} + \frac{1}{R_t}\bar{Q}$.
V_f	helicopter forward speed.
W	total weight of helicopter.
$\bar{X}_1$	chordwise distance from center of gravity to elastic axis.
$\bar{X}_2$	chordwise distance from center of gravity to the pitching axis ($\bar{X}_2 = \bar{X}_1 + e_1 - e$).
$\bar{X}_3$	chordwise distance from center of gravity to the blade reference line ($\bar{X}_3 = \bar{X}_2 - e_D - e_F$).
X, Y, Z	x-, y-, z-component of total force (including that due to blade inertia) acting on one blade.
x, y, z	right-hand orthogonal coordinate system with its xy-plane coincident with the reference plane (which is perpendicular to the rotor shaft and contains the flapping hinges), origin on the rotor shaft axis, x-axis pointing downstream and z-axis pointing upward.
$\bar{X}, \bar{Y}, \bar{Z}, \bar{M}, \bar{Q}$	twice the values of the averaged X, Y, Z, M, Q, such that $\bar{X} = \frac{1}{\pi}\int_0^{2\pi} X\, d\psi$, etc.

X_F, Z_F	x-, z-components of aerodynamic force acting on fuselage (which includes horizontal tail surface).
$\hat{X}_F, \hat{Z}_F, \hat{M}_F$	values of X_F, Z_F, M_F, when α_s is equal to a chosen reference value, $\hat{\alpha}_s$.
X'_F, Z'_F, M'_F	slopes of X_F, Z_F, M_F versus α_s plots at $\alpha_s = \hat{\alpha}_s$.
α_s	rotor shaft tilt angle in the zx-plane (positive α_s tends to move the fuselage nose down).
β_c	built-in coning angle.
γ	total number of torsional modes used for describing blade torsional deflection.
ϵ	induced angle so defined that $(\alpha_p + \epsilon\ell)$ is the drag (or inplane component of aerodynamic force) per unit span.
$\bar{\theta}$	total pitch $(\bar{\theta} = \bar{\theta}_0 + \bar{\theta}_{1c}\cos\psi + \bar{\theta}_{1s}\sin\psi)$.
θ_B	built-in twist, measured with respect to root section, positive nose up.
θ_j	generalized coordinate representing j^{th} torsional mode $(j = 1 \rightarrow \gamma)$.
$\bar{\theta}_{1c}$	longitudinal cyclic pitch.
$\bar{\theta}_{1s}$	lateral cyclic pitch.
$\bar{\theta}_0$	collective pitch.
μ	advance ratio $\left(\mu \equiv \frac{V_f}{\Omega R}\right)$.
ρ	air density.
ψ	blade azimuth angle, measured from the x-axis to the blade reference line (which line lies in the xy-plane, intersects the rotor shaft axis, and is perpendicular to the blade flapping hinge).
Ω	rotor shaft rotational speed.

SUPERSCRIPTS AND SUBSCRIPTS

$\tilde{\alpha}_s, \tilde{\theta}_0, \tilde{\theta}_{1c}, \tilde{\theta}_{1s}$	estimated or assumed values of α_s, $\bar{\theta}_0$, $\bar{\theta}_{1c}$, $\bar{\theta}_{1s}$.

$\bar{\alpha}_s, \bar{\theta}_0, \bar{\theta}_{1c}, \bar{\theta}_{1s}$	required adjustments to $\tilde{\alpha}_s, \tilde{\theta}_0, \tilde{\theta}_{1c}, \tilde{\theta}_{1s}$, as estimated from the trim equations.
0	as subscript, it indicates the value of a quantity averaged over $\psi = 0 \rightarrow 2\pi$.
nc	as subscripts, they indicate the amplitude of the n^{th} harmonic cosine component, in ψ, of a quantity.
ns	as subscripts, they indicate the amplitude of the n^{th} harmonic sine component, in ψ, of a quantity.
$()'_a, ()'_b, ()'_c$ & $()'_d$	as defined by Equation (36) may be interpreted as estimated partial derivatives of $(\bar{\ })$ with respect to $\alpha_s, \bar{\theta}_0, \bar{\theta}_{1c}$, and $\bar{\theta}_{1s}$, respectively.

INTRODUCTION

The U. S. Army Aviation Materiel Laboratories (USAAVLABS) has been directing a unified experimental and theoretical effort which has for one of its ultimate objectives the development of a means of predicting rotor-blade air loads, motions, and stresses in helicopters. That is, it is desired to develop the capability of predicting these quantities when all the rotor hub and blade physical parameters, the rotor operating flight condition, the helicopter weight and center of gravity location, and the fuselage aerodynamic characteristics are specified. As a participant in this Army effort, Cornell Aeronautical Laboratory, Inc. (CAL), has been working on the development of a method of prediction for a single-rotor helicopter in steady forward flight (Reference 1). This earlier development, however, used the assumptions that the blade motions are restricted to flapping and flapwise bending and that, for each flight condition, the blade pitch-control settings and the rotor-shaft tilt angle are specified by four given constants. In reality, these four trim constants are unknowns to be determined by the helicopter weight and center of gravity location and the fuselage aerodynamic characteristics, as explained later under "TRIM EQUATIONS". Furthermore, the blade inplane (or chordwise) and torsional motions could be important (directly and through their coupling with each other and the flapping motions) with respect to the blade stresses and aerodynamic loads. Consequently, the present program was undertaken to improve the previous development by removing the above-mentioned assumptions. The two diagrams in Figure 1 show the differences between the previous and present programs.

The same method and computer program developed in Reference 1 to predict the blade aerodynamic load distributions, when

the blade response and the trim constants are given, are used here.* This means automatically that the same wake and blade representations (both described fully in Reference 1) are used in both programs.*

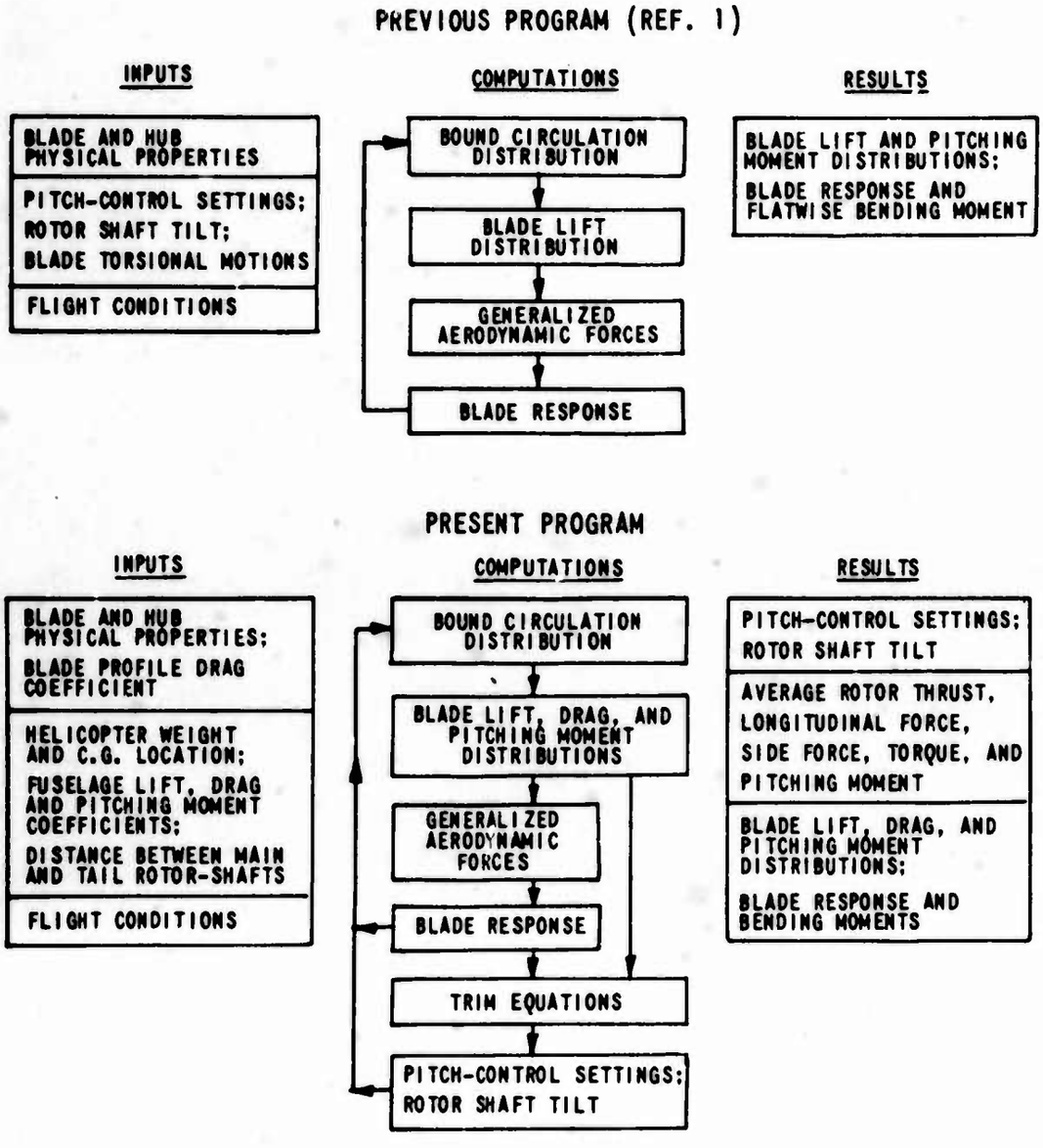

Figure 1. COMPARISON OF PREVIOUS AND PRESENT PROGRAMS.

* Except for minor modifications that are necessary for admitting blade profile drag coefficient as additional input and for having blade drag (profile plus induced) distribution as additional output.

TRIM EQUATIONS

Consider a single-rotor helicopter equipped with a tail rotor (which is assumed to produce a side force and yawing moment). When the helicopter is in steady level flight, the flight condition specifies its forward speed, V_f , and the rotor-shaft rotational speed, Ω . For each given flight condition, the average forces and moments (from both the aerodynamic and the inertia sources) acting on the rotor must be in equilibrium with the helicopter weight, the aerodynamic forces and moments acting on the fuselage, and the side force produced by the tail rotor. The equations that express the requirements to secure the equilibrium are called the trim equations. In a forward flight, the fuselage side force and yawing moment, as well as the net value between the rotor average rolling moment and the fuselage rolling moment, are all small.* Consequently, their effects on the trim equations will be ignored. Then, besides the forces and moments in the longitudinal plane, we need only to consider the presence of a tail force equal and opposite to the rotor average side force with its moment about the rotor shaft equal and opposite to the rotor average torque. Since the consideration of the forces and moments in the longitudinal plane leads to three trim equations, there will be a total of four trim equations. With the pitch-control system contributing a blade pitch angle $\bar{\theta}$ according to

$$\bar{\theta} = \bar{\theta}_0 + \bar{\theta}_{1C} \cos\psi + \bar{\theta}_{1S} \sin\psi , \tag{1}$$

---

* Their effects can actually be cancelled by secondary adjustments to the tail rotor force and location (perhaps combined with a lateral tilt of rotor shaft). In the derivation, the tail rotor location is considered to be fixed.

the constants $\bar{\theta}_0$, $\bar{\theta}_{1c}$, $\bar{\theta}_{1s}$ together with the rotor-shaft tilt angle, α_s, in the longitudinal plane may be called the four trim constants. Their values depend on flight conditions and must be so determined that they make the trim equations satisfied for the given flight condition.

Referring to Figure 2 and assuming that α_s is sufficiently small that $\cos\alpha_s = 1$ and $\sin\alpha_s = \alpha_s$, the trim equations may be written as

$$\frac{n_B}{2\pi}\int_0^{2\pi} X\,d\psi = W\alpha_s - X_F \tag{2}$$

$$\frac{n_B}{2\pi}\int_0^{2\pi} Z\,d\psi = W - Z_F \tag{3}$$

$$\frac{n_B}{2\pi}\int_0^{2\pi} M\,d\psi = (W\alpha_s - X_F)\,D_y - (W - Z_F)\,D_x - M_F \tag{4}$$

$$\frac{n_B}{2\pi}\int_0^{2\pi} Q\,d\psi + R_t\,\frac{n_B}{2\pi}\int_0^{2\pi} Y\,d\psi = 0\,. \tag{5}$$

Note that n_B is the number of rotor blades; X, Y, Z, M, Q are force and moment components acting on <u>one</u> rotor blade in the directions indicated in Figure 2; R_t is the distance (in the x-direction) between the main rotor and tail rotor shafts; and the tail rotor produces a force in the y-direction equal to

$$-\frac{n_B}{2\pi}\int_0^{2\pi} Y\,d\psi\,.$$

For a given flight condition, the blade loads (X, Y, Z, M and Q) depend on α_s and the blade motions, which may include flapping (h_1), lead-lag (h_2), pitching ($\bar{\theta}$), flapwise and inplane bending deflections (h_j, $j>1$ without lead-lag and $j>2$ with lead-lag), and torsional deflections (θ_j).

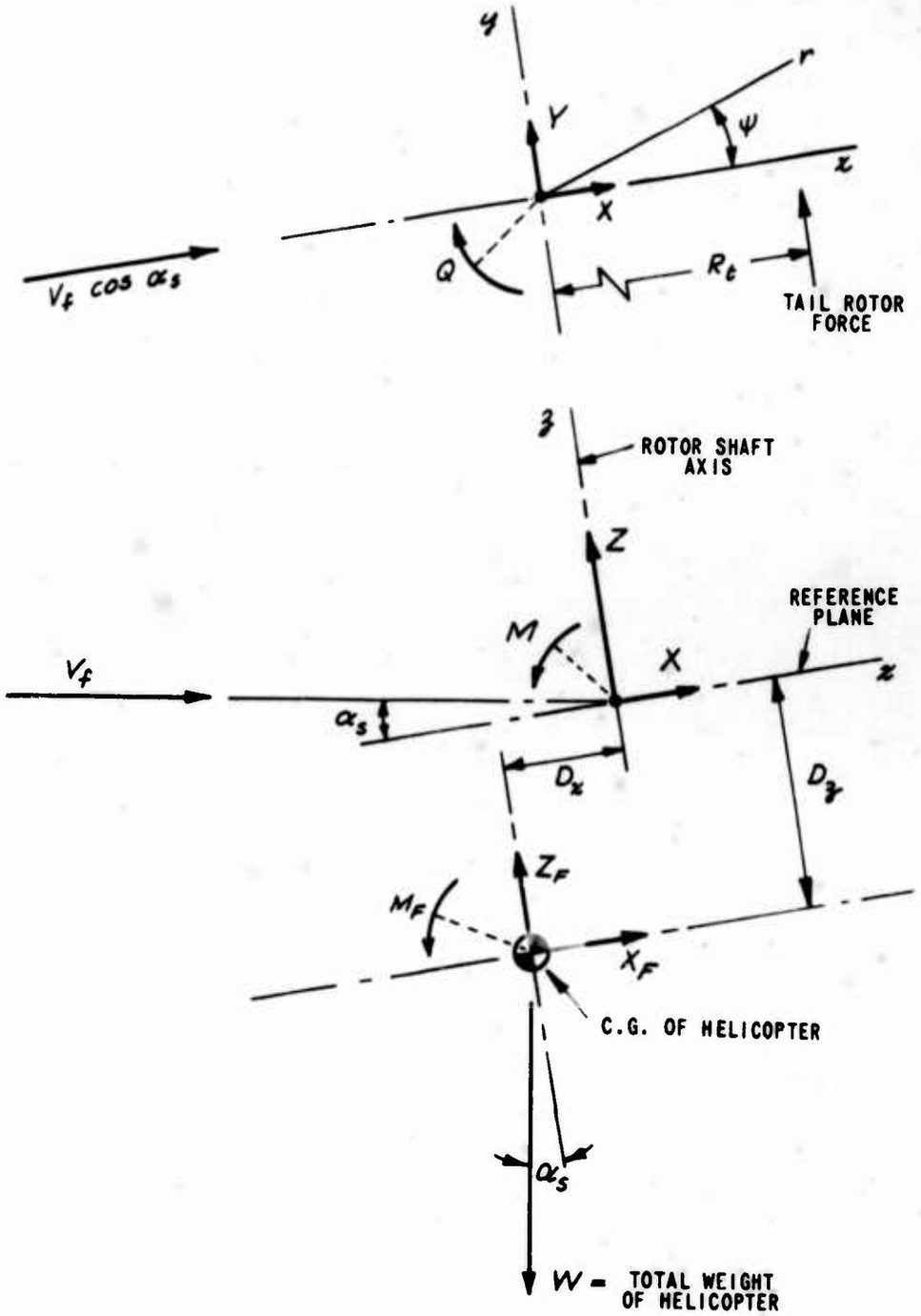

Figure 2. FORCES ACTING ON HELICOPTER.

The plane that is normal to the rotor shaft and contains the flapping axes will be chosen as the reference plane. Each bending mode, represented by h_j, will be described by two functions of the radial distance, r, from the rotor shaft of a blade section: f_{h_i} describes the radial variation of the deflection of the elastic axis normal to the reference plane, positive upward; f_{c_j} describes that parallel to the reference plane, positive forward. (Thus, for each j^{th} bending mode, $h_j f_{h_j}$ is the flapwise bending and $h_j f_{c_j}$ is the associated inplane bending.) Pure flapping or lead-lag may be considered as a special bending mode with $f_c = 0$ or $f_h = 0$, respectively, both with zero curvature.

In steady flight, the blade loads and motions are periodic so that they can be resolved into harmonic components. For example, the lift per blade may be expressed by

$$L = L_0 + \sum_{n=1}^{\infty} (L_{nc} \cos n\psi + L_{ns} \sin n\psi) \tag{6}$$

and the generalized coordinate representing the i^{th} bending mode may be expressed by

$$h_i = h_0^{(i)} + \sum_{n=1}^{\infty} \left(h_{nc}^{(i)} \cos n\psi + h_{ns}^{(i)} \sin n\psi \right). \tag{7}$$

Note that the pitching, $\bar{\theta}$, has $\theta_{nc} = \theta_{ns} = 0$ for $n \geq 2$. Throughout this report, the subscripts 0, nc and ns will only be used to indicate harmonic components in exactly the same manner as in (6) or (7).

Let $\bar{z}$ be the distance of local c.g. (i.e., the c.g. of a blade section at distance r from the rotor shaft) above the reference plane. Then

$$\bar{z} = (r - r_c)\beta_c + \sum_j h_j f_{h_j} - \bar{X}_1 \left(\theta_B + \sum_j \theta_j f_{\theta_j}\right)$$

$$-(e_1 - e + \bar{X}_1)(\bar{\theta}_0 + \bar{\theta}_{1c} \cos\psi + \bar{\theta}_{1s} \sin\psi) \tag{8}$$

where β_c is the built-in coning, r_c is the coning offset radius ($\beta_c = 0$ for $r < r_c$), θ_β is the blade built-in twist (about elastic axis), e_1 is the distance from midchord point to the pitching axis, e is the distance from midchord point to elastic axis, and $\bar{X}_1$ is the distance from c. g. to elastic axis. (All these distances are measured chordwise and positive forward; see Figure 3.) The acceleration* of the local c. g. in the z-direction, a_z, can now be obtained by taking the second derivative of $\bar{z}$ with respect to time, yielding

$$a_z = \sum_j \ddot{h}_j f_{h_j} - \bar{X}_1 \sum \ddot{\theta}_j f_{\theta_j} + (e_1 - e + \bar{X}_1)\Omega^2(\bar{\theta}_{1c}\cos\psi + \bar{\theta}_{1s}\sin\psi) . \quad (9)$$

Since a_z is actually tilted toward the rotor shaft by an angle equal to the flapping angle, $h_1/(R-r_F)$, plus β_c , it has a radial component equal to

$$-\left(\beta_c + \frac{h_1}{R-r_F}\right) a_z .$$

Thus, the total radial acceleration of the local c. g. is

$$a_r = -\left(\beta_c + \frac{h_1}{R-r_F}\right) a_z - \Omega^2 r . \quad (10)$$

The tangential acceleration (positive forward) of the local c. g. is

$$a_c = \sum_j \ddot{h}_j f_{c_j} + \Omega^2\left(\bar{X}_3 - \sum_j h_j f_{c_j}\right) \quad (11)$$

where

$$\bar{X}_3 = e_1 - e + \bar{X}_1 - e_D - e_P \quad (12)$$

and e_D and e_P are the chordwise offsets of the lead-lag hinge and the pitching axis as shown in Figure 3.

---

* All the Coriolis accelerations will be neglected.

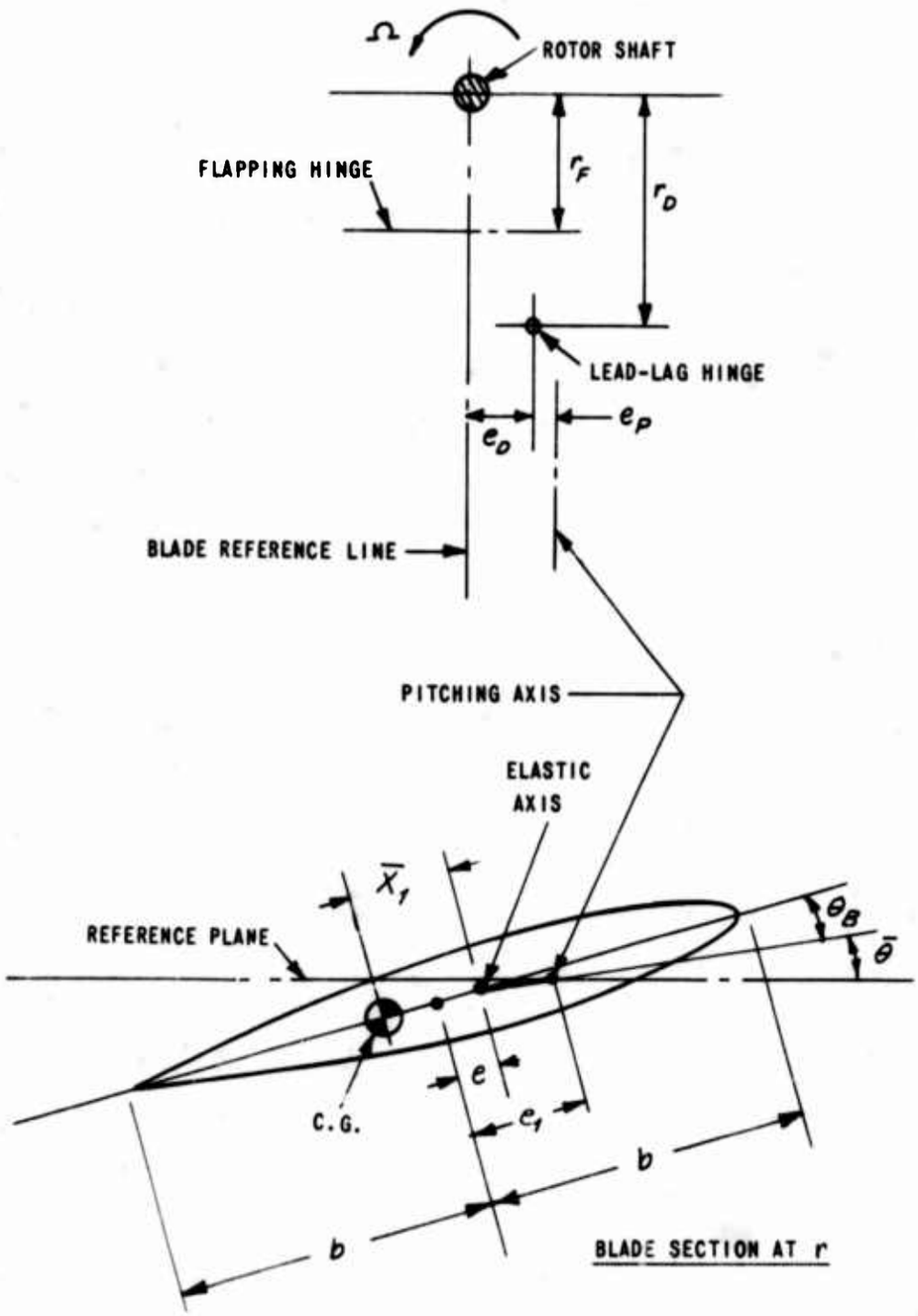

NOTES: (1) THE REFERENCE PLANE IS PERPENDICULAR TO THE ROTOR SHAFT AND CONTAINS THE FLAPPING HINGES.

(2) THE BLADE REFERENCE LINE LIES IN THE REFERENCE PLANE, INTERSECTS THE ROTOR SHAFT, AND IS PERPENDICULAR TO THE FLAPPING HINGE.

Figure 3. BLADE OFFSETS (POSITIVE SHOWN).

Letting m be the blade mass per unit span, ℓ be the lift per unit span, d_p be the profile drag per unit span, and ϵ be the induced angle (so defined that the total drag per unit span is equal to $d_p + \epsilon\ell$), the contribution per unit blade span to X can now be expressed as

$$\frac{dX}{dr} = (d_p + \epsilon\ell + ma_c)\sin\psi - \left\{\left(\beta_c + \frac{h_1}{R-r_F}\right)\ell + ma_r\right\}\cos\psi$$

$$= \left\{d_p + \epsilon\ell + m\sum_j \ddot{h}_j f_{c_j} + m\Omega^2\left(\bar{X}_3 - \sum_j h_j f_{c_j}\right)\right\}\sin\psi$$

$$- \left\{\left(\beta_c + \frac{h_1}{R-r_F}\right)(\ell - ma_z) - m\Omega^2 r\right\}\cos\psi . \tag{13}$$

Similarly,

$$\frac{dY}{dr} = -\left\{d_p + \epsilon\ell + m\sum_j \ddot{h}_j f_{c_j} + m\Omega^2\left(\bar{X}_3 - \sum_j h_j f_{c_j}\right)\right\}\cos\psi$$

$$- \left\{\left(\beta_c + \frac{h_1}{R-r_F}\right)(\ell - ma_z) - m\Omega^2 r\right\}\sin\psi \tag{14}$$

$$\frac{dZ}{dr} = \ell - ma_z \tag{15}$$

$$\frac{dQ}{dr} = \left(d_p + \epsilon\ell + m\sum_j \ddot{h}_j f_{c_j}\right) r \tag{16}$$

and, letting I_α be the blade mass moment of inertia (about the elastic axis) per unit span and η be the blade aerodynamic pitching moment (about the elastic axis, positive nose up) per unit span,

$$\frac{dM}{dr} = \left\{(\ell - ma_z)\, r - m\Omega^2 r\bar{z}\right\}\cos\psi$$

$$- \Big[ma_c\bar{z} + (d_p + \epsilon\ell)\left\{(r - r_c)\beta_c + \sum_j h_j f_{h_j} - (e_1 - e)\bar{\theta}\right\}$$

$$+ \left(I_\alpha - m\bar{X}_1^{\,2}\right)\left(\Omega^2\bar{\theta}_{1c}\cos\psi + \Omega^2\bar{\theta}_{1s}\sin\psi - \sum_j \ddot{\theta}_j f_{\theta_j}\right)$$

$$+ \eta - (e_1 - e - e_0 - e_p)\,\ell\Big]\sin\psi . \tag{17}$$

In obtaining $\int_0^{2\pi} X\,d\psi$, ..., $\int_0^{2\pi} M\,d\psi$ from Equation (13), ..., Equation (17) by double integration, it is essential to notice the following relations:

$$\int_0^{2\pi} d\psi = 2\pi \; ; \qquad \int_0^{2\pi} \cos^2\psi \cdot d\psi = \int_0^{2\pi} \sin^2\psi \cdot d\psi = \pi$$

$$\int_0^{2\pi} \cos n\psi \cdot d\psi = \int_0^{2\pi} \sin n\psi \cdot d\psi = 0 \; , \quad n \geq 1$$

$$\int_0^{2\pi} (\cos n\psi \text{ or } \sin n\psi) \cdot (\cos\psi \text{ or } \sin\psi) \cdot d\psi = 0 \; , \quad n \geq 2$$

$$(\ddot{h}_j)_0 = (\ddot{\theta}_j)_0 = (a_z)_0 = 0 \; ; \qquad (a_z)_{1C} = -\Omega^2 \bar{z}_{1C}$$

$$(\ddot{h}_j)_{1C} = -\Omega^2 h_{1C}^{(j)} \; ; \qquad (\ddot{h}_j)_{1S} = -\Omega^2 h_{1S}^{(j)}$$

$$(\ddot{\theta}_j)_{1C} = -\Omega^2 \theta_{1C}^{(j)} \; ; \qquad (\ddot{\theta}_j)_{1S} = -\Omega^2 \theta_{1S}^{(j)}$$

For example, taking the advantage of the above relations, the contribution of the first line of Equation (17) to $\int_0^{2} M\,d\psi$ can be obtained as follows:

$$\int_0^{2\pi} \left[\int_0^R \left\{ (l - ma_z)\, r - m\Omega^2 r \bar{z} \right\} \cos\psi \cdot dr \right] d\psi$$

$$= \int_0^R \left[\int_0^{2\pi} \left\{ l_{1C} - m(a_z)_{1C} - m\Omega^2 \bar{z}_{1C} \right\} \cos^2\psi \cdot d\psi \right] r\,dr$$

$$= \pi \int_0^R l_{1C}\, r\,dr = \pi B_{1C}$$

where B_{1C} is the amplitude of the first harmonic cosine component of $B = \int_0^R l\,dr$. The actual procedure of computing B_{1C} involves calculating B at $2N$ equally spaced azimuth positions. Denoting

$$\psi_k = \frac{k-1}{N}\pi \qquad \text{and} \qquad B_k = B_{\psi = \psi_k}$$

$(k = 1, 2, \cdots, 2N)$, B_{1C} is given by *

$$B_{1C} = \frac{1}{N} \sum_{k=1}^{2N} B_k \cos\psi_k \, .$$

---

* See Appendix III of Reference 1.

If the average value, B_0 , and the amplitude of the first harmonic sine component, B_{1S} , are also wanted, they can be computed from*

$$B_0 = \frac{1}{2N}\sum_{k=1}^{2N} B_k \quad \text{and} \quad B_{1S} = \frac{1}{N}\sum_{k=1}^{2N} B_k \sin\psi_k .$$

The contribution of the second line of Equation (17) to $\int_0^{2\pi} M\,d\psi$ can be obtained by writing it as

$$-\pi\int_0^R m\left\{(a_c)_{1S}\,\bar{z}_0 + (a_c)_0\,\bar{z}_{1S}\right\}dr$$
$$-\pi\int_0^R (d_p + \epsilon\ell)_{1S}\left\{(r-r_c)\beta_c + \sum_j h_0^{(j)} f_{h_j} - (e_1 - e)\bar{\theta}_0\right\}dr$$
$$-\pi\int_0^R (d_p + \epsilon\ell)_0\left\{\sum_j h_{1S}^{(j)} f_{h_j} - (e_1 - e)\bar{\theta}_{1S}\right\}dr .$$

However, in the first integral, an approximate expression,

$$\bar{z} = (r-r_c)\beta_c + \frac{r-r_F}{R-r_F}\,h_1 - (e_1 - e + \bar{x}_1)\bar{\theta},$$

will be used instead of Equation (8) to make

$$(a_c)_{1S}\,\bar{z}_0 + (a_c)_0\,\bar{z}_{1S}$$
$$= -2\Omega^2\left(\sum_j h_{1S}^{(j)} f_{c_j}\right)\left\{(r-r_c)\beta_c + \frac{r-r_F}{R-r_F}\,h_0^{(1)} - (e_1 - e + \bar{x}_1)\bar{\theta}_0\right\}$$
$$+\Omega^2\left(\bar{x}_3 - \sum_j h_0^{(j)} f_{c_j}\right)\left\{\frac{r-r_F}{R-r_F}\,h_{1S}^{(1)} - (e_1 - e + \bar{x}_1)\bar{\theta}_{1S}\right\}$$

while in the second and third integrals the replacements of

$$\sum_j h_0^{(j)} f_{h_j} \quad \text{with} \quad \frac{r-r_F}{R-r_F}\,h_0^{(1)}$$

and

$$\sum_j h_{1S}^{(j)} f_{h_j} \quad \text{with} \quad \frac{r-r_F}{R-r_F}\,h_{1S}^{(1)}$$

will be made. The complete set of results obtained by double integration of Equations (13) through (17) is as follows:

$$\frac{1}{\pi}\int_0^{2\pi} X\,d\psi = D_{1S} - 2\Omega^2\sum_j m_{c_j} h_{1S}^{(j)} - \frac{h_{1C}^{(1)}}{R-r_F}\,L_0$$
$$-\left(\beta_c + \frac{h_0^{(1)}}{R-r_F}\right)\left\{L_{1C} + \Omega^2\left(\sum_j m_{h_j} h_{1C}^{(j)} - \sum_j \tau_{\bar{x}_1\theta_j}\theta_{1C}^{(j)} - \tau_{\bar{x}_2}\bar{\theta}_{1C}\right)\right\} \quad (18)$$

*See Appendix III of Reference 1.

$$\frac{1}{\pi}\int_0^{2\pi} Y d\psi = -D_{1C} + 2\Omega^2 \sum_j m_{c_j} h_{1C}^{(j)} - \frac{h_{1S}^{(1)}}{R-r_F} L_0$$

$$-\left(B_C + \frac{h_0^{(1)}}{R-r_F}\right)\left\{L_{1S} + \Omega^2\left(\sum_j m_{h_j} h_{1S}^{(j)} - \sum_j \tau_{\bar{X}_1\theta_j}\theta_{1S}^{(j)} - \tau_{\bar{X}_2}\bar{\theta}_{1S}\right)\right\} \tag{19}$$

$$\frac{1}{\pi}\int_0^{2\pi} Z d\psi = 2L_0 \tag{20}$$

$$\frac{1}{\pi}\int_0^{2\pi} Q d\psi = 2C_0 \tag{21}$$

$$\frac{1}{\pi}\int_0^{2\pi} M d\psi = B_{1C} + 2\Omega^2 \sum_j h_{1S}^{(j)}\left\{\beta_C\left(\tau_{rc_j} - r_C m_{c_j}\right)\right.$$

$$\left. + \frac{h_0^{(1)}}{R-r_F}\left(\tau_{rc_j} - r_F m_{c_j}\right) - \bar{\theta}_0 \tau_{\bar{X}_2 c_j}\right\} - \Omega^2 \frac{h_{1S}^{(1)}}{R-r_F} H_{(r-r_F)\bar{X}_3} + \Omega^2 \bar{\theta}_{1S} H_{\bar{X}_2\bar{X}_3}$$

$$+ \Omega^2 \sum_j h_0^{(j)}\left\{\frac{h_{1S}^{(1)}}{R-r_F}\left(\tau_{rc_j} - r_F m_{c_j}\right) - \bar{\theta}_{1S}\,\tau_{\bar{X}_2 c_j}\right\}$$

$$-\beta_C C_{1S}'' - \frac{h_0^{(1)}}{R-r_F} C_{1S}' + \bar{\theta}_0 C_{1S}''' - \frac{h_{1S}^{(1)}}{R-r_F} C_0' + \bar{\theta}_{1S} C_0'''$$

$$-\Omega^2 \bar{\theta}_{1S} J_\alpha - \Omega^2 \sum_j \theta_{1S}^{(j)} J_{\theta_j} - (M_p)_{1S} \tag{22}$$

where

$$\bar{X}_2 = e_1 - e + \bar{X}_1 \qquad \bar{X}_3 = \bar{X}_2 - e_D - e_P$$

$$m_{c_j} = \int_{r_0}^{R} m f_{c_j}\, dr \qquad m_{h_j} = \int_{r_F}^{R} m f_{h_j}\, dr$$

$$\tau_{\bar{X}_1\theta_j} = \int_{r_\theta}^{R} m\bar{X}_1 f_{\theta_j}\, dr \qquad \tau_{\bar{X}_2} = \int_{r_\theta}^{R} m\bar{X}_2\, dr$$

$$\tau_{rc_j} = \int_{r_0}^{R} m r f_{c_j}\, dr \qquad \tau_{\bar{X}_2 c_j} = \int_{r_\theta}^{R} m\bar{X}_2 f_{c_j}\, dr$$

$$H_{r\bar{X}_3} = \int_0^{R} m r\bar{X}_3\, dr \qquad H_{(r-r_F)\bar{X}_3} = \int_{r_F}^{R} m(r-r_F)\bar{X}_3\, dr$$

$$H_{\bar{X}_2\bar{X}_3} = \int_{r_\theta}^{R} m\bar{X}_2\bar{X}_3\, dr$$

$$J_\alpha = \int_{r_\theta}^{R} (I_\alpha - m\bar{X}_1^2)\, dr \qquad J_{\theta_j} = \int_{r_\theta}^{R} (I_\alpha - m\bar{X}_1^2) f_{\theta_j}\, dr$$

$$L = \int_0^R l\, dr \qquad D = \int_0^R (d_p + \epsilon l)\, dr$$

$$B = \int_0^R l r\, dr \qquad C = \int_0^R (d_p + \epsilon l) r\, dr$$

$$C' = \int_{r_F}^{R} (d_p + \epsilon l)(r - r_F)\, dr$$

$$C'' = \int_{r_c}^{R} (d_p + \epsilon l)(r - r_c)\, dr$$

$$C''' = \int_{r_\theta}^{R} (d_p + \epsilon l)(e_o - e)\, dr$$

$$M_p = \int_0^R \left\{ \eta - (e_1 - e - e_o - e_p) l \right\} dr .$$

Note that the lower limits of the above integrals are based on: $f_{h_j} = 0$ for $r \le r_F$, $f_{c_j} = 0$ for $r \le r_0$, $\bar{\theta} = f_{\theta_j} = 0$ for $r \le r_\theta$, $r_F \le r_0 < r_\theta$, and $r_c < r_0$. For a teetering rotor, $r_F = r_0 = 0$. To be strictly correct, the $\angle_o$ in Equation (18) or (19) must be based on

$$L = \int_{r_F}^{R} l\, dr \quad ;$$

the $\angle_{1c}$ in Equation (18) or $\angle_{1s}$ in Equation (19) must be based on

$$L = \int_{r_c}^{R} l\, dr$$

when it multiplies β_c and on

$$L = \int_{r_F}^{R} l\, dr$$

when it multiplies $\frac{h_o^{(1)}}{R - r_F}$; and m_{h_j}, also in Equations (18) and (19), must be given by

$$m_{h_j} = \int_{r_c}^{R} m f_{h_j}\, dr$$

when it multiplies β_c. (These corrections are usually either not needed

or are negligible.)

Define

$$\bar{X} = \frac{1}{\pi}\int_0^{2\pi} X\,d\psi\,, \quad \bar{Y} = \frac{1}{\pi}\int_0^{2\pi} Y\,d\psi\,, \text{ etc.}$$

Then, Equations (2) through (5) become

$$\bar{X} = \frac{2}{n_B}\left(W\alpha_s - X_F\right) \tag{23}$$

$$\bar{Z} = \frac{2}{n_B}\left(W - Z_F\right) \tag{24}$$

$$\bar{M} = \frac{2}{n_B}\left\{W\alpha_s - X_F)D_y - (W-Z_F)D_x - M_F\right\} \tag{25}$$

$$\bar{T} = \bar{Y} + \frac{Q}{R_t} = 0\,, \tag{26}$$

and Equations (18) through (22) become

$$\bar{X} = D_{1s} - \frac{h_{1c}^{(1)}}{R-r_F}L_0 - \left(\beta_c + \frac{h_0^{(1)}}{R-r_F}\right)L_{1c} - \Omega^2\left\{2\sum_j m_{c_j}h_{1s}^{(j)}\right.$$

$$\left. + \left(\beta_c + \frac{h_0^{(1)}}{R-r_F}\right)\left(\sum_j m_{h_j}h_{1c}^{(j)} - \sum_j \tau_{\bar{x}_1\theta_j}\theta_{1c}^{(j)} - \tau_{\bar{x}_2}\bar{\theta}_{1c}\right)\right\} \tag{27}$$

$$\bar{Z} = 2L_0 \tag{28}$$

$$\begin{aligned}\bar{M} = {} & B_{1c} - \beta_c C_{1s}'' + \bar{\theta}_0 C_{1s}''' + \bar{\theta}_{1s}C_0''' - \frac{1}{R-r_F}\left(h_0^{(1)}C_{1s}' + h_{1s}^{(1)}C_0'\right) - (M_p)_{1s} \\ & - \Omega^2\left\{\bar{\theta}_{1s}\left(J_\alpha - H_{\bar{x}_2\bar{x}_3}\right) + \frac{h_{1s}^{(1)}}{R-r_F}H_{(r-r_F)\bar{x}_3} + \sum_j \theta_{1s}^{(j)}J_{\theta_j}\right\} \\ & - \Omega^2\sum_j h_0^{(j)}\left\{\bar{\theta}_{1s}\tau_{\bar{x}_2 c_j} - \frac{h_{1s}^{(1)}}{R-r_F}\left(\tau_{rc_j} - r_F m_{c_j}\right)\right\} \\ & + 2\Omega^2\sum_j h_{1s}^{(j)}\left\{\beta_c\left(\tau_{rc_j} - r_c m_{c_j}\right) - \bar{\theta}_0\tau_{\bar{x}_2 c_j} + \frac{h_0^{(1)}}{R-r_F}\left(\tau_{rc_j} - r_F m_{c_j}\right)\right\}\end{aligned} \tag{29}$$

$$\bar{T} = -D_{1c} - \frac{h_{1s}^{(1)}}{R-r_F}L_0 - \left(\beta_c + \frac{h_0^{(1)}}{R-r_F}\right)L_{1s} + \Omega^2\left\{2\sum_j m_{c_j}h_{1c}^{(j)}\right.$$

$$\left. - \left(\beta_c + \frac{h_0^{(1)}}{R-r_F}\right)\left(\sum_j m_{h_j}h_{1s}^{(j)} - \sum_j \tau_{\bar{x}_1\theta_j}\theta_{1s}^{(j)} - \tau_{\bar{x}_2}\bar{\theta}_{1s}\right)\right\} + \frac{2}{R_t}C_0 \tag{30}$$

The numerical values of the right-hand sides of Equations (27) through (30) depend on the computed blade air loads and motions; they will agree with the desired values given by Equations (23) through (26) only when the correct set of trim constants ($\alpha_s, \bar{\theta}_0, \bar{\theta}_{1c}$ & $\bar{\theta}_{1s}$) is used in the whole computation. The intricate dependence of blade loads on trim constants makes the determination of the trim constants for a given flight condition difficult. Only methods involving iteration or successive approximations can be used. One of such methods is described in the following paragraph.

Let ($\tilde{\alpha}_s, \tilde{\theta}_0, \tilde{\theta}_{1c}, \tilde{\theta}_{1s}$) be an arbitrary set of trim constants, different from the correct set ($\alpha_s, \bar{\theta}_0, \bar{\theta}_{1c}, \bar{\theta}_{1s}$) according to

$$\left.\begin{aligned} \tilde{\alpha}_s &= \alpha_s - \bar{\bar{\alpha}}_s \\ \tilde{\theta}_0 &= \bar{\theta}_0 - \bar{\bar{\theta}}_0 \\ \tilde{\theta}_{1c} &= \bar{\theta}_{1c} - \bar{\bar{\theta}}_{1c} \\ \tilde{\theta}_{1s} &= \bar{\theta}_{1s} - \bar{\bar{\theta}}_{1s} \end{aligned}\right\} . \tag{31}$$

When the arbitrary trim constants and their resultant computed blade air loads and motions are used in evaluating the right-hand sides of Equations (27) through (30), the resultant values will be designated

$$\tilde{X}, \tilde{Z}, \tilde{M} \text{ and } \tilde{T}$$

accordingly. In a similar manner, the following designations will be made:

$\tilde{X}_a$, $\tilde{Z}_a$, $\tilde{M}_a$, and $\tilde{T}_a$ pertinent to ($\tilde{\alpha}_s + \Delta_s$, $\tilde{\theta}_0$, $\tilde{\theta}_{1c}$, $\tilde{\theta}_{1s}$
$\tilde{X}_b$, $\tilde{Z}_b$, $\tilde{M}_b$, and $\tilde{T}_b$ pertinent to ($\tilde{\alpha}_s$, $\tilde{\theta}_0 + \Delta_0$, $\tilde{\theta}_{1c}$, $\tilde{\theta}_{1s}$);
$\tilde{X}_c$, $\tilde{Z}_c$, $\tilde{M}_c$, and $\tilde{T}_c$ pertinent to ($\tilde{\alpha}_s$, $\tilde{\theta}_0$, $\tilde{\theta}_{1c} + \Delta_c$, $\tilde{\theta}_{1s}$); and
$\tilde{X}_d$; $\tilde{Z}_d$, $\tilde{M}_d$, and $\tilde{T}_d$ pertinent to ($\tilde{\alpha}_s$, $\tilde{\theta}_0$, $\tilde{\theta}_{1c}$, $\tilde{\theta}_{1s} + \Delta_s$).

With reasonably chosen Δ's and ($\tilde{\alpha}_s$, $\tilde{\theta}_0$, $\tilde{\theta}_{1c}$, $\tilde{\theta}_{1s}$), it is reasonable to assume that the following four equations will determine a set of estimated values of $\bar{\bar{\alpha}}_s$, $\bar{\bar{\theta}}_0$, $\bar{\bar{\theta}}_{1c}$, and $\bar{\bar{\theta}}_{1s}$ to yield a new ($\tilde{\alpha}_s$, $\tilde{\theta}_0$, $\tilde{\theta}_{1c}$, $\tilde{\theta}_{1s}$) set closer to the correct set.

$$\tilde{X} + X'_a \bar{\bar{\alpha}}_s + X'_b \bar{\bar{\theta}}_0 + X'_c \bar{\bar{\theta}}_{1c} + X'_d \bar{\bar{\theta}}_{1s} = \bar{X} \tag{32}$$

$$\tilde{Z} + Z_a' \bar{\tilde{\alpha}}_s + Z_b' \bar{\tilde{\theta}}_o + Z_c' \bar{\tilde{\theta}}_{1c} + Z_d' \bar{\tilde{\theta}}_{1s} = \bar{Z} \tag{33}$$

$$\tilde{M} + M_a' \bar{\tilde{\alpha}}_s + M_b' \bar{\tilde{\theta}}_o + M_c' \bar{\tilde{\theta}}_{1c} + M_d \bar{\tilde{\theta}}_{1s} = \bar{M} \tag{34}$$

$$\tilde{T} + T_a' \bar{\tilde{\alpha}}_s + T_b' \bar{\tilde{\theta}}_o + T_c' \bar{\tilde{\theta}}_{1c} + T_d' \bar{\tilde{\theta}}_{1s} = 0 , \tag{35}$$

where

$$\left.\begin{aligned} (\ )_a' &= \frac{(\tilde{\ })_a - (\tilde{\ })}{\Delta_s} \\ (\ )_b' &= \frac{(\tilde{\ })_b - (\tilde{\ })}{\Delta_o} \\ (\ )_c' &= \frac{(\tilde{\ })_c - (\tilde{\ })}{\Delta_{1c}} \\ (\ )_d' &= \frac{(\tilde{\ })_d - (\tilde{\ })}{\Delta_{1s}} \end{aligned}\right\} \quad (\ ) = X, Z, M, \text{or } T. \tag{36}$$

The quantities $\bar{X}$, $\bar{Z}$, and $\bar{M}$ appearing in Equations (32), (33), and (34) must be computed from (23), (24), and (25). The aerodynamic loads on the fuselage for $\alpha_s = \hat{\alpha}_s + \hat{\tilde{\alpha}}_s$, $|\hat{\tilde{\alpha}}_s|$ small, may be expressed by

$$\left.\begin{aligned} X_F &= \hat{X}_F + X_F' \hat{\tilde{\alpha}}_s \\ Z_F &= \hat{Z}_F + Z_F' \hat{\tilde{\alpha}}_s \\ M_F &= \hat{M}_F + M_F' \hat{\tilde{\alpha}}_s \end{aligned}\right\} , \tag{37}$$

where $\hat{X}_F$, X_F', etc. are constants depending on flight conditions and the chosen reference shaft angle, $\hat{\alpha}_s$. Substituting (37) into (23) through (25),

$$\bar{X} = \frac{2}{n_B}\left(W\alpha_s - \hat{X}_F - X_F' \hat{\tilde{\alpha}}_s\right)$$

$$\bar{Z} = \frac{2}{n_B}\left(W - \hat{Z}_F - Z_F' \hat{\tilde{\alpha}}_s\right)$$

$$\bar{M} = \frac{2}{n_B}\left\{\left(W\alpha_s - \hat{X}_F\right) D_y - \left(W - \hat{Z}_F\right) D_x - \hat{M}_F - \left(X_F' D_y - Z_F' D_x + M_F'\right) \hat{\tilde{\alpha}}_s\right\} .$$

With $\alpha_s = \tilde{\alpha}_s + \bar{\tilde{\alpha}}_s$ and $\hat{\tilde{\alpha}}_s = -(\hat{\alpha}_s - \tilde{\alpha}_s) + \bar{\tilde{\alpha}}_s$, the above three equations may be written

$$\bar{X} = \frac{2}{n_B}\left\{W\hat{\alpha}_s - \hat{X}_F - (W - X_F')(\hat{\alpha}_s - \tilde{\alpha}_s)\right\} + \frac{2}{n_B}(W - X_F')\,\bar{\tilde{\alpha}}_s \tag{38}$$

$$\bar{Z} = \frac{2}{n_B}\left\{W - \hat{Z}_F + Z'_F(\hat{\alpha}_s - \tilde{\alpha}_s)\right\} - \frac{2}{n_B} Z'_F \bar{\bar{\alpha}}_s \tag{39}$$

$$\bar{M} = \frac{2}{n_B}\left[(W\hat{\alpha}_s - \hat{X}_F)D_z - (W - \hat{Z}_F)D_x - \hat{M}_F - \left\{(W - X'_F)D_z + Z'_F D_x - M'_F\right\}(\hat{\alpha}_s - \tilde{\alpha}_s)\right]$$

$$+ \frac{2}{n_B}\left\{(W - X'_F)D_z + Z'_F D_x - M'_F\right\}\bar{\bar{\alpha}}_s . \tag{40}$$

By substituting these into (32) through (34) and rearranging, (32) through (35) become

$$X'_b\bar{\bar{\theta}}_0 + X'_c\bar{\bar{\theta}}_{1c} + X'_d\bar{\bar{\theta}}_{1s} + \left\{X'_a - \frac{2}{n_B}(W - X'_F)\right\}\bar{\bar{\alpha}}_s = \frac{2}{n_B}\left\{W\hat{\alpha}_s - \hat{X}_F - (W - X'_F)(\hat{\alpha}_s - \tilde{\alpha}_s)\right\} - \tilde{X} \tag{41}$$

$$Z'_b\bar{\bar{\theta}}_0 + Z'_c\bar{\bar{\theta}}_{1c} + Z'_d\bar{\bar{\theta}}_{1s} + \left(Z'_a + \frac{2}{n_B}Z'_F\right)\bar{\bar{\alpha}}_s = \frac{2}{n_B}\left\{W - \hat{Z}_F + Z'_F(\hat{\alpha}_s - \tilde{\alpha}_s)\right\} - \tilde{Z} \tag{42}$$

$$M'_b\bar{\bar{\theta}}_0 + M'_c\bar{\bar{\theta}}_{1c} + M'_d\bar{\bar{\theta}}_{1s} + \left[M'_a - \frac{2}{n_B}\left\{(W - X'_F)D_z + Z'_F D_x - M'_F\right\}\right]\bar{\bar{\alpha}}_s$$

$$= \frac{2}{n_B}\left[(W\hat{\alpha}_s - \hat{X}_F)D_z - (W - \hat{Z}_F)D_x + \hat{M}_F - \left\{(W - X'_F)D_z + Z'_F D_x - M'_F\right\}(\hat{\alpha}_s - \tilde{\alpha}_s)\right] - \tilde{M} \tag{43}$$

$$T'_b\bar{\bar{\theta}}_0 + T'_c\bar{\bar{\theta}}_{1c} + T'_d\bar{\bar{\theta}}_{1s} + T'_a\bar{\bar{\alpha}}_s = -\tilde{T}. \tag{44}$$

These are a set of four linear equations, from which the four unknowns ($\bar{\bar{\alpha}}_s$, $\bar{\bar{\theta}}_0$, $\bar{\bar{\theta}}_{1c}$, and $\bar{\bar{\theta}}_{1s}$) pertaining to a given ($\tilde{\alpha}_s$, $\tilde{\theta}_0$, $\tilde{\theta}_{1c}$, $\tilde{\theta}_{1s}$) set can be solved. A new ($\tilde{\alpha}_s$, $\tilde{\theta}_0$, $\tilde{\theta}_{1c}$, $\tilde{\theta}_{1s}$) set can then be formed in accordance with (31) and the computation can be repeated until $\bar{\bar{\alpha}}_s$, $\bar{\bar{\theta}}_0$, $\bar{\bar{\theta}}_{1c}$, and $\bar{\bar{\theta}}_{1s}$ become sufficiently small.

EQUATIONS OF BLADE MOTIONS

When those Coriolis forces which do not have Ω as a factor are neglected, Lagrange's equation of blade motions with respect to any i^{th} generalized coordinate (q_i) has the following general form:*

$$\sum_j \left[M_{q_i q_j} \ddot{q}_j - \Omega 2 C_{q_i q_j} \dot{q}_j + \left\{ (1 + j g_{q_j}) K_{q_i q_j} - \Omega^2 T_{q_i q_j} \right\} q_j \right] = C_{q_i} + G_{q_i} \qquad (45)$$

where

$$q_j = (h_j \text{ or } \theta_j) = (h_1, \cdots, h_S ; \theta_1, \cdots, \theta_\gamma).$$

There will be a total number of ($S + \gamma$) equations of the form (45). According to Reference 2, $M_{q_i q_j}$ is called the generalized mass coefficient, $2C_{q_i q_j}$ the generalized Coriolis force coefficient, $T_{q_i q_j}$ the generalized centrifugal force coefficient, and $K_{q_i q_j}$ the generalized restraining (elastic) force coefficient. (Formulas for these coefficients can be obtained by the method given in Reference 3.) Symbolically, $j g_{q_j}$ indicates the presence of a generalized structural damping force (associated with q_j) equal to

$$g_{q_j} K_{q_i q_j} \sum_{n=1}^{\infty} \left(-q_{nc}^{(j)} \sin n\psi + q_{ns}^{(j)} \cos n\psi \right) \qquad (46)$$

if q_j is expanded into Fourier's series as

$$q_j = q_0^{(j)} + \sum_{n=1}^{\infty} \left(q_{nc}^{(j)} \cos n\psi + q_{ns}^{(j)} \sin n\psi \right). \qquad (47)$$

The constant g_{q_j} for each q_j is called the structural damping factor of the degree of freedom represented by q_j . G_{q_i} is the generalized aerodynamic force in coordinate q_i and can be calculated from one of the

---

* If the blade pitch-control system were rigid, it would contribute a blade pitch angle $\bar{\theta}$ given by

$$\bar{\theta} = \bar{\theta}_0 + \bar{\theta}_{1c} \cos\psi + \bar{\theta}_{1s} \sin\psi.$$

For a flexible control system, the equation of motion with respect to pitch deflection (which is the difference between $\bar{\theta}$ and the actual pitch) is similar to that with respect to a torsional mode θ_i having $f_{\theta_i} = 1$.

following two formulas:

$$G_{h_i} = \int \ell f_{h_i}\, dr - \int (d_p + \epsilon \ell) f_{c_i}\, dr \tag{48}$$

$$G_{\theta_i} = \int m f_{\theta_i}\, dr \tag{49}$$

Finally, C_{q_i} is the generalized force in q_i when the blade is rotating in vacuum with all h_j and θ_j held zero. C_{h_i} and C_{θ_i} depend on the blade configuration (β_c , θ_B and offsets) and pitch control ($\bar{\theta}$), and can be calculated from the following two general formulas:*

$$\begin{aligned} C_{h_i} = {} & \Omega^2 \bar{\theta}_0 \int m r \bar{X}_1 f'_{h_i}\, dr - \Omega^2 \beta_c \int m r f_{h_i}\, dr \\ & + \Omega^2 (\bar{\theta}_{1c} \cos\psi + \bar{\theta}_{1s} \sin\psi) \left\{ \int m r \bar{X}_1 f'_{h_i}\, dr - \int m (e_1 - e + \bar{X}_1) f_{h_i}\, dr \right\} \\ & - \Omega^2 \int m (-e_D - e_P + e_1 - e + \bar{X}_1) f_{c_i}\, dr + \Omega^2 \int m r \bar{X}_1 \theta_B f'_{h_i}\, dr + \Omega^2 \int m r \bar{X}_1 f'_{c_i}\, dr \end{aligned} \tag{50}$$

$$\begin{aligned} C_{\theta_i} = {} & -\Omega^2 \bar{\theta}_0 \int \left\{ I_\alpha + m \bar{X}_1 (-e_D - e_P + e_1 - e) \right\} f_{\theta_i}\, dr + \Omega^2 (\bar{\theta}_{1c} \cos\psi + \bar{\theta}_{1s} \sin\psi)(e_D + e_P) \int m \bar{X}_1 f_{\theta_i}\, dr \\ & + \Omega^2 \beta_c \int m r \bar{X}_1 f_{\theta_i}\, dr - \Omega^2 \int k_A^2 \frac{d\theta_B}{dr} \left(\int_r^R m r\, dr \right) f'_{\theta_i}\, dr \\ & - \Omega^2 \int \left\{ I_\alpha + m \bar{X}_1 (-e_D - e_P + e_1 - e) \right\} \theta_B f_{\theta_i}\, dr \end{aligned} \tag{51}$$

where k_A is the radius of gyration of the local blade sectional area which is effective in taking the centrifugal force. Due to the blade built-in twist, θ_B , the centrifugal force is, in effect, accompanied by a torsional moment equal to

$$-\Omega^2 \left(\int_r^R m r\, dr \right) \frac{d\theta_B}{dr} k_A^2$$

---

* Unless noted otherwise, a prime indicates derivative with respect to blade radius. The first and second $\bar{X}_1$ appearing in (50) must be replaced with $(e_1 - e + \bar{X}_1)$, if h_i represents pure flapping; the last $\bar{X}_1$ appearing in (50) must be replaced with $(-e_p + e_1 - e + \bar{X}_1)$, if h_i represents pure lead-lag.

acting on a thin blade section at r. The contributions to C_{h_i} and C_θ due to

$$\bar{\theta} = \bar{\theta}_o + \bar{\theta}_{1c}\cos\psi + \bar{\theta}_{1s}\sin\psi$$

may be first written as

$$-\left(M_{h_i\bar{\theta}}\ddot{\bar{\theta}} - \Omega^2 T_{h_i\bar{\theta}}\bar{\theta}\right)$$

and

$$-\left(M_{\theta_i\bar{\theta}}\ddot{\bar{\theta}} - \Omega^2 T_{\theta_i\bar{\theta}}\bar{\theta}\right), \text{ respectively,}$$

where

$$T_{h_i\bar{\theta}} = \int mr\bar{X}_1 f'_{h_i}\,dr$$

$$M_{h_i\bar{\theta}} = -\int m(e_1 - e + \bar{X}_1) f_{h_i}\,dr$$

$$T_{\theta_i\bar{\theta}} = -\int \left\{I_\alpha + m\bar{X}_1(-e_D - e_P + e_1 - e)\right\} f_{\theta_i}\,dr$$

$$T_{\theta_i\bar{\theta}} + M_{\theta_i\theta} = (e_D + e_P)\int m\bar{X}_1 f_{\theta_i}\,dr.$$

It is now easy to verify (50) and (51). It may be noted that $(C_{q_i})_{nc} = (C_{q_i})_{ns} = 0$ for $n \geq 2$.

If viscous damping exists in a certain j^{th} degree of freedom (such as lead-lag) and does virtual work equal to $D_{q_i q_j}$ to a certain i^{th} degree of freedom, only the term $D_{q_i q_j}/\Omega$ needs to be added to $2C_{q_i q_j}$ for the appropriate set of (i, j). The part of $2C_{q_i q_j}$ that really represents Coriolis force is usually negligible for blade loads computation. For a blade with offsets shown in Figure 3 and with a rigid link connecting the flapping and lead-lag hinges, the following formulas for the M-, Γ-, and K-coefficients have been obtained:*

$$M_{h_i h_j} = \int_{r_D}^{R} m\left(f_{h_i} f_{h_j} + f_{c_i} f_{c_j}\right)dr + J_H\left(f'_{h_i} f'_{h_j}\right)_{r=r_D}$$

$$M_{h_i\theta_j} = -\int_{r_\theta}^{R} m\bar{X}_1 f_{h_i} f_{\theta_j}\,dr = M_{\theta_j h_i}$$

$$M_{\theta_i\theta_j} = \int_{r_\theta}^{R} I_\alpha f_{\theta_i} f_{\theta_j}\,dr$$

---

* The lower limits of the integrals are based on the assumption that $r_\theta > r_D \geq r_f \geq 0$. (Note that $\bar{\theta} = f_{\theta_j} = 0$ for $r \leq r_\theta$.)

$$T_{h_i h_j} = \int_{r_0}^{R} m f_{c_i} f_{c_j}\, dr - \int_{r_F}^{R} \left(f'_{h_i} f'_{h_j} + f'_{c_i} f'_{c_j}\right)\left(\int_r^R mr\,dr\right)dr$$
$$- \left\{J_H - 2J_{HZ} + (r_0 - r_F)\int_{r_0}^{R} mr\,dr + r_F(\bar{r}_H - r_F)\, m_H\right\}\left(f'_{h_i} f'_{h_j}\right)_{r=r_0}$$

$$T_{h_i \theta_j} = \int_{r_\theta}^{R} mr\bar{X}_1 f'_{h_i} f_{\theta_j}\, dr = T_{\theta_j h_i}$$

$$T_{\theta_i \theta_j} = -M_{\theta_i \theta_j} - \int_{r_\theta}^{R} m\bar{X}_1(-e_0 - e_p + e_1 - e_0) f_{\theta_i} f_{\theta_j}\, dr$$

$$K_{h_i h_j} = \int_{r_0}^{R} \left\{EI_B\left(f''_{h_i}\cos\theta - f''_{c_i}\sin\theta\right)\left(f''_{h_j}\cos\theta - f''_{c_j}\sin\theta\right)\right.$$
$$\left. + EI_C\left(f''_{c_i}\cos\theta + f''_{h_i}\sin\theta\right)\left(f''_{c_j}\cos\theta + f''_{h_j}\sin\theta\right)\right\}dr$$

$$K_{h_i \theta_j} = 0 = K_{\theta_j h_i}$$

$$K_{\theta_i \theta_j} = \int_{r_\theta}^{R} \left\{GJ + \Omega^2 k_A^2\left(\int_r^R mr\,dr\right)\right\} f'_{\theta_i} f'_{\theta_j}\, dr$$

where EI_B, EI_C and GJ are the elastic properties of the blade section (flatwise flexural, chordwise flexural, and conventional torsional rigidities, respectively); J_H, J_{HZ}, $\bar{r}_H$ and m_H are the inertial properties of the link connecting the flapping and lead-lag hinges (J_H is the moment of inertia about the flapping hinge, J_{HZ} is the part of J_H due to spread of mass in the direction parallel to the lead-lag hinge, $\bar{r}_H$ is the c. g. radius, and m_H is the mass); and $\theta = \bar{\theta} + \theta_B$ (but the approximation $\theta \approx \bar{\theta}_0 + \theta_B$ has to be used in practice). It may be noted that the formulas are applicable to a teetering rotor blade without lead-lag hinge by setting $r_F = r_0 = 0$ and using appropriate values of J_H and J_{HZ} (both belong to the hub mass that flaps with the blade); they are also applicable to a rigid hub rotor blade by setting $r_F = r_0 = \left(f'_{h_i} f'_{h_j}\right)_{r=r_0} = 0$.

One part of the air load program will first compute each G_{q_i} according to the appropriate formula [(48) or (49)] for $2N$ equally spaced azimuthal positions and then, by harmonic analysis, express it as the following finite series:

$$G_{q_i} = \left(G_{q_i}\right)_0 + \sum_{n=1}^{N}\left(G_{q_i}\right)_{nc}\cos n\psi + \sum_{n=1}^{N-1}\left(G_{q_i}\right)_{ns}\sin n\psi\,, \qquad (52)$$

which contains $2N$ coefficients and gives the actually computed values of G_{q_i} at those $2N$ equally spaced azimuthal positions. By making N reasonably large ($2N = 24$ for the present program), it is usual to consider that it is accurate enough to substitute (52) into (45). By doing this, all harmonic components of any q_j higher than the N^{th} harmonic are automatically nullified.

By equating the coefficients of $\cos n\psi$ of the two sides of (45),

$$\sum_j \left\{ K_{q_i q_j} - \Omega^2 \left(n^2 M_{q_i q_j} + T_{q_i q_j} \right) \right\} q_{nc}^{(j)} + \sum_j \left(K_{q_i q_j} g_{q_j} - \Omega^2 n 2 \mathcal{C}_{q_i q_j} \right) q_{ns}^{(j)}$$

$$= \left(C_{q_i} \right)_{nc} + \left(G_{q_i} \right)_{nc} . \tag{53}$$

By equating the coefficients of $\sin n\psi$ of the two sides of (45),

$$- \sum_j \left(K_{q_i q_j} g_{q_j} - \Omega^2 n 2 \mathcal{C}_{q_i q_j} \right) q_{nc}^{(j)} + \sum_j \left\{ K_{q_i q_j} - \Omega^2 \left(n^2 M_{q_i q_j} + T_{q_i q_j} \right) \right\} q_{ns}^{(j)}$$

$$= \left(C_{q_i} \right)_{ns} + \left(G_{q_i} \right)_{ns} . \tag{54}$$

Equations (53) and (54) may be called the equations for n^{th} harmonic components with respect to q_i. Note that either (53) or (54) involves both the cosine and sine amplitudes of q_j in n^{th} harmonic. There is only one corresponding equation for the 0^{th} harmonic components (or the constant terms, or the average values):

$$\sum_j \left(K_{q_i q_j} - \Omega^2 T_{q_i q_j} \right) q_0^{(j)} = \left(C_{q_i} \right)_0 + \left(G_{q_i} \right)_0 . \tag{55}$$

Since, according to (50) through (52), the right-hand sides of both (53) and (54) are identically zero for $n > N$,

$$q_{nc}^{(j)} = q_{ns}^{(j)} = 0 \qquad \text{for} \qquad n > N, \tag{56}$$

as pointed out at the end of the last paragraph. Thus, there are

$(1 + 2N)$ equations with respect to each q_i, and each q_j assumes the form

$$q_j = q_0^{(j)} + \sum_{j=1}^{N} \left(q_{nc}^{(j)} \cos n\psi + q_{ns}^{(j)} \sin n\psi \right). \tag{57}$$

As there will be a total number of $(S + \gamma)$ different q_i, there will be $(S + \gamma)$ equations of the form (55) to determine the $(S + \gamma)$ different $q_0^{(j)}$. There will also be $2(S + \gamma)$ equations, half of them of the form (53) and the other half of the form (54), for each n, $1 \le n \le N$, to determine the $(S + \gamma)$ different $q_{nc}^{(j)}$ plus the $(S + \gamma)$ different $q_{ns}^{(j)}$.

Torsional vibration modes of twisted rotating blade, cantilevered at $r = r_\theta$, will be used for f_θ. Then f_{θ_i} satisfies the following equilibrium condition:

$$\left\{ GJ + \Omega^2 k_A^2 \left(\int_r^R m r dr \right) \right\} f'_{\theta_i}$$
$$= \omega_{\theta_i}^2 \int_r^R I_\alpha f_{\theta_i} dr - \Omega^2 \int_r^R I_\alpha f_{\theta_i} \cos 2(\bar{\theta} + \theta_B) dr,$$

where ω_{θ_i} is the natural frequency associated with f_{θ_i}. Using $\cos 2(\bar{\theta} + \theta_B) \approx 1$, the above equilibrium condition may be written as

$$\left\{ GJ + \Omega^2 k_A^2 \left(\int_r^R m r dr \right) \right\} f'_{\theta_i} = (\omega_{\theta_i}^2 - \Omega^2) \int_r^R I_\alpha f_{\theta_i} dr. \tag{58}$$

Multiplying both sides of (58) by f'_{θ_j} and then integrating over r_θ to R,

$$\int_{r_\theta}^R \left\{ GJ + \Omega^2 k_A^2 \left(\int_r^R m r dr \right) \right\} f'_{\theta_i} f'_{\theta_j} dr$$
$$= (\omega_{\theta_j}^2 - \Omega^2) \int_{r_\theta}^R I_\alpha f_{\theta_i} f_{\theta_j} dr. \tag{59}$$

(Note that the right-hand side of the above equation has been integrated by parts once, using $f_\theta = 0$ at $r = r_\theta$ and $\int_r^R I_\alpha f_\theta dr = 0$ at $r = R$.) Using the expressions for $K_{\theta_i \theta_j}$ and $M_{\theta_i \theta_j}$ as given before, (59) states simply

$$K_{\theta_i \theta_j} = (\omega_{\theta_i}^2 - \Omega^2) M_{\theta_i \theta_j}. \tag{60}$$

Similarly, starting with (58) for the j^{th} mode,

$$K_{\theta_i \theta_j} = (\omega_{\theta_j}^2 - \Omega^2) M_{\theta_i \theta_j} . \tag{61}$$

From (60) and (61), it can be concluded that

$$M_{\theta_i \theta_j} = 0, \quad j \neq i \tag{62}$$

$$K_{\theta_i \theta_j} = 0, \quad j \neq i \tag{63}$$

and

$$K_{\theta_i \theta_i} = (\omega_{\theta_i}^2 - \Omega^2) M_{\theta_i \theta_i} . \tag{64}$$

Relations like (62), (63), and (64) are usually called orthogonality relations of vibration modes.

Bending vibration modes of twisted rotating blades will be used for f_h and f_c. The existing method of Reference 4 yields modal shapes each described by deflection components in two mutally perpendicular directions, from which the f_h and f_c used herein can be easily obtained for each mode. The derivations of the orthogonality relations among these modes are presented in the appendix. The results are

$$M_{h_i h_j} = 0, \quad j \neq i \tag{65}$$

$$K_{h_i h_j} - \Omega^2 T_{h_i h_j} = 0, \quad j \neq i \tag{66}$$

and

$$K_{h_i h_i} - \Omega^2 T_{h_i h_i} = \omega_{h_i}^2 M_{h_i h_i} . \tag{67}$$

By the use of $K_{h_i\theta_j} = 2\mathcal{C}_{h_i\theta_j} = 0$ and (65) through (67), (53) and (54) may be written as

$$(\omega_{h_i}^2 - n^2\Omega^2) M_{h_ih_i} h_{nc}^{(i)} - \Omega^2 \sum_{j=1}^{\gamma} (n^2 M_{h_i\theta_j} + T_{h_i\theta_j}) \theta_{nc}^{(j)} + \sum_{j=1}^{s} (K_{h_ih_j} q_{h_j} - n\Omega^2 2\mathcal{C}_{h_ih_j}) h_{ns}^{(j)} = (C_{h_i})_{nc} + (G_{h_i})_{nc} \qquad (i = 1 \text{ to } s) \qquad (68)$$

and

$$-\sum_{j=1}^{s} (K_{h_ih_j} q_{h_j} - n\Omega^2 2\mathcal{C}_{h_ih_j}) h_{nc}^{(j)} + (\omega_{h_i}^2 - n^2\Omega^2) M_{h_ih_i} h_{ns}^{(i)} - \Omega^2 \sum_{j=1}^{\gamma} (n^2 M_{h_i\theta_j} + T_{h_i\theta_j}) \theta_{ns}^{(j)} = (C_{h_i})_{ns} + (G_{h_i})_{ns} \qquad (i = 1 \text{ to } s). \qquad (69)$$

By the use of $K_{\theta_ih_j} = 2\mathcal{C}_{\theta_iq_j} = 0$ and (62) through (64), (53) and (54) become

$$-\Omega^2 \sum_{j=1}^{s} (n^2 M_{\theta_ih_j} + T_{\theta_ih_j}) h_{nc}^{(j)} + (\omega_{\theta_i}^2 - n^2\Omega^2) M_{\theta_i\theta_i} \theta_{nc}^{(i)} - \Omega^2 \sum_{j=1}^{\gamma} \hat{T}_{\theta_i\theta_j} \theta_{nc}^{(j)} + (\omega_{\theta_i}^2 - \Omega^2) M_{\theta_i\theta_i} q_{\theta_i} \theta_{ns}^{(i)} = (C_{\theta_i})_{nc} + (G_{\theta_i})_{nc} \qquad (i = 1 \text{ to } \gamma) \qquad (70)$$

and

$$-(\omega_{\theta_i}^2 - \Omega^2) M_{\theta_i\theta_i} q_{\theta_i} \theta_{nc}^{(i)} - \Omega^2 \sum_{j=1}^{s} (n^2 M_{\theta_ih_j} + T_{\theta_ih_j}) h_{ns}^{(j)} + (\omega_{\theta_i}^2 - n^2\Omega^2) M_{\theta_i\theta_i} \theta_{ns}^{(i)} - \Omega^2 \sum_{j=1}^{\gamma} \hat{T}_{\theta_i\theta_j} \theta_{ns}^{(j)} = (C_{\theta_i})_{ns} + (G_{\theta_i})_{ns} \qquad (i = 1 \text{ to } \gamma) \qquad (71)$$

where

$$\hat{T}_{\theta_i\theta_j} \equiv T_{\theta_i\theta_j} + M_{\theta_i\theta_j} = -\int_{r_\theta}^{R} m\bar{X}_1 (-e_D - e_P + e_1 - e) f_{\theta_i} f_{\theta_j} \, dr .$$

The two equations for 0^{th} harmonic can be obtained by substituting $n = h_{ns}^{(j)} = 0$ into (68) and $n = \theta_{ns}^{(i)} = 0$ into (70), respectively, and replacing nc by 0.

The blade weight (mg pounds per unit span) may be taken into account by modifying (48) and (49) as follows: subtract mg from the first ℓ and add $mg\bar{x}_1$ to $\mathcal{M}$. Since the blade lift usually amounts to over 20 times the blade outboard weight, it is permissible (until a more accurate method of predicting becomes available) to treat the predicted air loads as if they included the blade weight effects. In actual computation, the blade weight can be more conveniently taken into account by adding

$$-\int mg f_{h_i}\, dr \qquad \text{and} \qquad +\int mg \bar{x}_1 f_{\theta_i}\, dr$$

to the right-hand sides of (50) and (51), respectively.

During forward flight, the cyclic pitch makes the blade root angle vary with the blade azimuthal position. The blade bending modes (and their associated radial variations of bending moments) are usually based on some constant blade root angle, approximately equal to the collective pitch. In other words, the blade elastic properties with reference to a coordinate system fixed to the rotor hub are usually assumed to be constant, approximately equal to the average values. This assumption is believed to be satisfactory for obtaining the blade motions. For the flatwise and chordwise bending moments, however, the following compensation may be suggested: after the flatwise and chordwise bending moments based on the assumed blade root angle are computed (by summing the contributions from all the bending modes employed), transform them to the actual directions according to the difference between the actual (various) and the assumed (constant) root angles. (Then the resultant loading is taken by the actual blade, although the bending deformation and its associated inertia loading are based on a slightly modified blade.)

COMPUTATIONAL PROCEDURE

The trim constants are obtained by a successive approximation method described in the last paragraph of the section entitled "TRIM EQUATIONS". The method starts with an assumed or estimated set of trim constants and then adjusts them systematically so as to make the average force and moment components acting on the rotor cancel the corresponding force and moment components acting on the rest of the helicopter, until the required adjustments are within prescribed limits. A flow diagram indicating the main conceptual elements of this procedure is presented in Figure 4.

The computational procedure described in Reference 1 is for computing blade loadings and response when the trim constants are given. It is an iterative procedure which starts with a first approximation to the blade response and repeatedly computes the blade aerodynamic loadings (that depend on the blade response) and solves the equations of blade motions (with the generalized aerodynamic forces based on the blade response obtained in the previous iteration cycle), until the blade response converges to within prescribed limits. The same general procedure is used here to compute the blade loadings and response for each prevailing set of trim constants (corresponding to the flow diagram shown in Figure 4 marked with solid lines only). In order to admit the additional blade motions and to include the drag distribution in the blade loadings, the following four modifications are made. First, the quasi-steady bound circulation, I, defined by (21) of Reference 1 as *

$$I = C_{\ell_\alpha}\, b\left(-\dot{h} + V_t\,\alpha + \frac{b}{2}\,\dot{\alpha}\right), \tag{72}$$

* Note that $V_t = \Omega r + (V_f \cos\alpha_s)\sin\psi$ and C_{ℓ_α} is the slope of the blade sectional lift coefficient versus angle-of-attack plot.

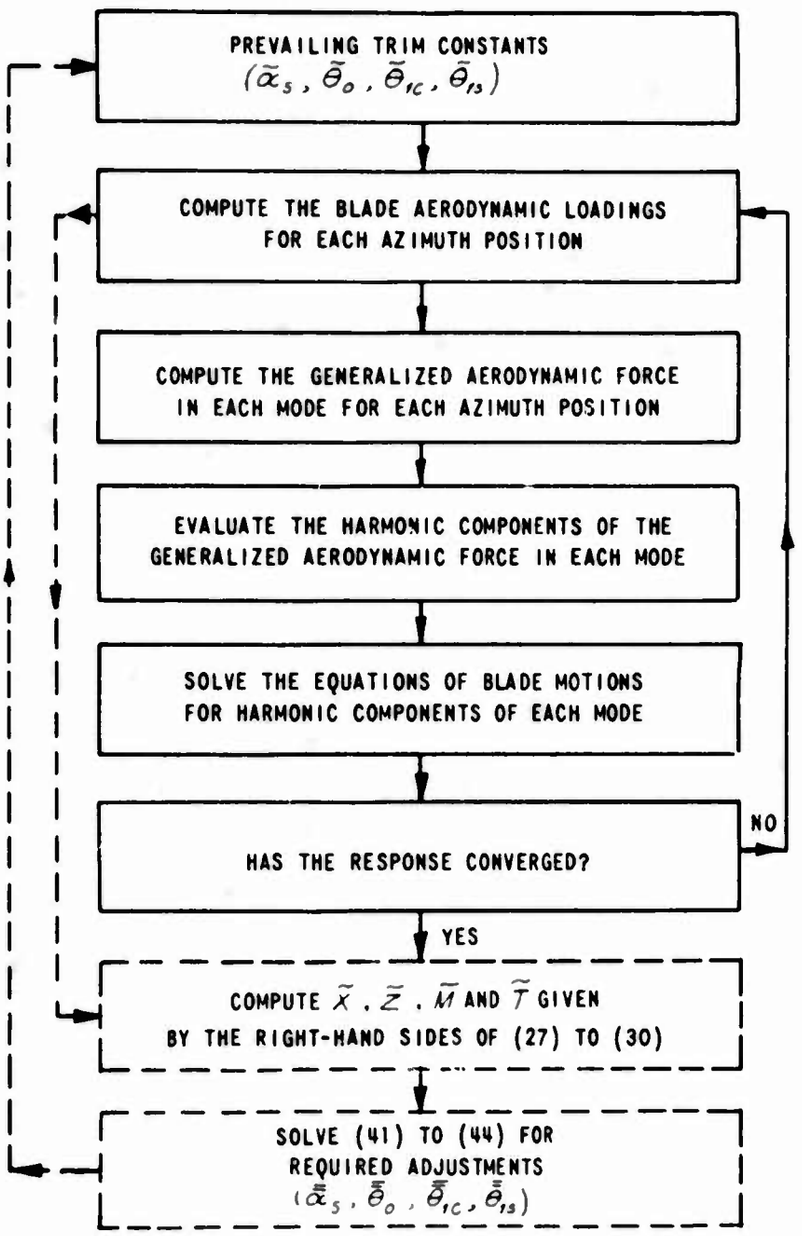

NOTES: ONCE $\bar{\tilde{\alpha}}_s$, $\bar{\tilde{\theta}}_o$, $\bar{\tilde{\theta}}_{1c}$ AND $\bar{\tilde{\theta}}_{1s}$ BECOME WITHIN PRESCRIBED LIMITS, THE NEXT (ALSO THE LAST) CYCLE WILL ONLY ENCOMPASS THE PORTION MARKED WITH SOLID LINES, WITH YES COMMANDING THE DRAWING OF DESIRED OUTPUTS.

Figure 4. MAJOR STEPS IN THE COMPUTATIONAL PROCEDURE.

has now

$$\alpha = \theta_\beta + \bar{\theta}_o + \bar{\theta}_{1c}\cos\psi + \bar{\theta}_{1s}\sin\psi + \sum_{j=1}^{\gamma}\theta_j f_{\theta_j} \tag{73}$$

$$\dot{\alpha} = -\Omega\bar{\theta}_{1c}\sin\psi + \Omega\bar{\theta}_{1s}\cos\psi + \sum_{j=1}^{\gamma}\dot{\theta}_j f_{\theta_j} + \Omega\left(\beta_c + \sum_{j=1}^{s} h_j f'_{h_j}\right) \tag{74}$$

$$\dot{h} = V_f \sin\alpha_s + e_1\Omega(\bar{\theta}_{1c}\sin\psi - \bar{\theta}_{1s}\cos\psi) + \sum_{j=1}^{s}\dot{h}_j f_{h_j} - e\sum_{j=1}^{\gamma}\dot{\theta}_j f_{\theta_j}$$

$$+ (V_f\cos\alpha_s)\left(\beta_c + \sum_{j=1}^{s} h_j f'_{h_j}\right)\cos\psi\,. \tag{75}$$

Second, the profile drag coefficient, C_{d_p}, of blade section is a new input that depends on Mach number (which is proportional to V_1) and α_e, the effective angle of attack defined by

$$\alpha_e = \alpha + \frac{1}{V_1}\frac{b}{2}\dot{\alpha} - \epsilon \tag{76}$$

where

$$\epsilon = \tan^{-1}\left(\frac{-V_2}{V_1}\right) = \tan^{-1}\left(\frac{\dot{h} - w_{3/4}}{V_1}\right) \tag{77}$$

is the induced angle, with $w_{3/4}$ being the upwash at the three-quarter-chord point induced by the wake. Third, the drag per unit span is equal to $(d_p + \epsilon\ell)$, with

$$d_p = \rho V_1^2 b C_{d_p} \tag{78}$$

being the profile drag per unit span. It was found in Reference 1 that the convergence of the procedure was improved by subtracting a part of the generalized aerodynamic force, approximately equal to the part that depends on the response or generalized coordinates, from both sides of each equation of blade motions. (The part subtracted from the right or left side is based on blade response obtained in the previous or the present cycle, respectively; they approach each other as the response converges.) In effect, it means that the convergence can be

accelerated by estimating the generalized aerodynamic forces for the present iteration cycle closer than those based on the blade response obtained in the previous cycle. As the fourth modification, therefore, the terms

$$\Omega^2 \left\{ \sum_{j=1}^{\gamma} A_{h_i \theta_j} \theta_{nc}^{(j)} + n \sum_{j=1}^{s} A_{h_i \dot{h}_j} h_{ns}^{(j)} + n \sum_{j=1}^{\gamma} A_{h_i \dot{\theta}_j} \theta_{ns}^{(j)} \right\} \tag{79}$$

$$\Omega^2 \left\{ -n \sum_{j=1}^{s} A_{h_i \dot{h}_j} h_{nc}^{(j)} - n \sum_{j=1}^{\gamma} A_{h_i \dot{\theta}_j} \theta_{nc}^{(j)} + \sum_{j=1}^{\gamma} A_{h_i \theta_j} \theta_{ns}^{(j)} \right\} \tag{80}$$

$$\Omega^2 \left\{ \sum_{j=1}^{\gamma} A_{\theta_i \theta_j} \theta_{nc}^{(j)} + n \sum_{j=1}^{s} A_{\theta_i \dot{h}_j} h_{ns}^{(j)} + n \sum_{j=1}^{\gamma} A_{\theta_i \dot{\theta}_j} \theta_{ns}^{(j)} \right\} \tag{81}$$

and

$$\Omega^2 \left\{ -n \sum_{j=1}^{s} A_{\theta_i \dot{h}_j} h_{nc}^{(j)} - n \sum_{j=1}^{\gamma} A_{\theta_i \dot{\theta}_j} \theta_{nc}^{(j)} + \sum_{j=1}^{\gamma} A_{\theta_i \theta_j} \theta_{ns}^{(j)} \right\} \tag{82}$$

are subtracted from both sides of (68), (69), (70), and (71), respectively, resulting in using (83) through (86) as the formulas of the equations of blade motions for the present computation. A superscript (-1) appearing in (83) through (86) indicates a quantity based on blade response obtained in the previous cycle. The formulas for the A-coefficients appearing in (79) through (82), and in (83) through (86), are the following:

$$A_{h_i \dot{h}_j} = -2\pi\rho \int r b f_{h_i h_j} \, dr$$

$$A_{h_i \dot{\theta}_j} = 2\pi\rho \int r b (b+e) f_{h_i} f_{\theta_j} \, dr$$

$$A_{h_i \theta_j} = 2\pi\rho \int r^2 b f_{h_i} f_{\theta_j} \, dr$$

$$A_{\theta_i \dot{h}_j} = -2\pi\rho \int r b \left(\frac{b}{2} - e\right) f_{\theta_i} f_{h_j} \, dr$$

$$A_{\theta_i \dot{\theta}_j} = -2\pi\rho \int r b e \left(\frac{b}{2} + e\right) f_{\theta_i} f_{\theta_j} \, dr$$

$$A_{\theta_i \theta_j} = 2\pi\rho \int r^2 b \left(\frac{b}{2} - e\right) f_{\theta_i} f_{\theta_j} \, dr .$$

The terms (79) through (82) are derived from the generalized forces in h_i and θ_i coordinates due to the quasi-steady portion and the apparent mass contribution (as called by von Karman and Sears in Reference 5) of the aerodynamic loads* resulting from $\dot{h}_j$, $\dot{\theta}_j$ and θ_j. (The apparent masses associated with $\ddot{h}_j$ and $\ddot{\theta}_j$ are negligible compared with the corresponding blade inertial properties.) In other words, (79) and (80) are the n^{th} harmonic cosine and sine components, respectively, of the generalized force in h_i due to a lift distribution

$$2\pi\rho b \Omega r \left(\Omega r \sum_{j=1}^{\gamma} \theta_j f_{\theta_j} - \sum_{j=1}^{s} \dot{h}_j f_{h_j} + e \sum_{j=1}^{\gamma} \dot{\theta}_j f_{\theta_j}\right)$$

acting at quarter chord and another lift distribution

$$2\pi\rho b \Omega r \left(b \sum_{j=1}^{\gamma} \dot{\theta}_j f_{\theta_j}\right)$$

acting at half chord, while (81) and (82) are those in θ_i due to the same two lift distributions. (The first lift distribution is entirely quasi-steady, but half of the second one is apparent mass contribution.)

---

* Based on airfoil theory of two-dimensional thin plate and assumed Ωr to be the stream velocity.

$$\left(\omega_{h_i}^2 - n^2\Omega^2\right) M_{h_i h_i} h_{nc}^{(i)} - \Omega^2 \sum_{j=1}^{\gamma} \left(n^2 M_{h_i \theta_j} + T_{h_i \theta_j} + A_{h_i \theta_j}\right) \theta_{nc}^{(j)}$$

$$+ \sum_{j=1}^{s} \left\{ K_{h_i h_j} q_{h_j} - n\Omega^2 \left(2\zeta_{h_i h_j} + A_{h_i h_j}\right) \right\} h_{ns}^{(j)} - n\Omega^2 \sum_{j=1}^{\gamma} A_{h_i \dot{\theta}_j} \theta_{ns}^{(j)}$$

$$= \left(C_{h_i}\right)_{nc} + \left(G_{h_i}\right)_{nc}^{(-1)} \qquad \left[\left(C_{h_i}\right)_{nc} = 0 \quad \text{for} \quad n > 1.\right]$$

$$- \Omega^2 \left\{ \sum_{j=1}^{\gamma} A_{h_i \theta_j} \theta_{nc}^{(j)} + n \sum_{j=1}^{s} A_{h_i h_j} h_{ns}^{(j)} + n \sum_{j=1}^{\gamma} A_{h_i \dot{\theta}_j} \theta_{ns}^{(j)} \right\}^{(-1)} \tag{83}$$

$$- \sum_{j=1}^{s} \left\{ K_{h_i h_j} q_{h_j} - n\Omega^2 \left(2\zeta_{h_i h_j} + A_{h_i h_j}\right) \right\} h_{nc}^{(j)} + n\Omega^2 \sum_{j=1}^{\gamma} A_{h_i \dot{\theta}_j} \theta_{nc}^{(j)}$$

$$+ \left(\omega_{h_i}^2 - n^2\Omega^2\right) M_{h_i h_i} h_{ns}^{(i)} - \Omega^2 \sum_{j=1}^{\gamma} \left(n^2 M_{h_i \theta_j} + T_{h_i \theta_j} + A_{h_i \theta_j}\right) \theta_{ns}^{(j)}$$

$$= \left(C_{h_i}\right)_{ns} + \left(G_{h_i}\right)_{ns}^{(-1)} \qquad \left[\left(C_{h_i}\right)_{ns} = 0 \quad \text{for} \quad n > 1.\right]$$

$$- \Omega^2 \left\{ - n \sum_{j=1}^{s} A_{h_i h_j} h_{nc}^{(j)} - n \sum_{j=1}^{\gamma} A_{h_i \dot{\theta}_j} \theta_{nc}^{(j)} + \sum_{j=1}^{\gamma} A_{h_i \theta_j} \theta_{ns}^{(j)} \right\}^{(-1)} \tag{84}$$

$$- \Omega^2 \sum_{j=1}^{s} \left(n^2 M_{\theta_i h_j} + T_{\theta_i h_j}\right) h_{nc}^{(j)} + \left(\omega_{\theta_i}^2 - n^2\Omega^2\right) M_{\theta_i \theta_i} \theta_{nc}^{(i)} - \Omega^2 \sum_{j=1}^{\gamma} \left(\hat{T}_{\theta_i \theta_j} + A_{\theta_i \theta_j}\right) \theta_{nc}^{(j)}$$

$$- n\Omega^2 \sum_{j=1}^{s} A_{\theta_i h_j} h_{ns}^{(j)} + \sum_{j=1}^{\gamma} \left\{ \left(\omega_{\theta_i}^2 - \Omega^2\right) M_{\theta_i \theta_j} q_{\theta_j} - n\Omega^2 A_{\theta_i \dot{\theta}_j} \right\} \theta_{ns}^{(j)}$$

$$= \left(C_{\theta_i}\right)_{nc} + \left(G_{\theta_i}\right)_{nc}^{(-1)} \qquad \left[\left(C_{\theta_i}\right)_{nc} = 0 \quad \text{for} \quad n > 1.\right]$$

$$- \Omega^2 \left\{ \sum_{j=1}^{\gamma} A_{\theta_i \theta_j} \theta_{nc}^{(j)} + n \sum_{j=1}^{s} A_{\theta_i h_j} h_{ns}^{(j)} + n \sum_{j=1}^{\gamma} A_{\theta_i \dot{\theta}_j} \theta_{ns}^{(j)} \right\}^{(-1)} \tag{85}$$

$$n\Omega^2 \sum_{j=1}^{s} A_{\theta_i h_j} h_{nc}^{(j)} - \sum_{j=1}^{\gamma} \left\{ \left(\omega_{\theta_i}^2 - \Omega^2\right) M_{\theta_i \theta_j} q_{\theta_j} - n\Omega^2 A_{\theta_i \dot{\theta}_j} \right\} \theta_{nc}^{(j)}$$

$$- \Omega^2 \sum_{j=1}^{s} \left(n^2 M_{\theta_i h_j} + T_{\theta_i h_j}\right) h_{ns}^{(j)} + \left(\omega_{\theta_i}^2 - n^2\Omega^2\right) M_{\theta_i \theta_i} \theta_{ns}^{(i)} - \Omega^2 \sum \left(\hat{T}_{\theta_i \theta_j} + A_{\theta_i \theta_j}\right) \theta_{ns}^{(j)}$$

$$= \left(C_{\theta_i}\right)_{ns} + \left(G_{\theta_i}\right)_{ns}^{(-1)} \qquad \left[\left(C_{\theta_i}\right)_{ns} = 0 \quad \text{for} \quad n > 1.\right]$$

$$- \Omega^2 \left\{ - n \sum_{j=1}^{s} A_{\theta_i h_j} h_{nc}^{(j)} - n \sum_{j=1}^{\gamma} A_{\theta_i \dot{\theta}_j} \theta_{nc}^{(j)} + \sum_{j=1}^{\gamma} A_{\theta_i \theta_j} \theta_{ns}^{(j)} \right\}^{(-1)} \tag{86}$$

COMPUTER PROGRAM

Initially, the computer program was written in FORTRAN IV for the IBM 7044. In the latter stages of the project, the program was simply converted for use on the IBM 360/65; no effort was expended to optimize the program in order to take advantage of the 360/65 system capabilities. Physically, because of core storage limitations of the 7044 and for convenience in solving the equations of blade motions, the program was separated into six parts. Each part is also divided into several subroutines for further convenience in programming, checkout, and program modification. The major steps in each part of the computer program are shown in the flow chart presented in Figure 5. Parts 1 and 2 of the program are identical to those presented in Reference 1, since the representations of the blade and the wake were not altered. The principal functions of each part of the program are listed below.

Part 1

1. Reads the necessary inputs for Parts 1 and 2.
2. Computes the blade and wake coordinates.

Two tape drives are used in this part of the program. The first is used for temporary storage of the blade and wake coordinates used in computing the induced velocity coefficients, and the second is used to transfer variables and the matrix of induced velocity coefficients which are used in Part 2 of the program.

Part 2

1. Reads the necessary inputs for Parts 2 and 3.
2. Computes the initial trial circulations (represented by Γ's in Reference 1) about blade segments at chosen azimuth positions, the initial blade motions and other variables used in Parts 2 and 3.
3. Normalizes the matrix of induced velocity coefficients. (The normalized matrix is used in solving the Γ equations in Part 3.)

Three tape drives are used in this part of the program. The first tape is used to read in the variables and the matrix of induced velocity coefficients from Part 1. The second tape stores the normalized matrix of induced velocity coefficients used in solving the Γ equations in Part 3; the third tape transfers the initial trial Γ, the initial trial blade motions and other variables used in Part 3.

Part 3

1. Solves the Γ equations.
2. Solves the equations of blade motions.
3. Computes time histories of blade lift, drag and pitching moment distributions.
4. Computes the generalized aerodynamic forces.
5. Computes the time histories of the rotor aerodynamic forces and moments (due to one blade) used in Part 5.

Four tape drives are used in Part 3 of the program. The first is used to read in the initial trial Γ, the initial trial blade motions and other variables used in Parts 3, 4, and 5. The second tape retains the normalized matrix of induced velocity coefficients used in solving the equations. The third tape, which has been generated in Part 6 of the program, is used to retain all the inverses of all the matrices used in solving the blade equations of motions for each harmonic order. The fourth tape is used to store the time histories of the variables to be harmonically analyzed and other variables used in Part 4 of the program. The time histories of the rotor aerodynamic forces and moments used in Part 5 of the program are machine-punched on data cards.

Part 4

Harmonically analyzes the time histories of the variables generated in Part 3 of the program.

One tape drive is used in Part 4; namely, that which contains the time histories of the variables to be harmonically analyzed.

Part 5

1. Computes the harmonic components of the rotor aerodynamic forces and moments that appear in the trim equations.
2. Computes the partial derivatives of the average rotor forces and moments with respect to the trim constants. (See(36).)
3. Computes the forces and moments on the fuselage.
4. Computes a new set of trim variables.

No tape drives are used in this part of the program. The time histories of the rotor aerodynamic forces and moments are inputs from data cards which have been machine-punched in Part 3 of the program. The integrals used in Part 5 which are dependent solely on the blade geometric and inertial properties and mode shapes are computed and machine-punched in Part 6 of the program and, thus, inputed on data cards in Part 5.

Part 6

1. Computes the coefficients of the equations of blade motions, (83) through (86), to form a matrix for each harmonic order.
2. Computes the inverses of the matrices which are used in solving the equations of blade motions in Part 3.
3. Computes the integrals which are dependent on the blades' geometric and inertial properties and mode shapes to be used in Parts 5 and 3.

One tape drive is used in this part of the program; namely, that which retains the inverses of the matrices and the integrals appearing in C_{q_i}.

Parts 1 and 6 of the program are run initially, and the binary output tapes from each part are saved. Parts 2 and 3 are then run sequentially a total of five times to provide the input for computing the rotor forces and moments and for computing the partial derivatives of the rotor forces and moments with respect to each of the trim constants. Part 5 is then run to compute a new set of trim constants. If the difference between the initial set of trim constants and the new set is not within prescribed limits, Parts 2 and 3 are then rerun with the new set of trim constants to provide the input for recomputing the rotor forces and moments. Part 5 is then rerun with this new input to compute a third set of trim variables The process is repeated until the trim variables converge within prescribed limits. When the process has converged, the output tape from Part 3 is used in Part 4 to harmonically analyze the last-obtained results.

It has been assumed in the above processes that the partial derivatives of the rotor forces and moments with respect to the trim constants are nearly constant within the range under consideration. If this were not true, then Part 3 would need to be rerun to obtain a new set of partial derivatives for each new set of trim constants.

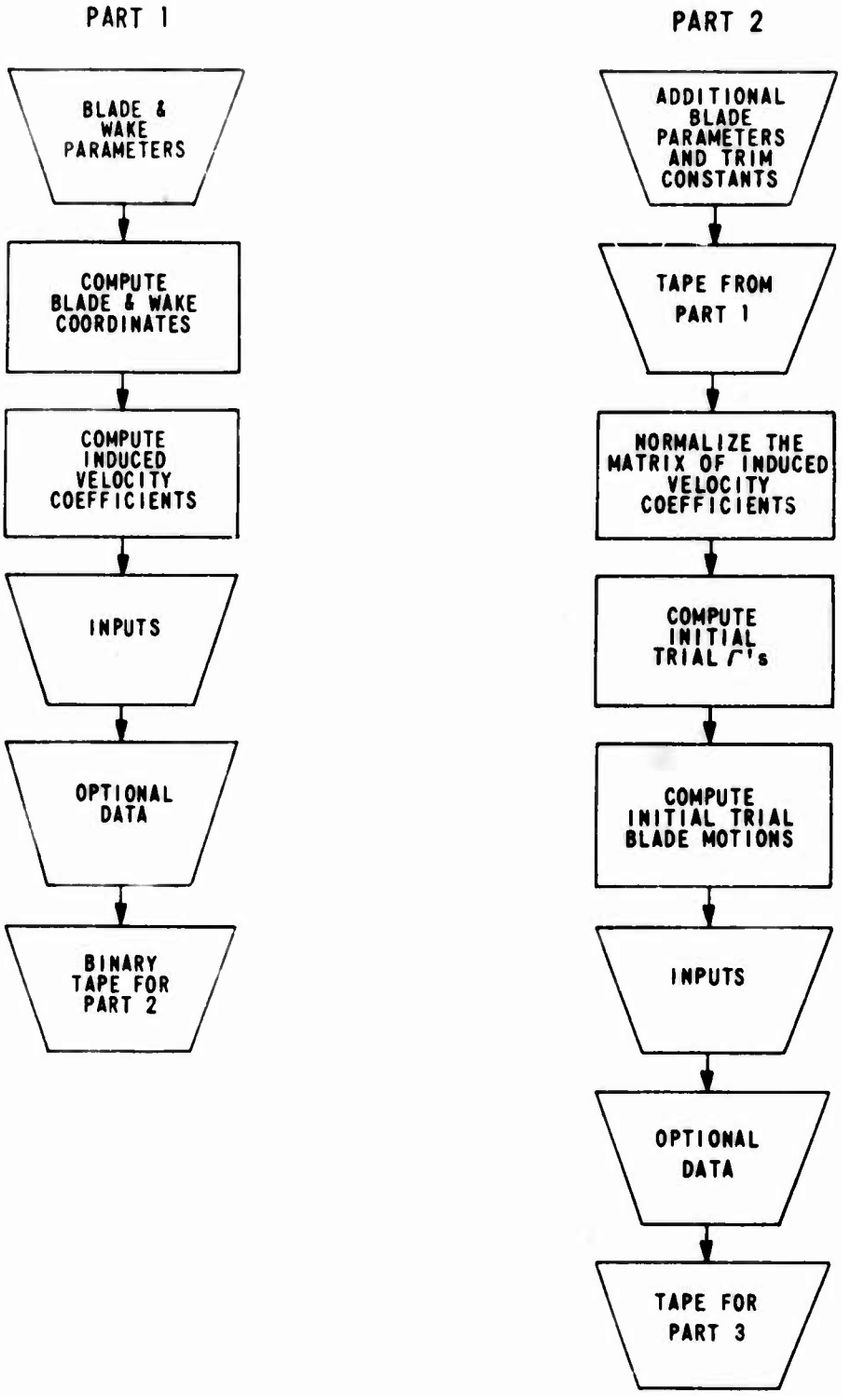

Figure 5. COMPUTER PROGRAM FLOW CHART.

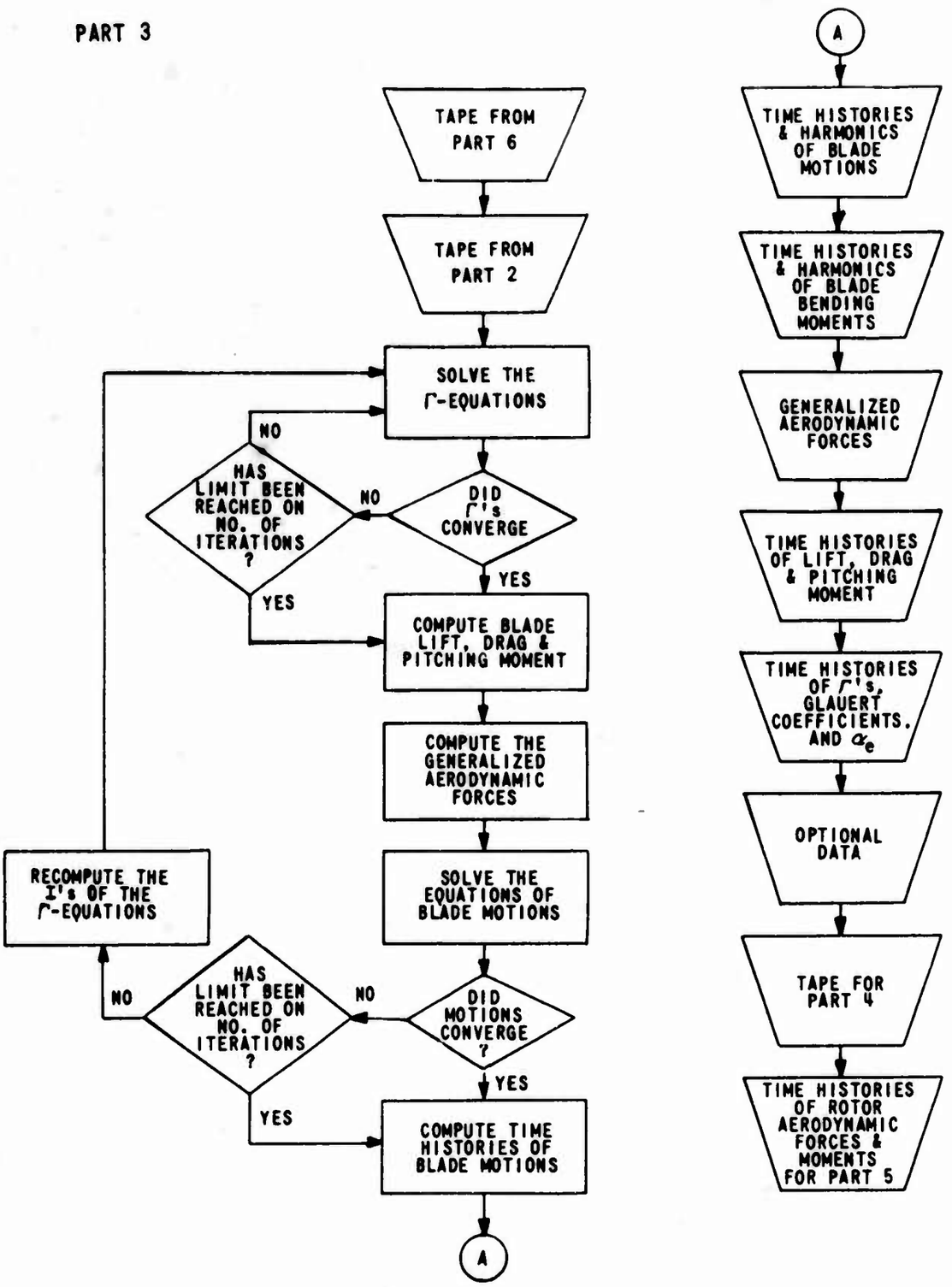

Figure 5 (CONTD). COMPUTER PROGRAM FLOW CHART.

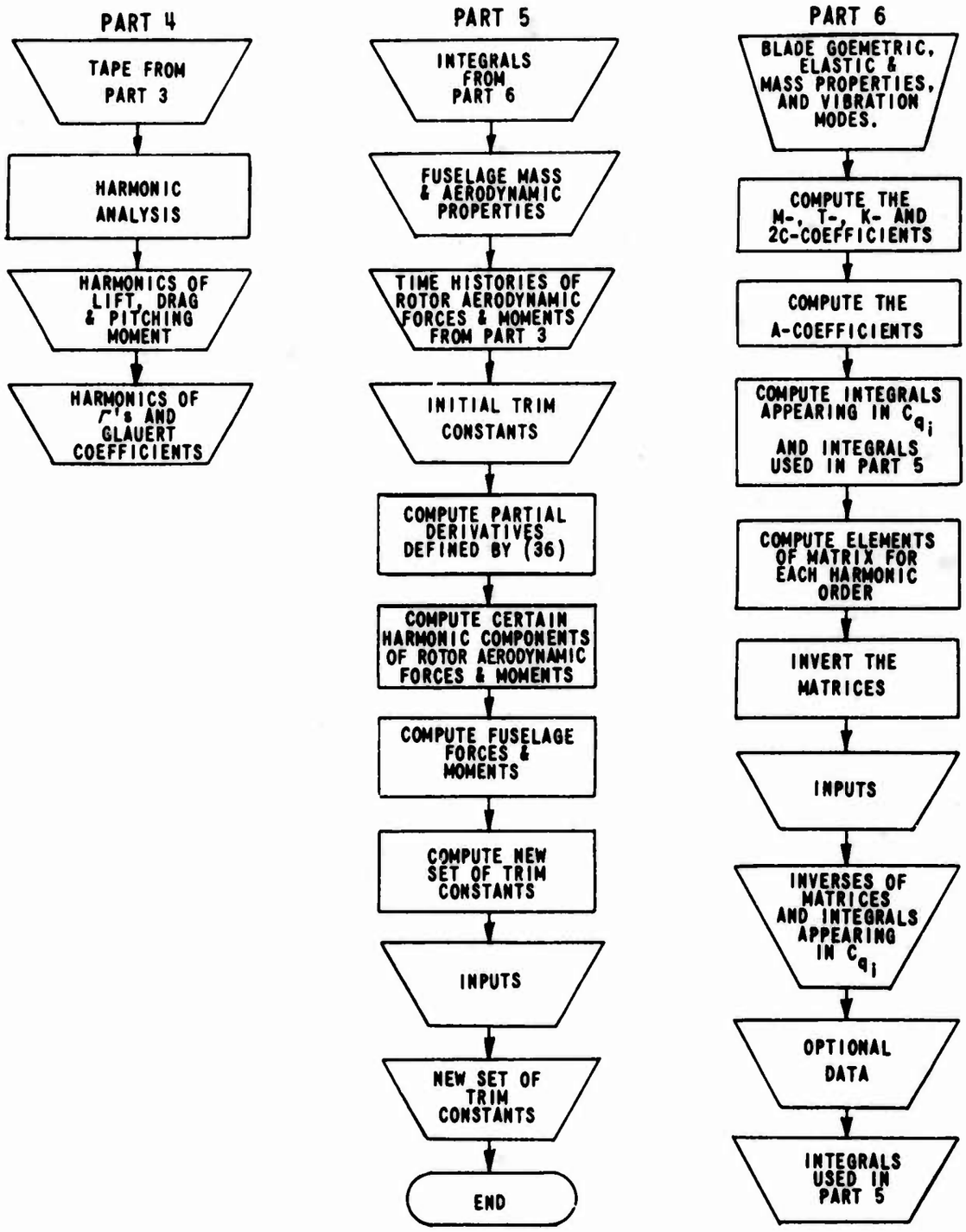

Figure 5 (CONTD). COMPUTER PROGRAM FLOW CHART.

COMPUTED RESULTS AND COMPARISONS WITH MEASURED RESULTS

The computational procedure was used to analyze the same four flight conditions that have been analyzed in Reference 1. They are for the teetering UH-1A rotor at advance ratios 0.26 and 0.08 (identified as Flights No. 67 and No. 65, respectively, in Reference 7) and for the H-34 rotor, which consists of four fully articulated blades, at advance ratios 0.29 (identified as Flight No. 18 in Reference 8) and 0.18 (for which measured data are obtained similarly to those in Reference 8 and are given in Table III of Reference 13). The profile drag coefficients, which are expressed as functions of angle of attack and Mach number in the computing program, are based on data from Reference 9 for the NACA 0015 airfoil section used in the UH-1A rotor blades and on data from Reference 10 for the modified NACA 0012 airfoil section used in the H-34 rotor blades. The fuselage aerodynamic characteristics are obtained from Reference 11 for UH-1A and Reference 12 for H-34.

The azimuthal variations (or the time histories with the steady components at each specified radial station removed) of the resulting blade aerodynamic loadings (lift, pitching moment, and drag, per unit span) and blade bending moments are plotted for a number of radial stations.* The bending moments are obtained by summing the contributions from the responses of all the bending modes used. They automatically include the influence of inertia loadings. Available measured data (lift distributions and flatwise bending moments) are shown in the appropriate plots for convenient comparisons in Figures 6 through 31. For the lift distribution or flatwise bending moment, the radial variation of the steady component (or time average) is presented together with the radial variations of the cosine and sine components of the harmonics in blade rotational speed.

* Positive flatwise and chordwise bending moments tend to compress the upper surface and leading edges, respectively.

For each flight condition, the same wake model and the same values of the parameters that specify the wake model used in Reference 1 are used here. Five flapwise modes (based on an unwisted blade with zero blade angle) are used in Reference 1, while five or six bending modes (in which both flapwise and chordwise deflections are admitted and twist effects are included) and two torsional modes are used here.* The computed lift and flapwise bending moment results obtained here are not significantly closer to the measured results than those obtained in Reference 1. Therefore, the establishment of both a better wake model and further refinements in the prediction of blade motions may be necessary for the configurations studied. However, the present results do demonstrate that the computational procedure developed by the present effort is suitable for taking additional blade motions into account and can be used to yield trim constants.

Reasonable agreement between measured and computed lift distributions is obtained (Figures 6, 7, 13, 14, 19, 20, 26, 27), but the flatwise bending moment agreement is less satisfactory (Figures 8, 9, 15, 16, 21, 22, 28, 29). The disagreement in the flatwise bending moment values may be the result of an accuracy problem. The moments are relatively small, and they represent small differences of large numbers (lift moments and inertial force moments) for the configurations studied. In all cases, both the measured and computed flatwise bending moments on any blade section have magnitudes less than the moment acting on some inboard blade section due to the blade weight alone, while the lift distribution over the outboard portion of the blade goes as high as 20 to 30 times the blade weight distribution. Thus, small differences between the measured and computed lift distributions can result in large percentage differences in flatwise bending moments. Similarly, small errors between computed and actual natural frequencies lead to large errors in inertial forces at forcing frequencies near the resonance frequencies.

---

* Five bending modes are used in the UH-1A cases and six in the H-34 cases, with the natural frequency of the highest order mode slightly over ten times the rotor shaft rotational speed. (The present computer program can handle a total of ten bending and torsional modes.)

Calculated drag distributions and pitching moment distributions are shown on Figures 10, 11, 17, 18, 23, 24, 30, and 31.

Chordwise bending moments are shown on Figures 12 (UH-1A) and 25 (H-34). The chordwise bending moments as computed by summing the contributions from the responses of all the bending modes used do not agree with estimates based on computed blade drag loading. Superposition of natural modes is ineffective for the cases considered because the blade chordwise elastic deflection is small and is almost all due to a single bending mode which is dominated by chordwise deflection.* Thus, in effect, the chordwise deflection distribution is approximated by only one curve which can have a curvature (or bending moment) distribution quite different from the actual one. That is, unless the loading has the same shape as the inertial loading in that single natural mode, the corresponding moment distributions will not have the same shape.

Measured chordwise bending moments are available at four stations for the H-34 case. Both the measured and computed chordwise bending moments for the H-34 rotor at an advance ratio of 0.29 are shown in Figure 25. The poor agreement is attributed to the factors given above, although it must be admitted that more cases should be investigated before a strong conclusion can be formed. By considering that the moment about the lead-lag hinge due to chordwise centrifugal loading cancels that due to the computed drag, the resulting steady inplane bending moment distributions have been computed by hand. They are shown in the table on page 43, together with the measured and computed steady chordwise bending moments, all in inch-pounds. The measured value of -13921 at $r/R = 0.825$ corresponds to a uniform drag loading on the blade outboard of that station of about 97 pounds per foot, which can hardly be considered reasonable. The disagreement between the two sets of computed results is disturbing (this would be true even if no measured

*All the other natural bending modes are dominated by the flatwise motion.

TABLE
STEADY INPLANE BENDING MOMENTS, H-34, $\mu = 0.29$

r/R	STEADY INPLANE BENDING MOMENT COMPUTED FROM BLADE LOADING	MEASURED STEADY CHORDWISE BENDING MOMENT	COMPUTED STEADY CHORDWISE BENDING MOMENT
0.150	-2670	2379	390
0.275	-4530	--	291
0.375	-4800	3776	190
0.575	-3293	-4418	-5
0.825	-820	-13921	15

values were available). In effect, the calculated results suggest that it would be advisable to calculate steady deflections (and moments) from the steady loads and to use the modal description to account for the time varying deflections (and moments).

The calculated and measured trim data are given below for each flight case considered. It should be recalled that the gross weight, c.g. position, fuselage aerodynamic forces (lift, drag, pitching moment), rotor rotational speed, and flight velocity are input data. Direct comparison of the angle components (α, θ_i , β_i) calculated with those measured should be made with caution for several reasons. First, aerodynamic effects usually depend on a combination of the components; e.g., location of the "control plane". Second, the accuracy of the experimental data has not been specified. Third, the induced angles of attack were not measured and they can have magnitudes comparable to the magnitudes of some of the control angles. Fourth, the structural deformation effects have not been explicitly shown, and these can be important.

UH-1A at $\mu = 0.26$

The computed trim constants in degrees are listed below (with the corresponding measured values, obtained from Reference 7, shown in parentheses):

α_s =	5.35 deg	(6.50, measured)
$\bar{\theta}_o$ =	19.03 deg	(19.20, measured)
$\bar{\theta}_{1c}$ =	1.10 deg	(2.86, measured)
$\bar{\theta}_{1s}$ =	-6.47 deg	(-7.34, measured)

The computed average rotor forces are

$$\text{thrust} = \frac{n_B}{2}\bar{Z} = 6,610 \text{ pounds}$$

$$\text{longitudinal force} = \frac{n_B}{2}\bar{X} = -535 \text{ pounds}$$

$$\text{side force} = \frac{n_B}{2}\bar{Y} = -271 \text{ pounds}$$

$$\text{torque} = \frac{n_b}{2}\bar{Q} = 7,250 \text{ foot-pounds}$$

$$\text{pitching moment} = \frac{n_B}{2}\bar{M} = 606 \text{ foot-pounds}$$

In the expression of steady plus cyclic blade flapping responses,

$$\beta_F = \beta_o + \beta_{1c}\cos\psi + \beta_{1s}\sin\psi$$

The results, all given in degrees, are

β =	0 deg	(-0.07, measured)
β_{1c} =	0.24 deg	(-1.10, measured)
β_{1s} =	-0.23 deg	(2.39, measured)

UH-1A at $\mu = 0.08$

Using the same notations and units as in the previous case, the results for this case are

α_s	=	5.03 deg	(4.50, measured)
$\bar{\theta}_o$	=	17.57 deg	(14.97, measured)
$\bar{\theta}_{1c}$	=	0.81 deg	(1.49, measured)
$\bar{\theta}_{1s}$	=	-2.56 deg	(-1.73, measured)

thrust	=	6,620 pounds
longitudinal force	=	-396 pounds
side force	=	-203 pounds
torque	=	5,420 foot-pounds
pitching moment	=	358 foot-pounds

β_o	=	0 deg	(0.16, measured)
β_{1c}	=	0.83 deg	(-2.07, measured)
β_{1s}	=	-1.53 deg	(-0.33, measured)

H-34 at $\mu = 0.29$

The following results are obtained for the present case:

α_s	=	5.29 deg	(5.40, measured)
$\bar{\theta}_o$	=	16.04 deg	(17.35, measured)
$\bar{\theta}_{1c}$	=	2.24 deg	(2.61, measured)
$\bar{\theta}_{1s}$	=	-6.37 deg	(-7.82, measured)

thrust	=	11,630 pounds
longitudinal force	=	46 pounds
side force	=	-721 pounds
torque	=	23,780 foot-pounds
pitching moment	=	372 foot-pounds

β_o	=	3.82 deg	(3.71, measured)
β_{1c}	=	-0.01 deg	(-0.02, measured)
β_{1s}	=	0.58 deg	(-0.24, measured)
τ_o	=	8.16 deg	(9.15, measured)
τ_{1c}	=	0.16 deg	(-0.31, measured)
τ_{1s}	=	0.10 deg	(0.14, measured)

The last three items, all in degrees, are the quantities as defined in the expression of steady plus cyclic blade lagging responses;

$$\beta_L = \tau_o + \tau_{1c} \cos\psi + \tau_{1s} \sin\psi$$

H-34 at $\mu = 0.18$

α_s	=	2.37 deg	(2.50, measured)
$\bar{\theta}_o$	=	13.12 deg	(13.69, measured)
$\bar{\theta}_{1c}$	=	3.05 deg	(1.19, measured)
$\bar{\theta}_{1s}$	=	-3.25 deg	(-4.70, measured)

thrust	=	11,820 pounds
longitudinal force	=	81 pounds
side force	=	-444 pounds
torque	=	14,640 foot-pounds
pitching moment	=	646 foot-pounds

β_o	=	3.86 deg	(3.93, measured)
β_{1c}	=	-0.07 deg	(0.61, measured)
β_{1s}	=	0.55 deg	(-0.52, measured)
τ_o	=	5.01 deg	(5.99, measured)
τ_{1c}	=	0.00 deg	(-0.13, measured)
τ_{1s}	=	0.11 deg	(0.04, measured)

CONCLUSIONS AND RECOMMENDATIONS

A computational procedure has been developed that predicts rotor-blade aerodynamic loadings, bending moments, and realistic blade motions, as well as trim constants. The scope of the blade motion analysis of Reference 1 was extended by incorporation of lead-lag and edgewise bending and torsional degrees of freedom. Although these additional blade motion degrees of freedom have been included, the computed lift and flapwise bending moment distributions for the UH-1A and CH-34 rotors obtained here are not significantly closer to the measured results than those obtained in Reference 1. Therefore, it appears that, at least for these configurations, further improvement in the correlations will probably require the establishment of a better wake model and an even more complete representation of the blade motions.

In both Reference 1 and the present work, a fixed skewed helix was assumed for the location of the vorticity in the wake. It appears that a realistic wake model is needed and, to this end, both theoretical and experimental studies of the disposition of vortical elements in rotor wakes are recommended. An experimental program alone probably will not suffice since quantitative data are required which can be extended to any desired rotor configuration. Current experimental techniques are susceptible to errors which are not adequately predictable. For instance, the presence of boundaries (such as wind tunnel walls) must be accounted for in the interpretation of experimental data. Direct application of the wake positions measured on one configuration might introduce serious errors. A concommitant theoretical effort is recommended, therefore, to enable evaluation of experimental techniques and to develop a means of theoretically predicting the wake location for any specified rotor system.

Further improvement of the correlations, particularly in the bending moments, might necessitate a better representation of the blade motions. Configurations such as the UH-1A and CH-34 rotors are designed to maintain low bending moments of the blades. Consequently, small errors in predicting the blade motions and the resultant lift can produce

relatively large errors in the computed bending moments, good prediction of the bending moments might depend, therefore, on a precise description of the inertial and elastic characteristics of the blade as well as the definition of the wake.

Finally, it is recommended that, if this computer program is to see practical utilization it should be revised to make efficient use of the capabilities of the IBM 360/65 on which it is now being run. This computer program was written initially in FORTRAN IV for the 7044. Later in the project, the program was simply converted to the IBM 360/65. There is no effort to optimize the program to the new equipment.

In summary, the following further efforts are recommended: (a) investigate means for improving the wake model, (b) determine the relative advantages of alternative representations of blade motion equations, and (c) refine the computer program in order to take advantage of the IBM 360/65 system capabilities.

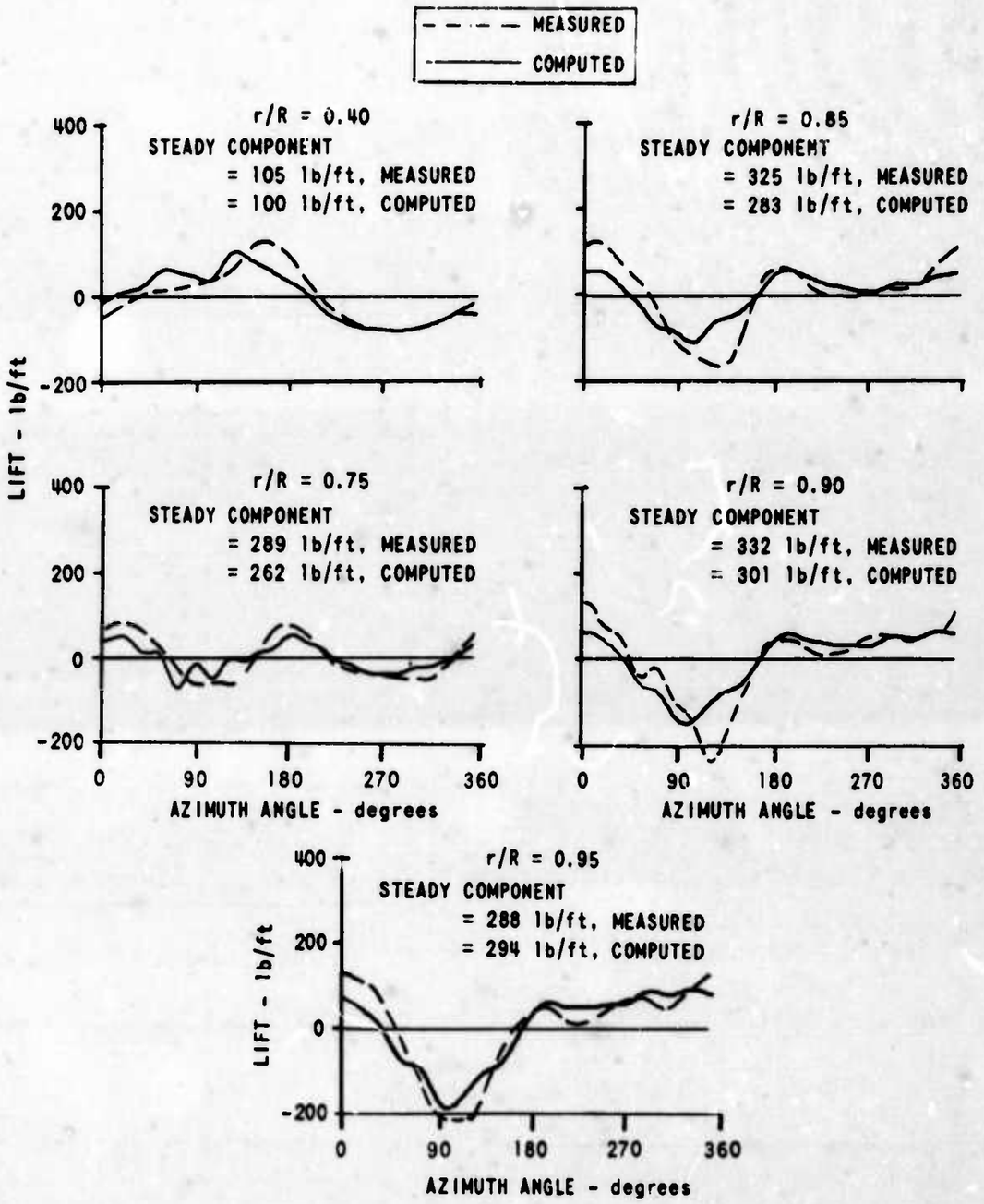

Figure 6. MEASURED AND COMPUTED AZIMUTHAL VARIATIONS OF BLADE LIFT DISTRIBUTION; UH-1A AT $\mu = 0.26$.

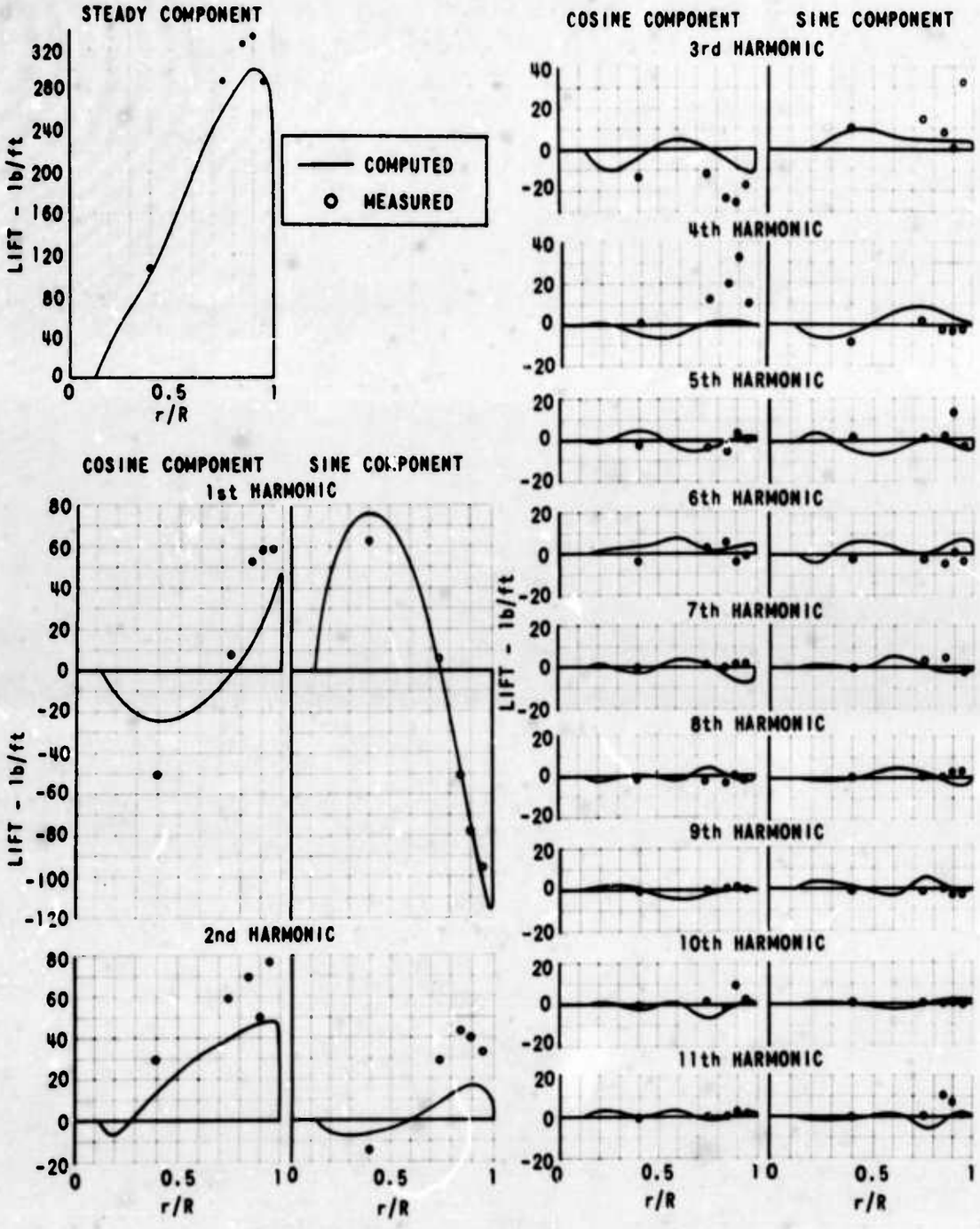

Figure 7. MEASURED AND COMPUTED HARMONICS OF BLADE LIFT DISTRIBUTION; UH-1A AT μ = 0.26.

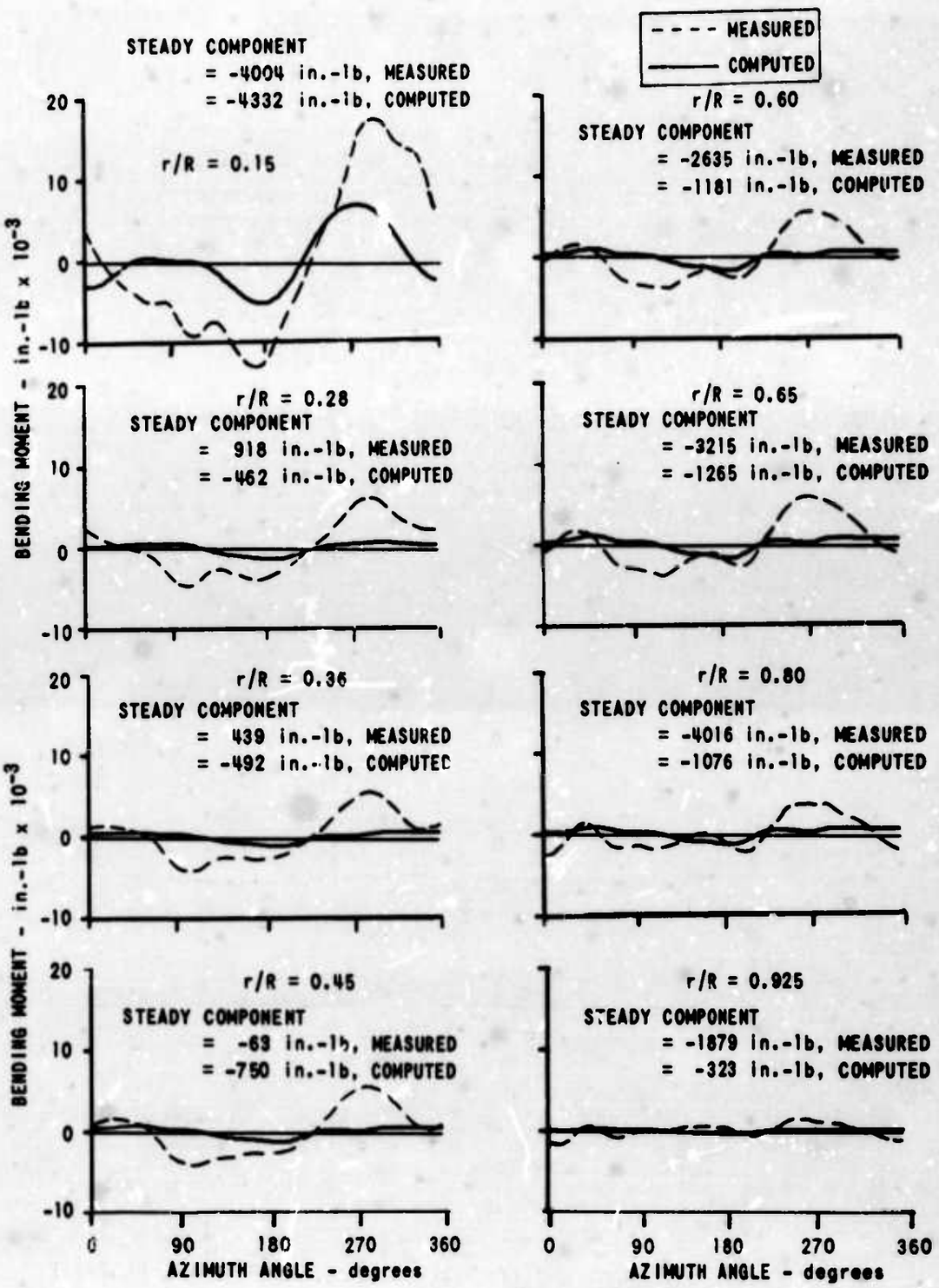

Figure 8. MEASURED AND COMPUTED AZIMUTHAL VARIATIONS OF BLADE FLATWISE BENDING MOMENTS; UH-1A AT $\mu = 0.26$.

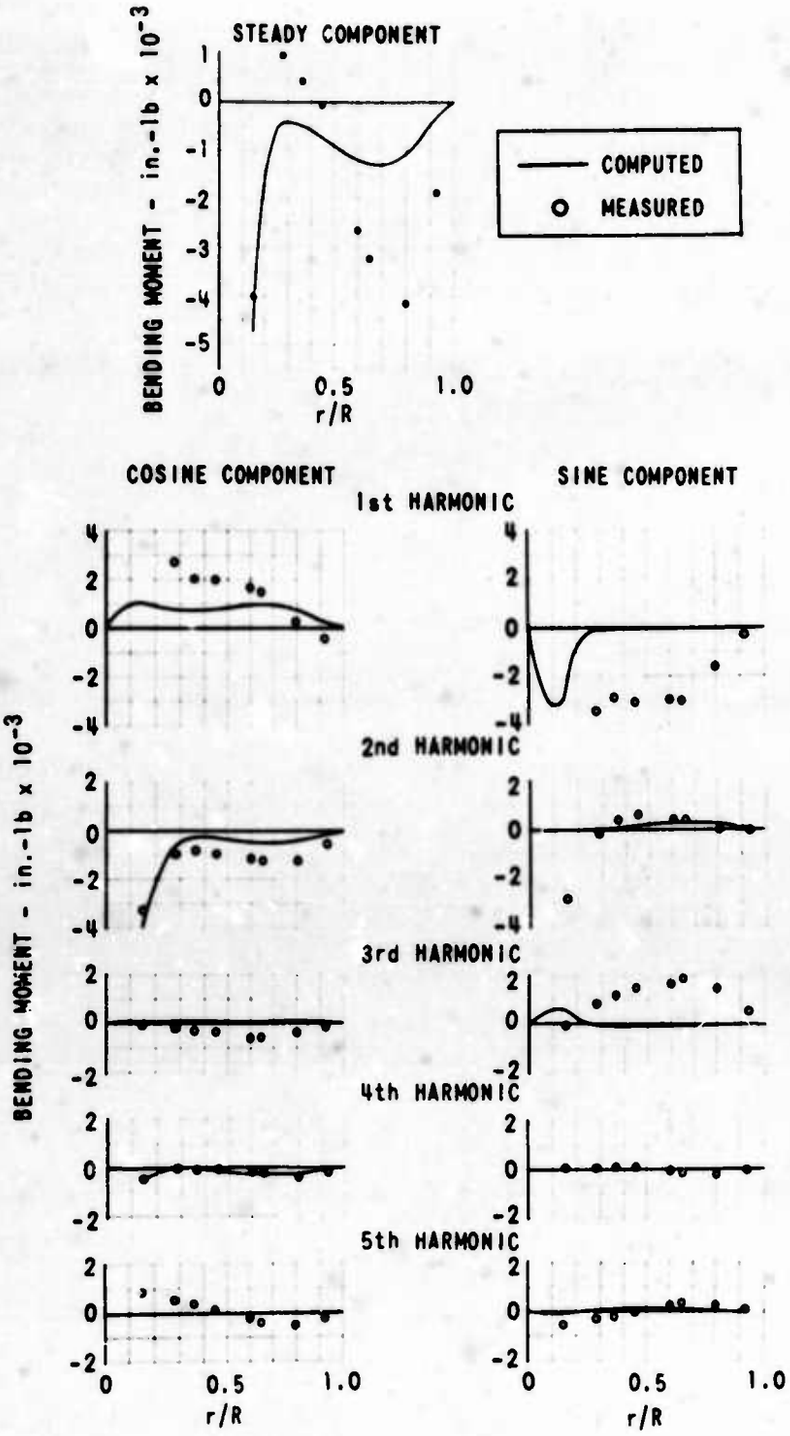

Figure 9. MEASURED AND COMPUTED HARMONICS OF BLADE FLATWISE BENDING MOMENT; UH-1A AT μ = 0.26.

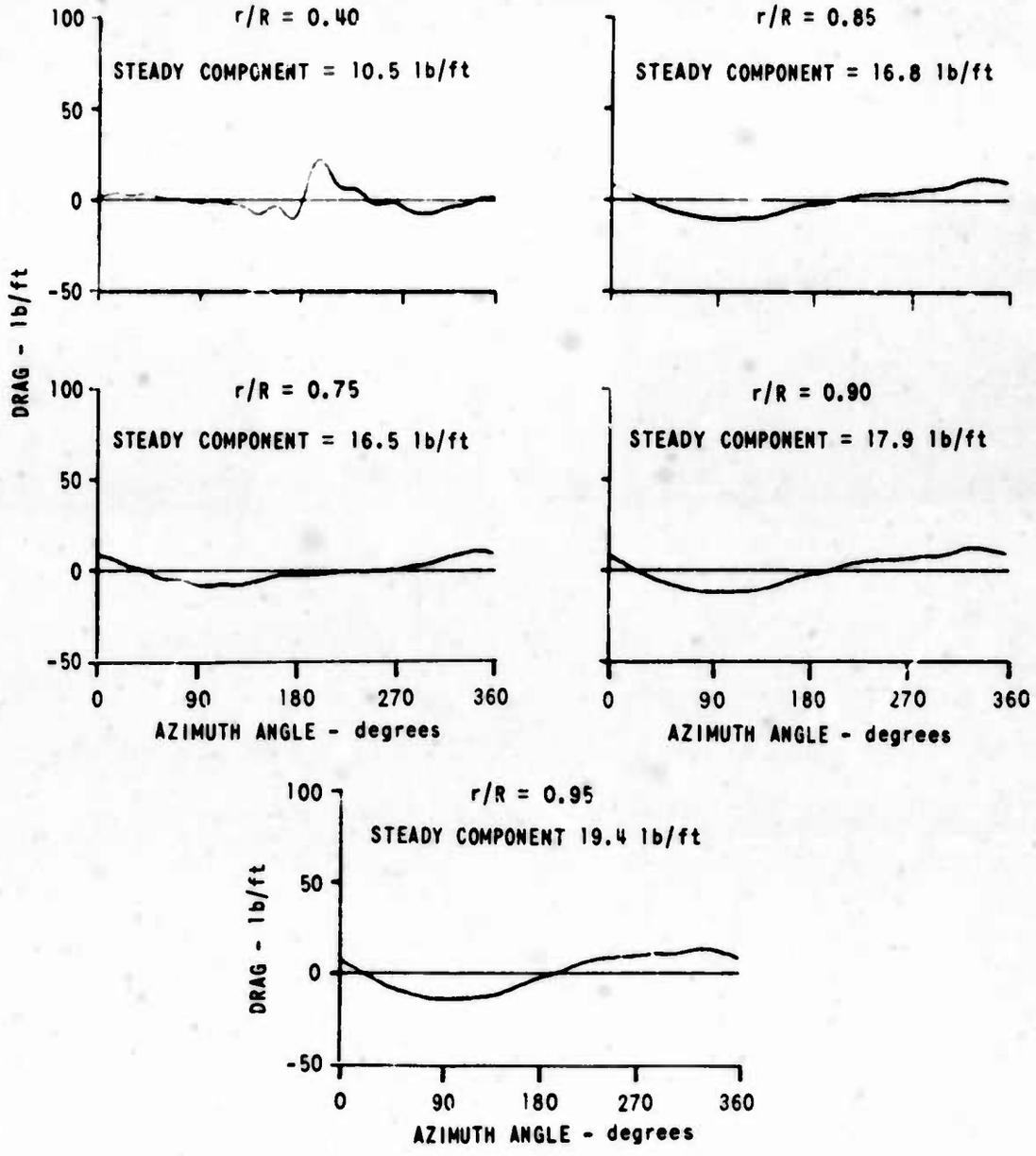

Figure 10. COMPUTED AZIMUTHAL VARIATIONS OF BLADE DRAG DISTRIBUTION; UH-1A AT μ = 0.26.

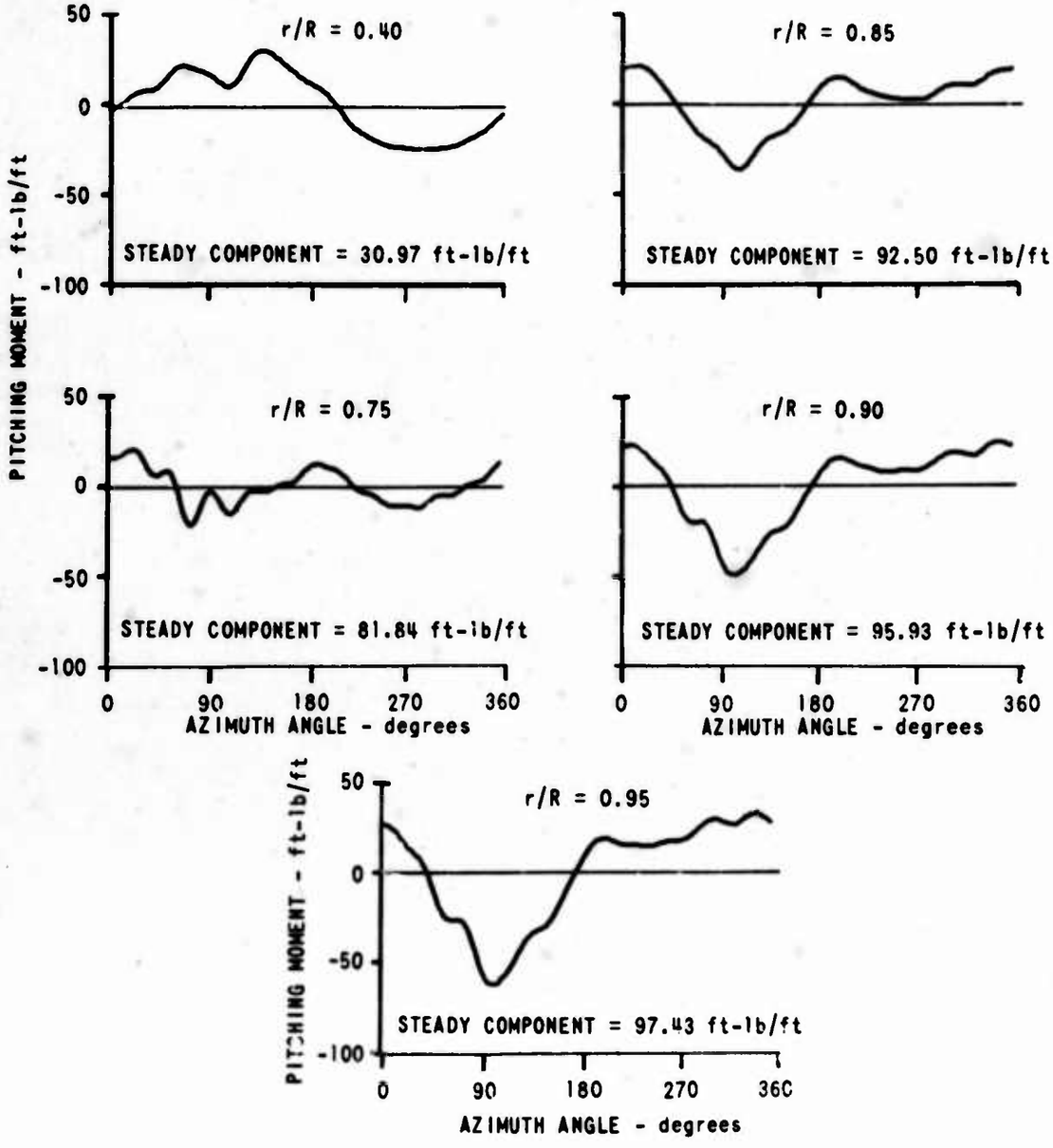

Figure 11. COMPUTED AZIMUTHAL VARIATIONS OF BLADE PITCHING MOMENT (ABOUT MIDCHORD) DISTRIBUTION; UH-1A AT μ = 0.26.

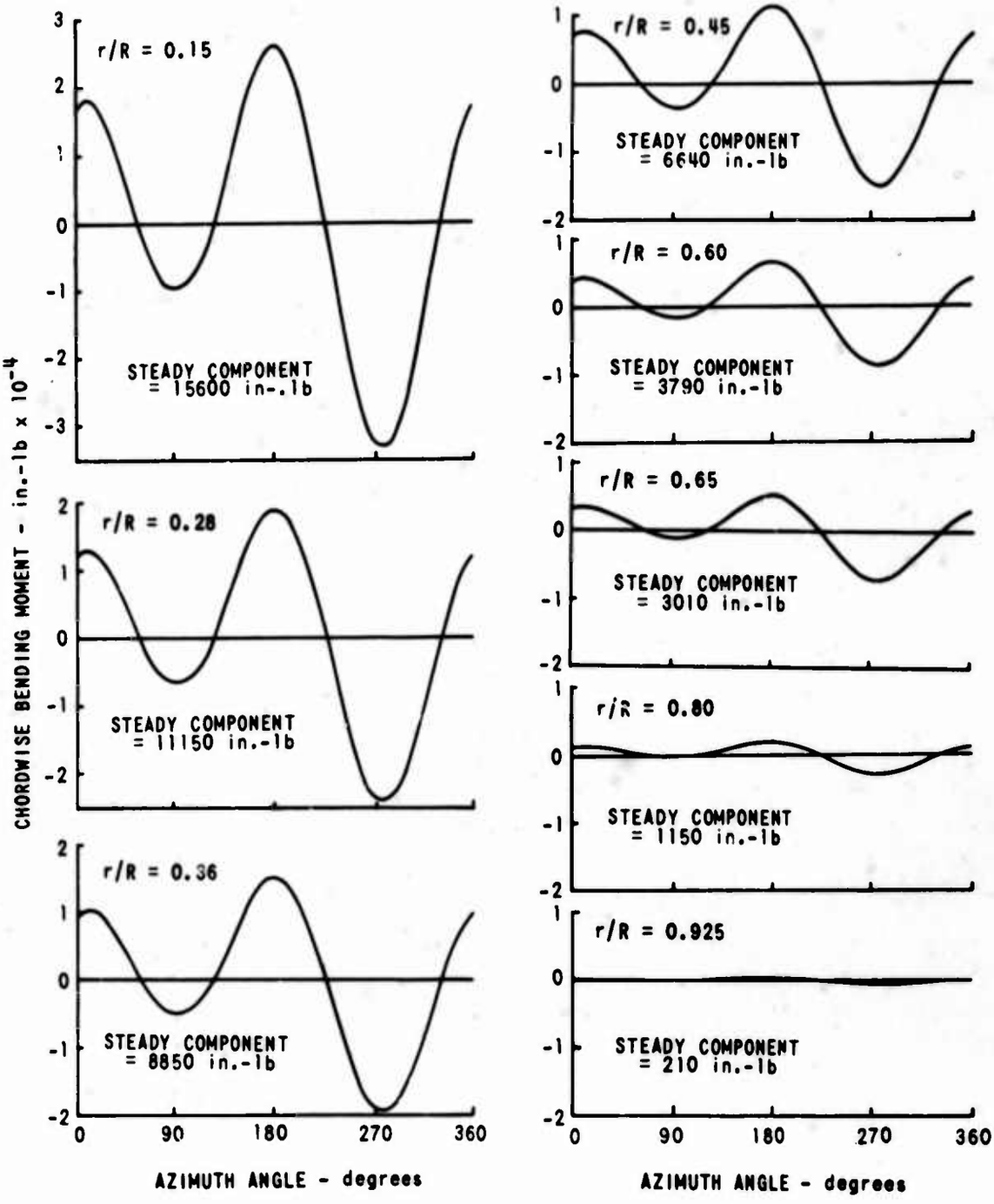

Figure 12. COMPUTED AZIMUTHAL VARIATIONS OF BLADE CHORDWISE BENDING MOMENTS; UH-1A AT μ = 0.26.

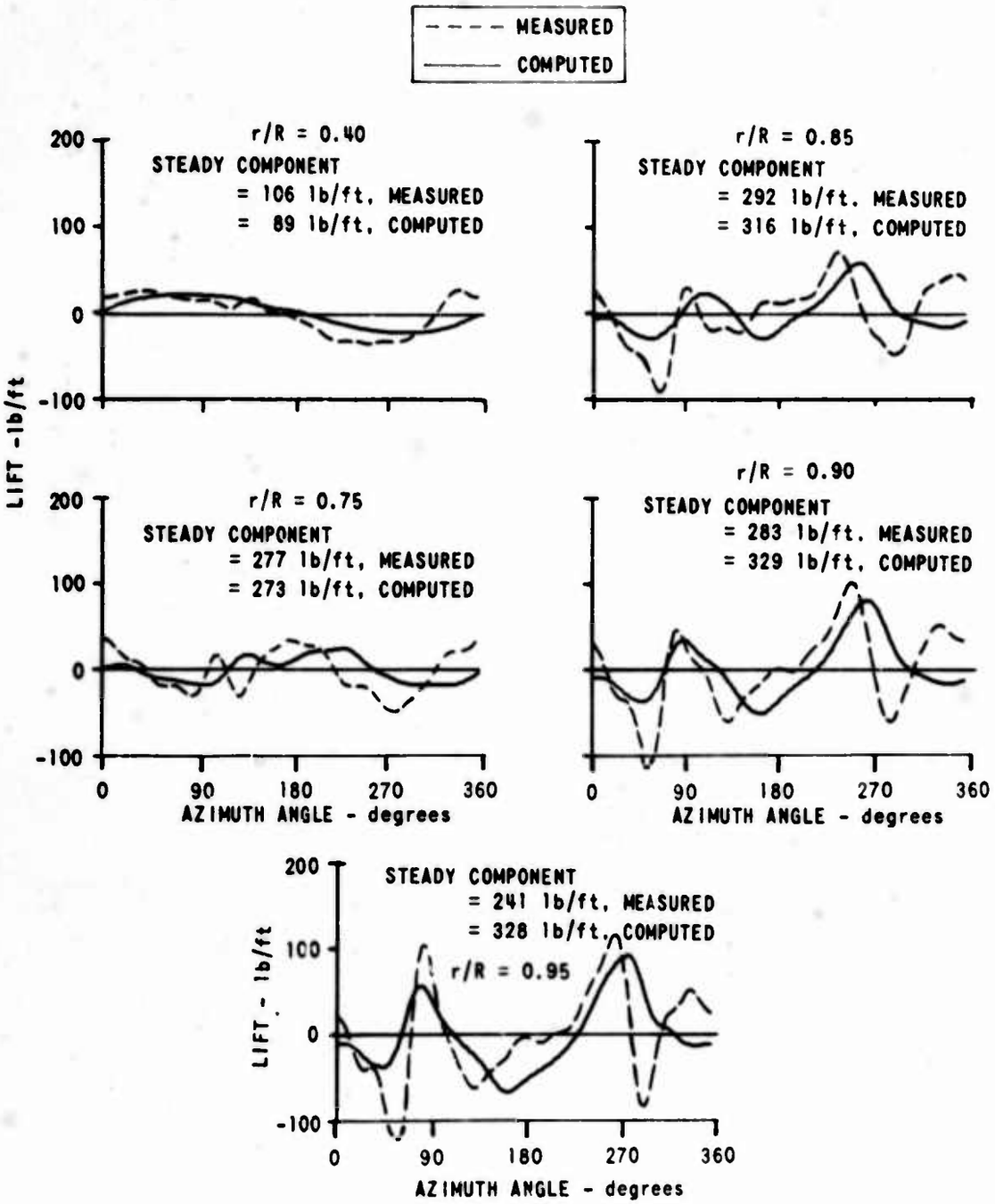

Figure 13. MEASURED AND COMPUTED AZIMUTHAL VARIATIONS OF BLADE LIFT DISTRIBUTION; UH-1A AT μ = 0.08.

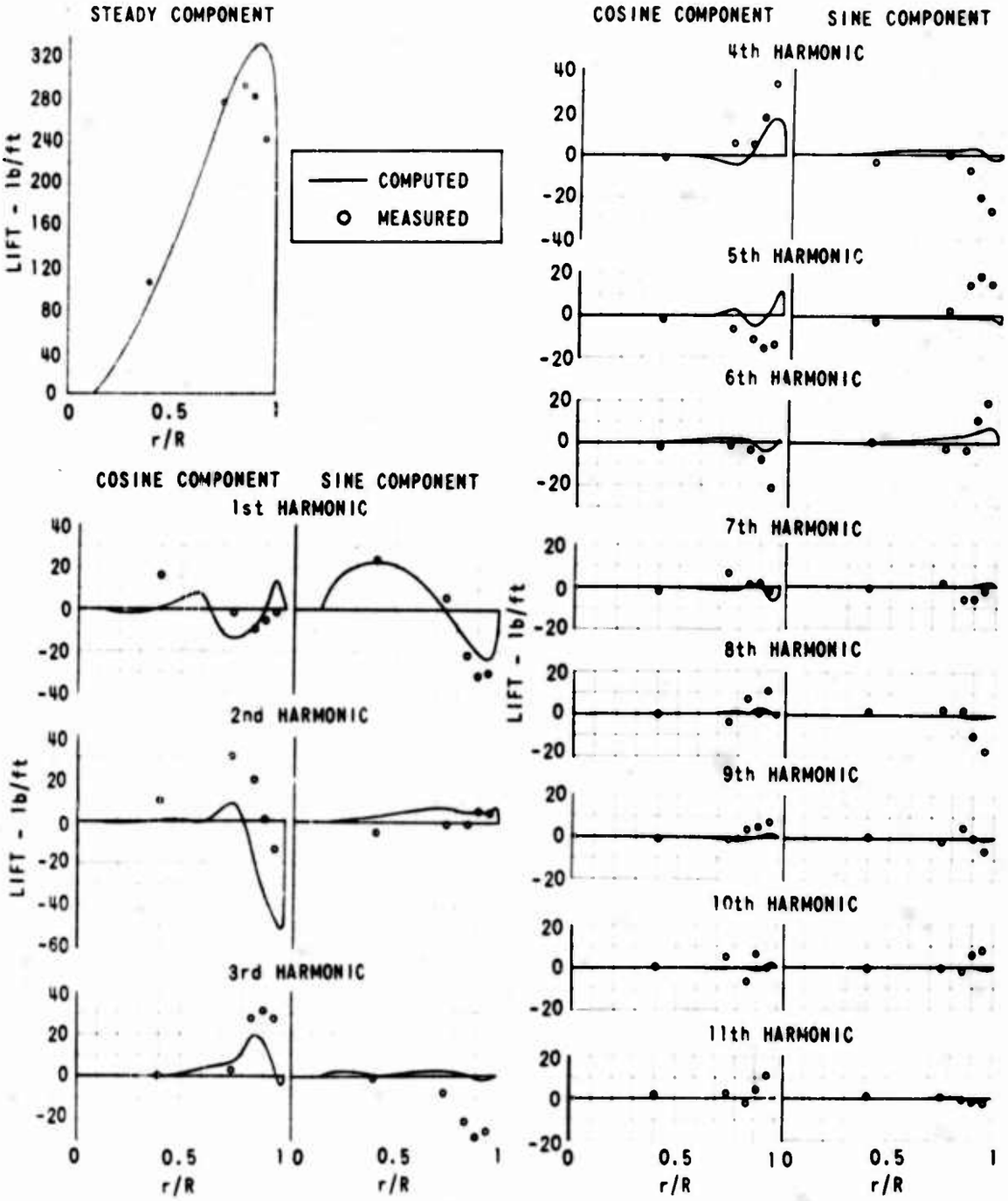

Figure 14. MEASURED AND COMPUTED HARMONICS OF BLADE LIFT DISTRIBUTION; UH-1A AT μ = 0.08.

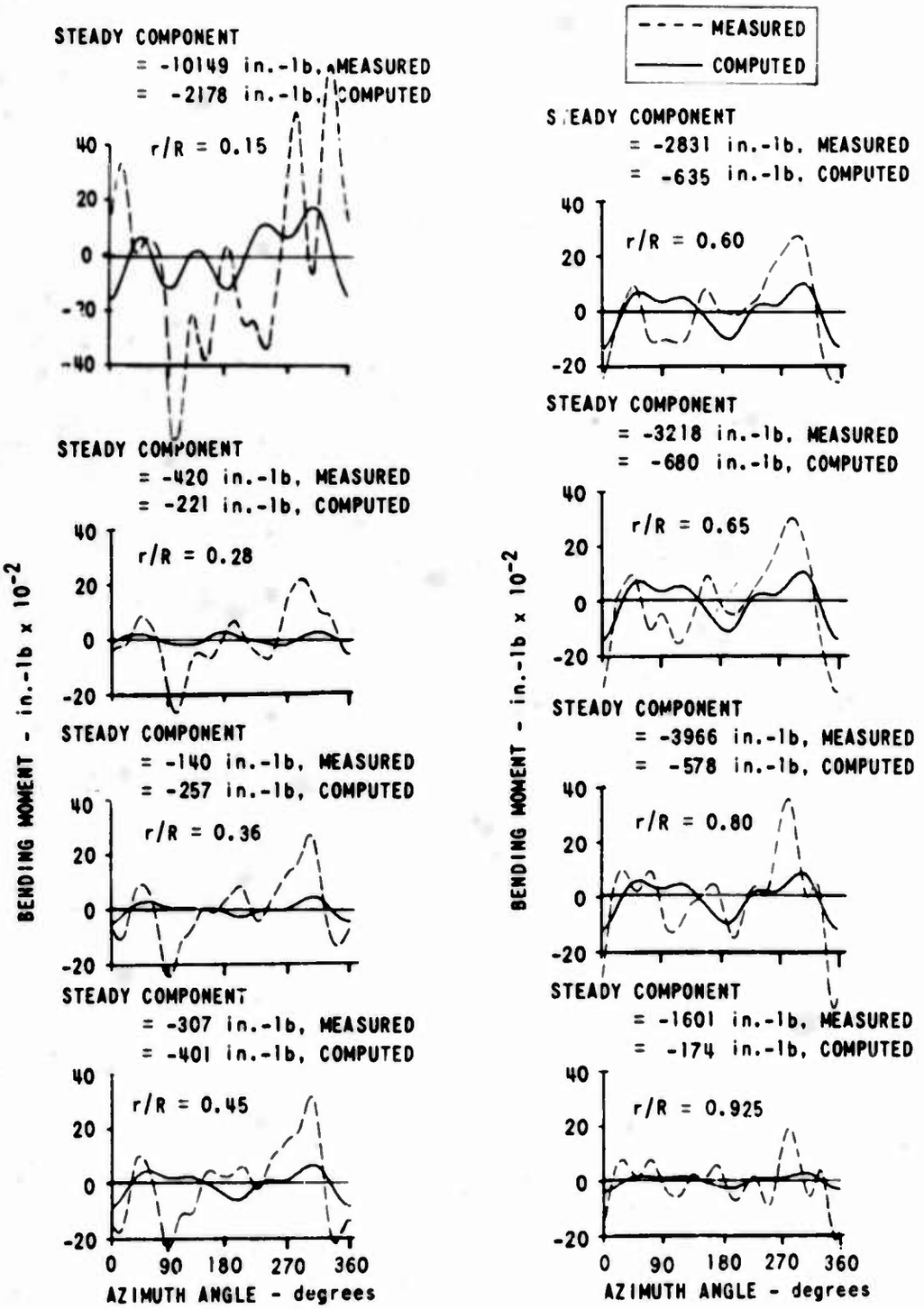

Figure 15. MEASURED AND COMPUTED AZIMUTHAL VARIATIONS OF BLADE FLATWISE BENDING MOMENTS: UH-1A AT μ = 0.08.

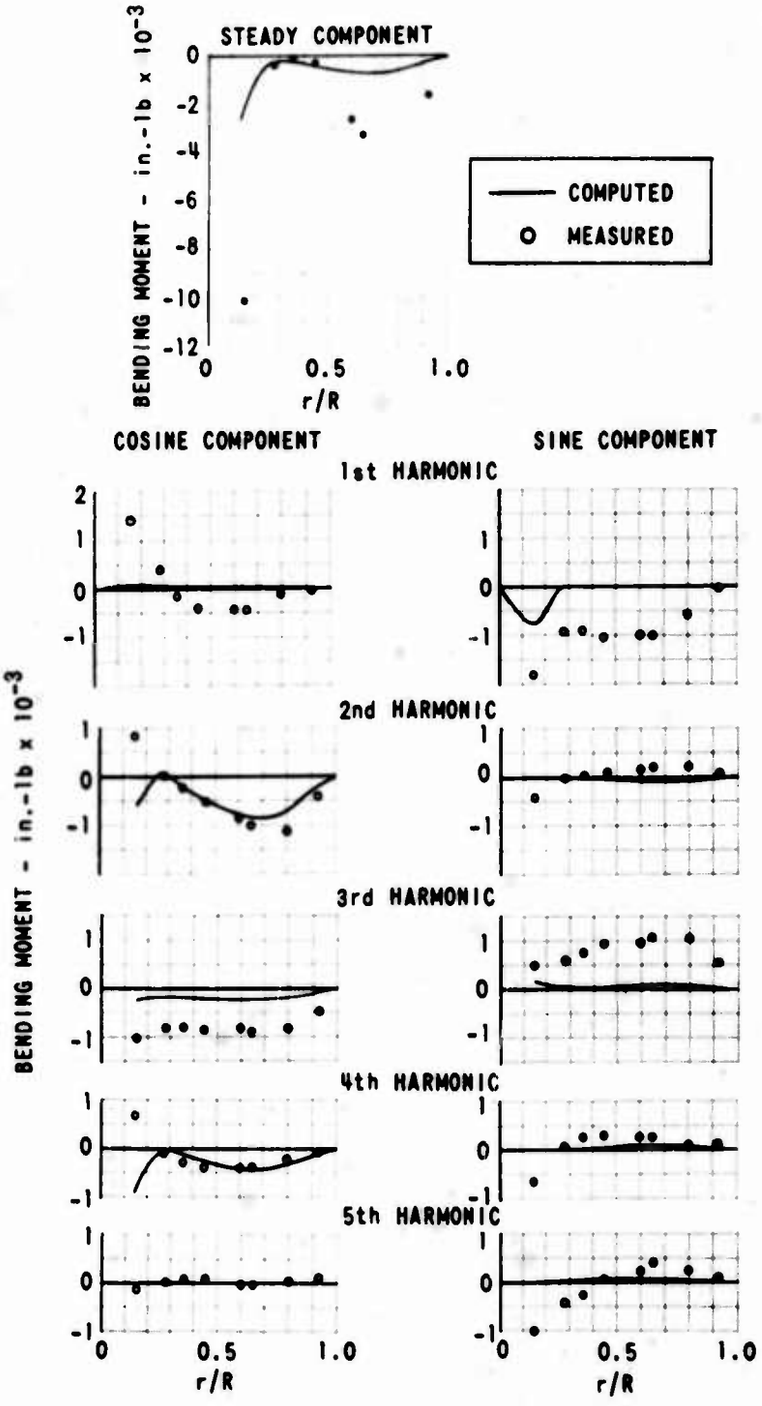

Figure 16. MEASURED AND COMPUTED HARMONICS OF BLADE FLATWISE BENDING MOMENT; UH-1A AT μ = 0.08.

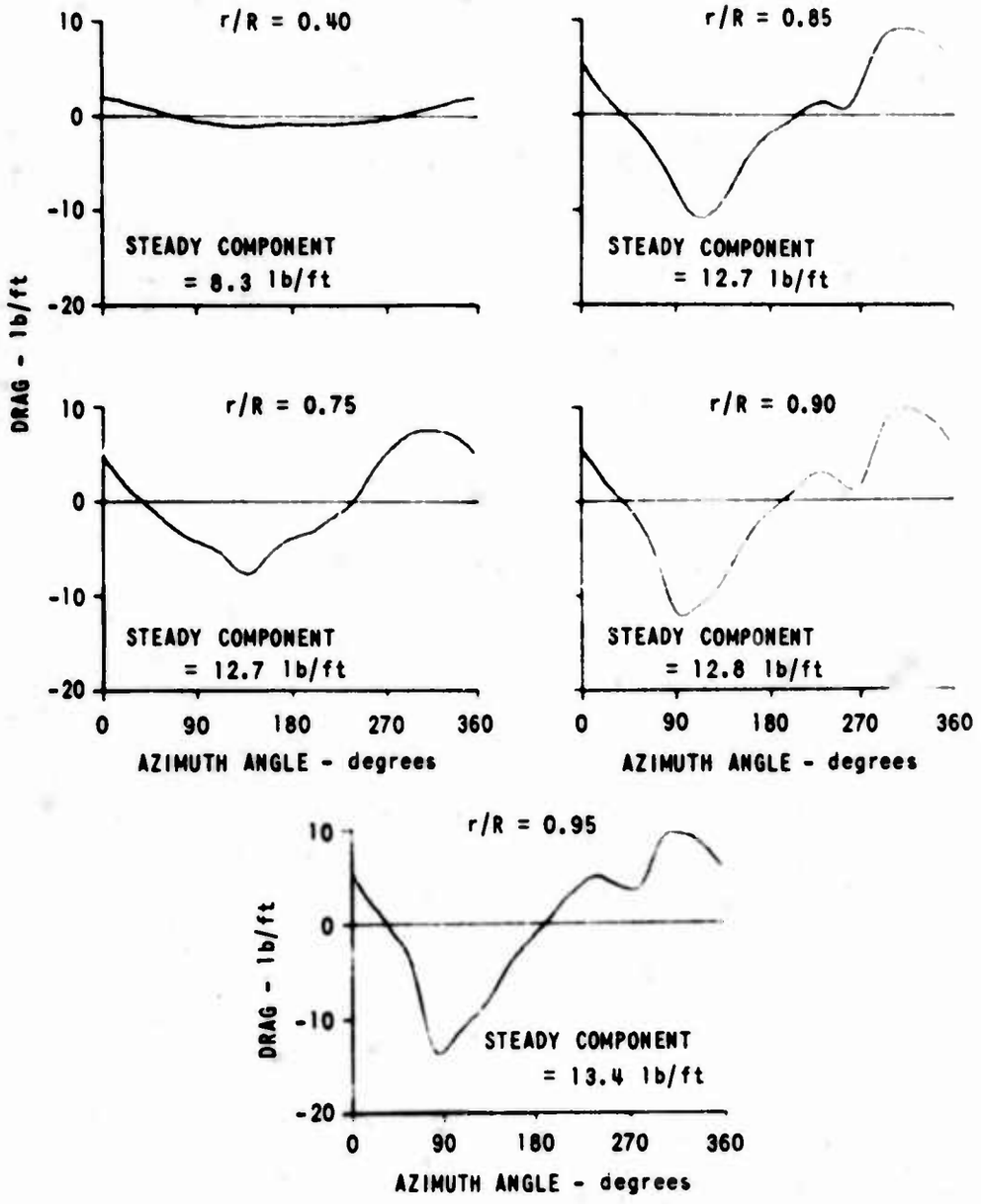

Figure 17. COMPUTED AZIMUTHAL VARIATIONS OF BLADE DRAG DISTRIBUTION; UH-1A AT μ = 0.08.

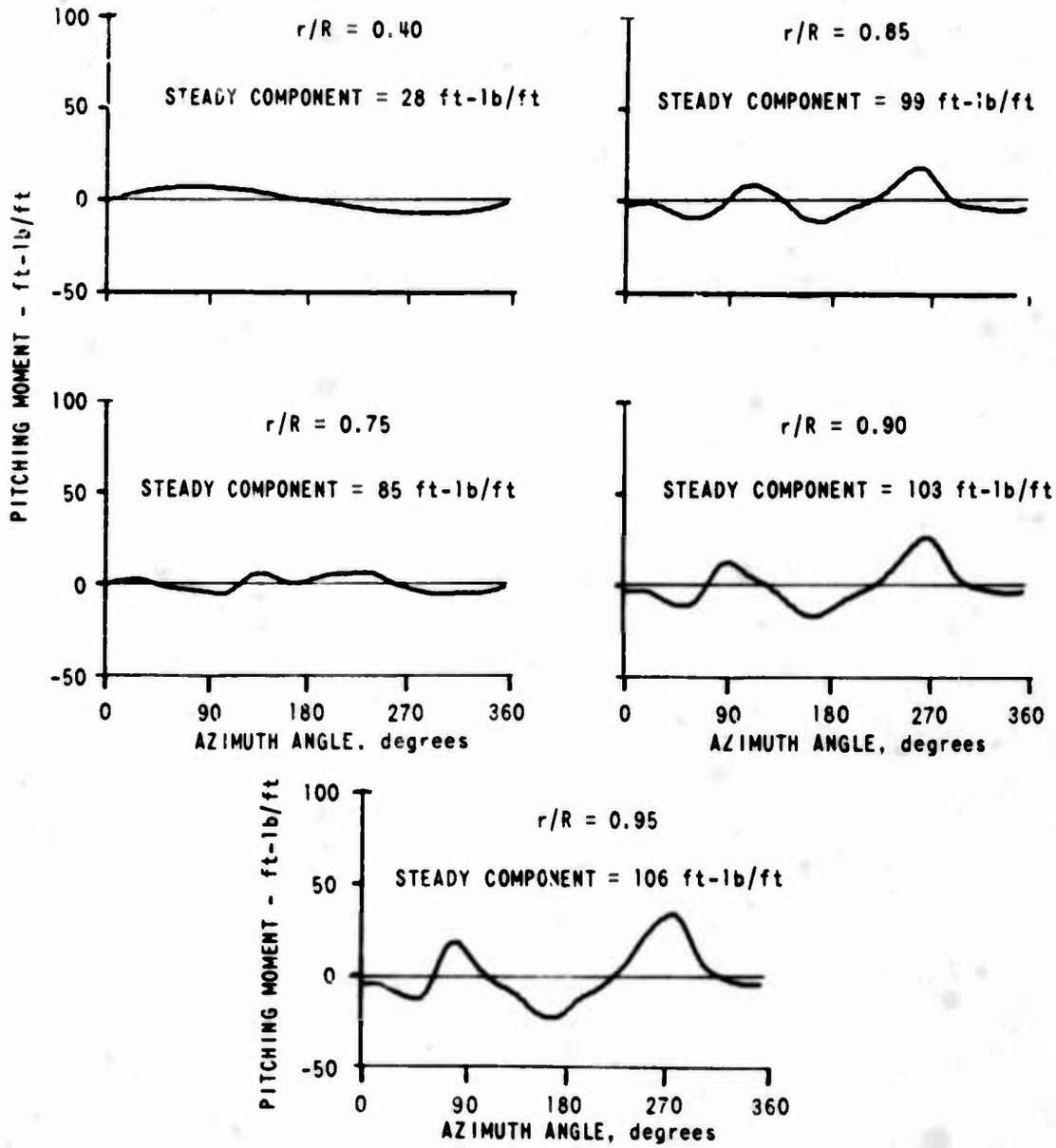

Figure 18. COMPUTED AZIMUTHAL VARIATIONS OF BLADE PITCHING MOMENT (ABOUT MIDCHORD) DISTRIBUTION; UH-1A AT μ = 0.08.

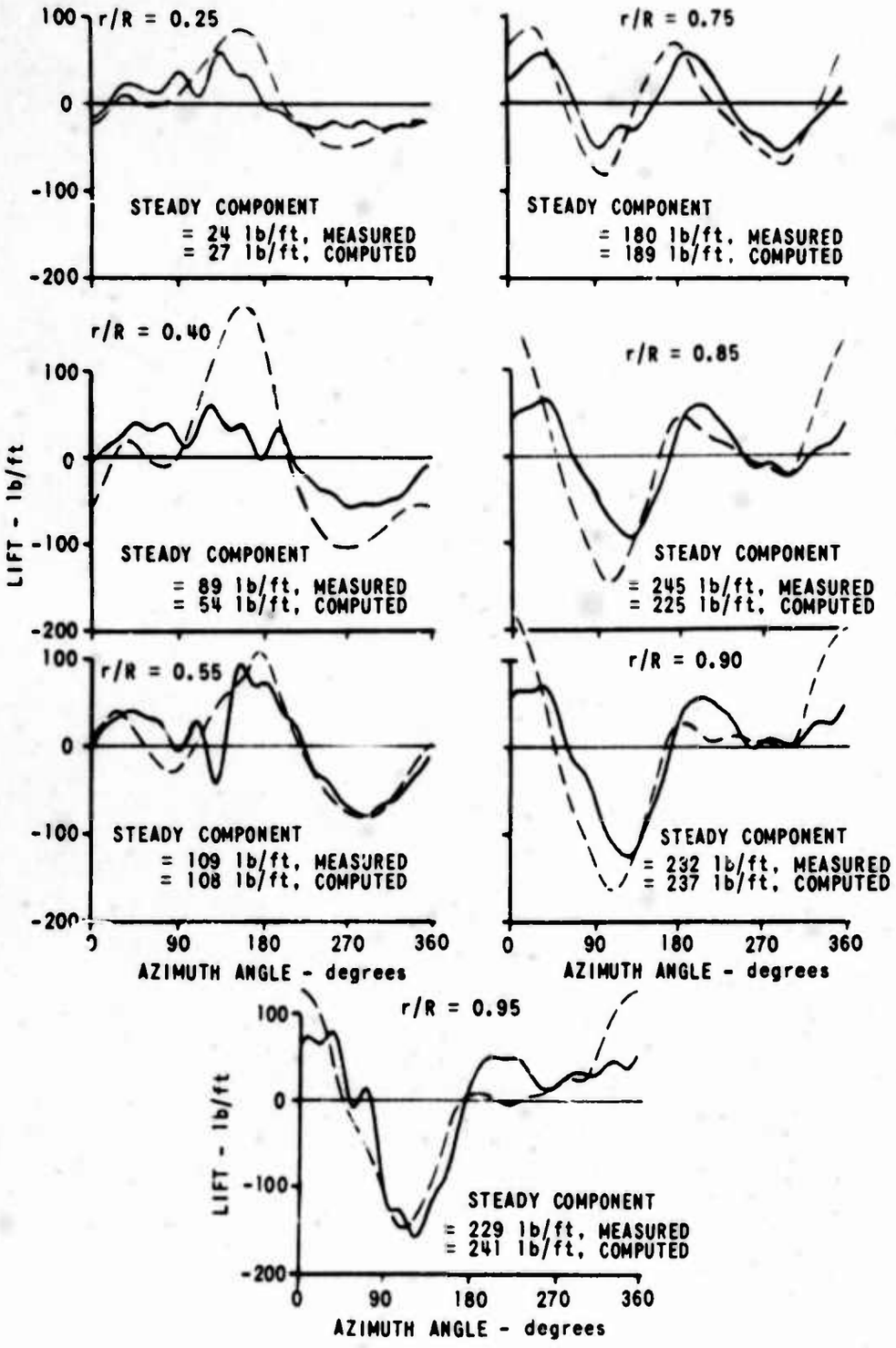

Figure 19. MEASURED AND COMPUTED AZIMUTHAL VARIATIONS OF BLADE LIFT DISTRIBUTION; H-34 AT $\mu = 0.29$.

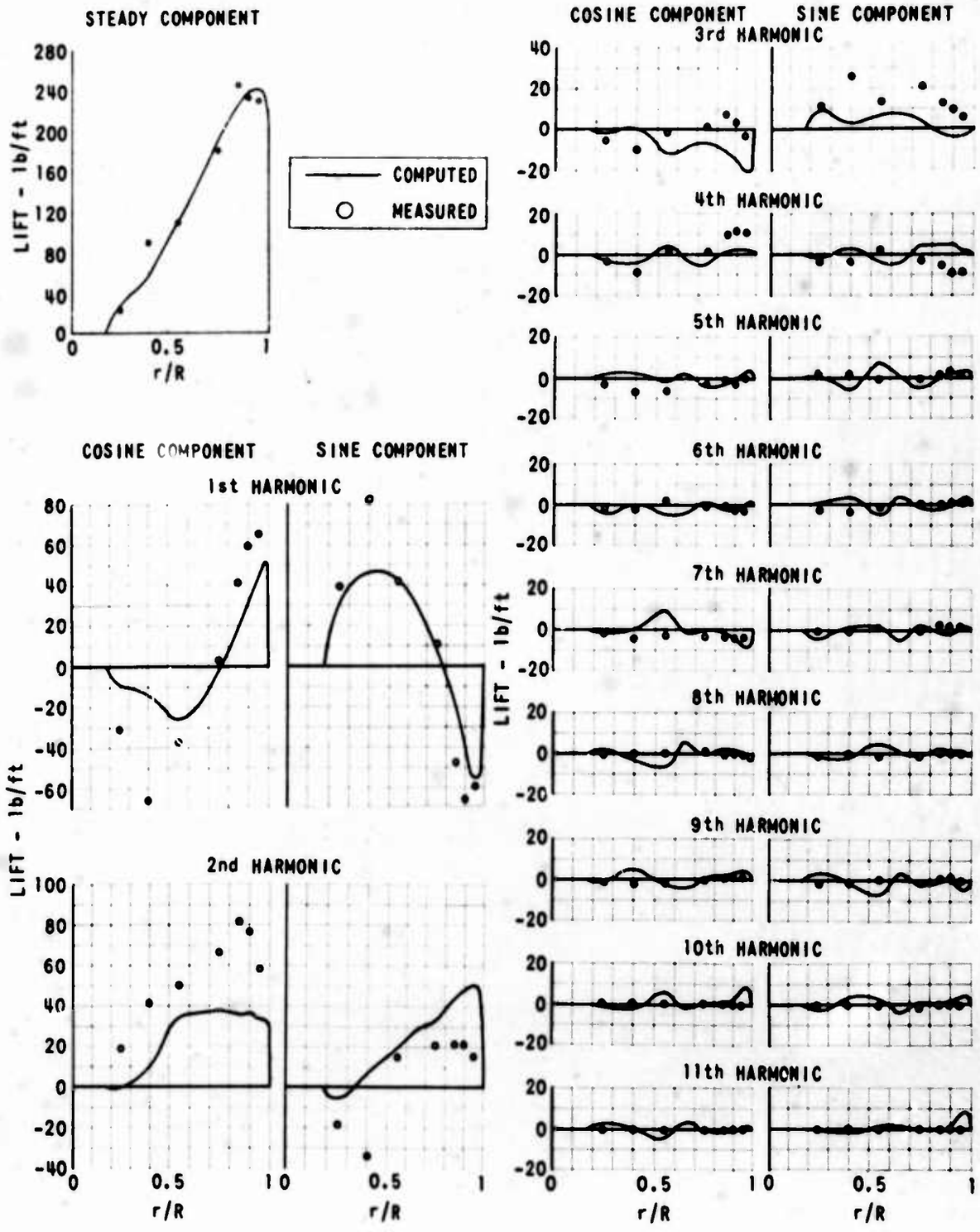

Figure 20. MEASURED AND COMPUTED HARMONICS OF BLADE LIFT DISTRIBUTION; H-34 AT μ = 0.29.

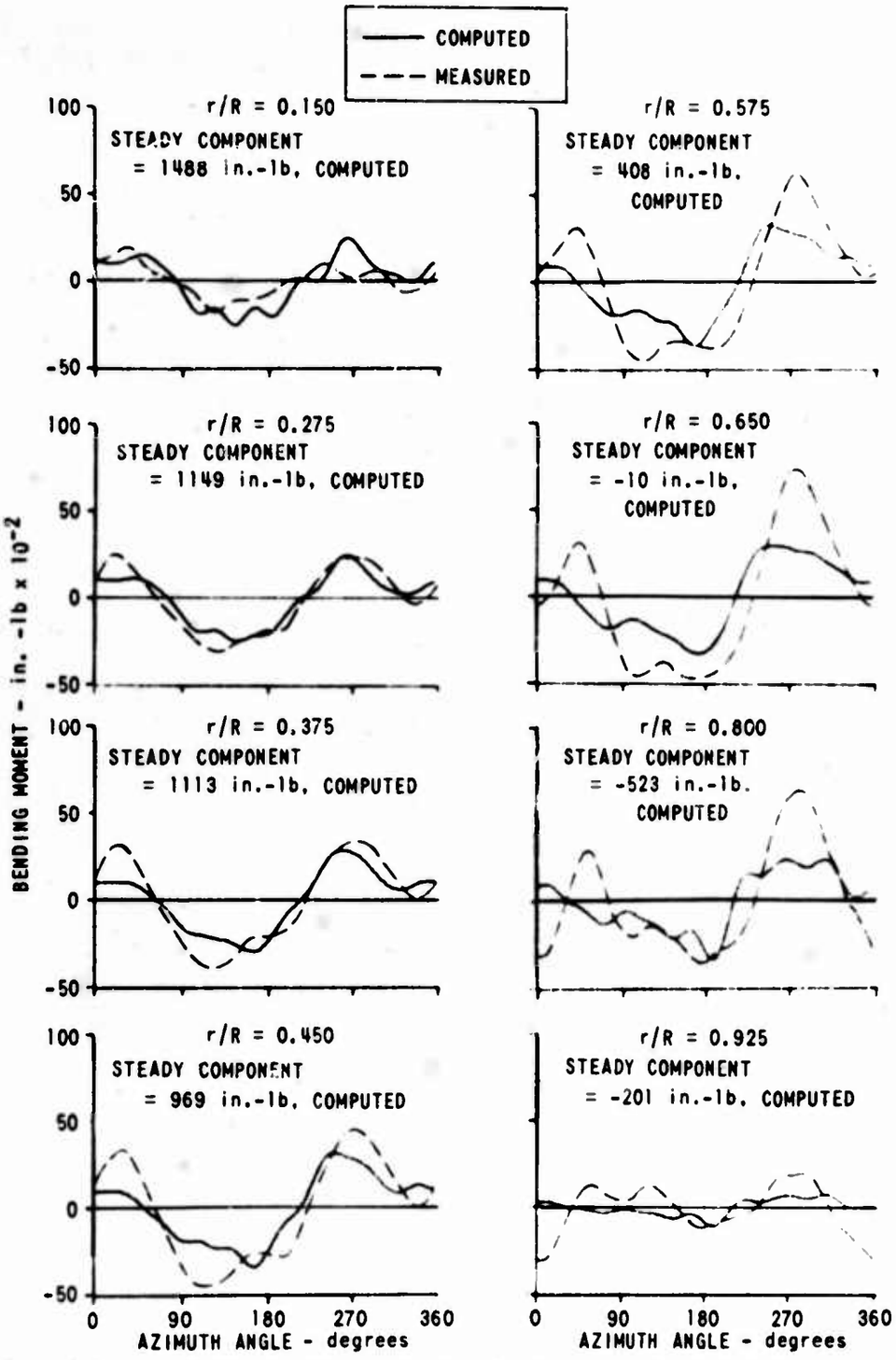

Figure 21. MEASURED AND COMPUTED AZIMUTHAL VARIATIONS OF BLADE FLATWISE BENDING MOMENTS; H-34 AT μ = 0.29.

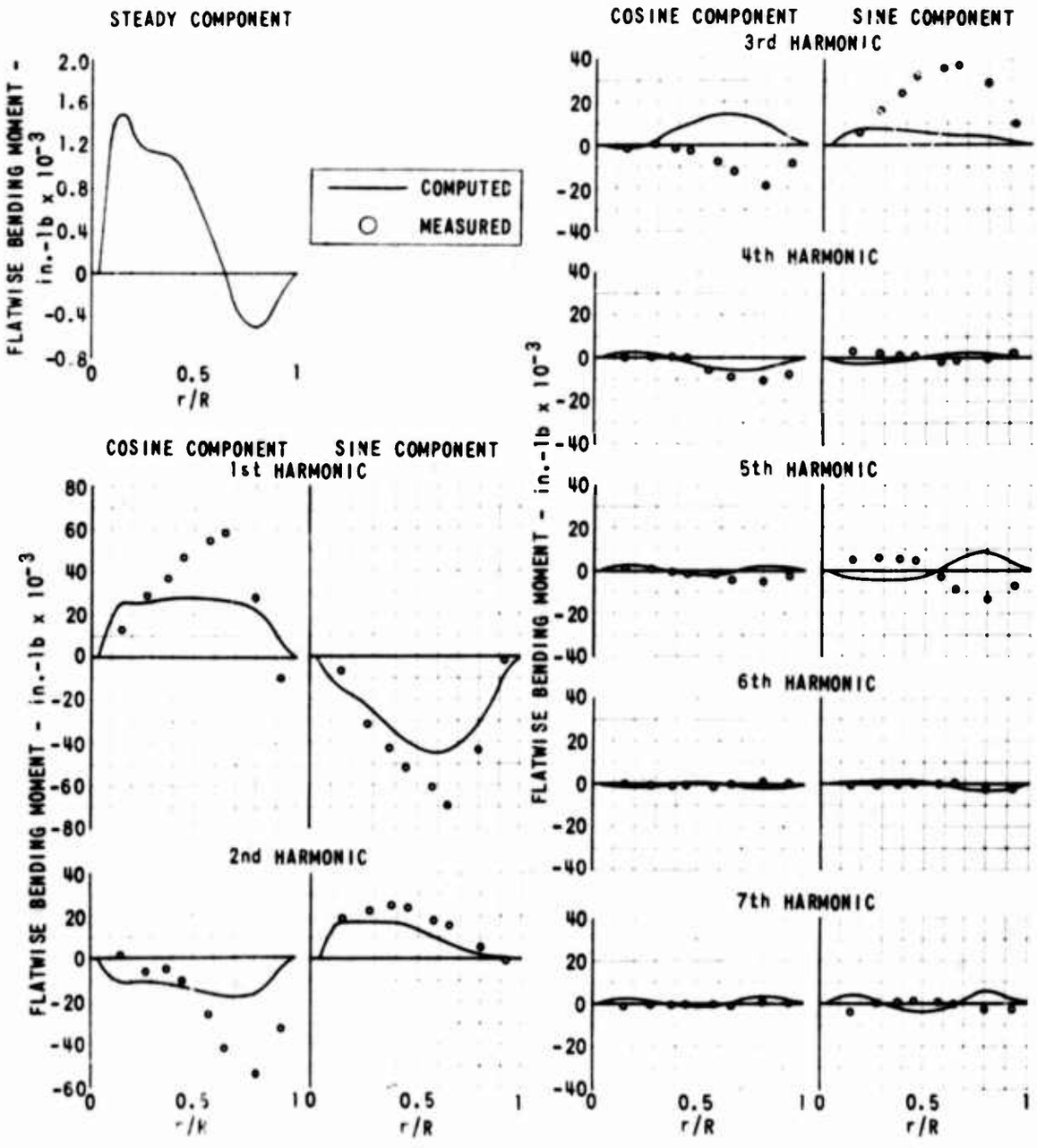

Figure 22. MEASURED AND COMPUTED HARMONICS OF BLADE FLATWISE BENDING MOMENT: H-34 AT μ = 0.29.

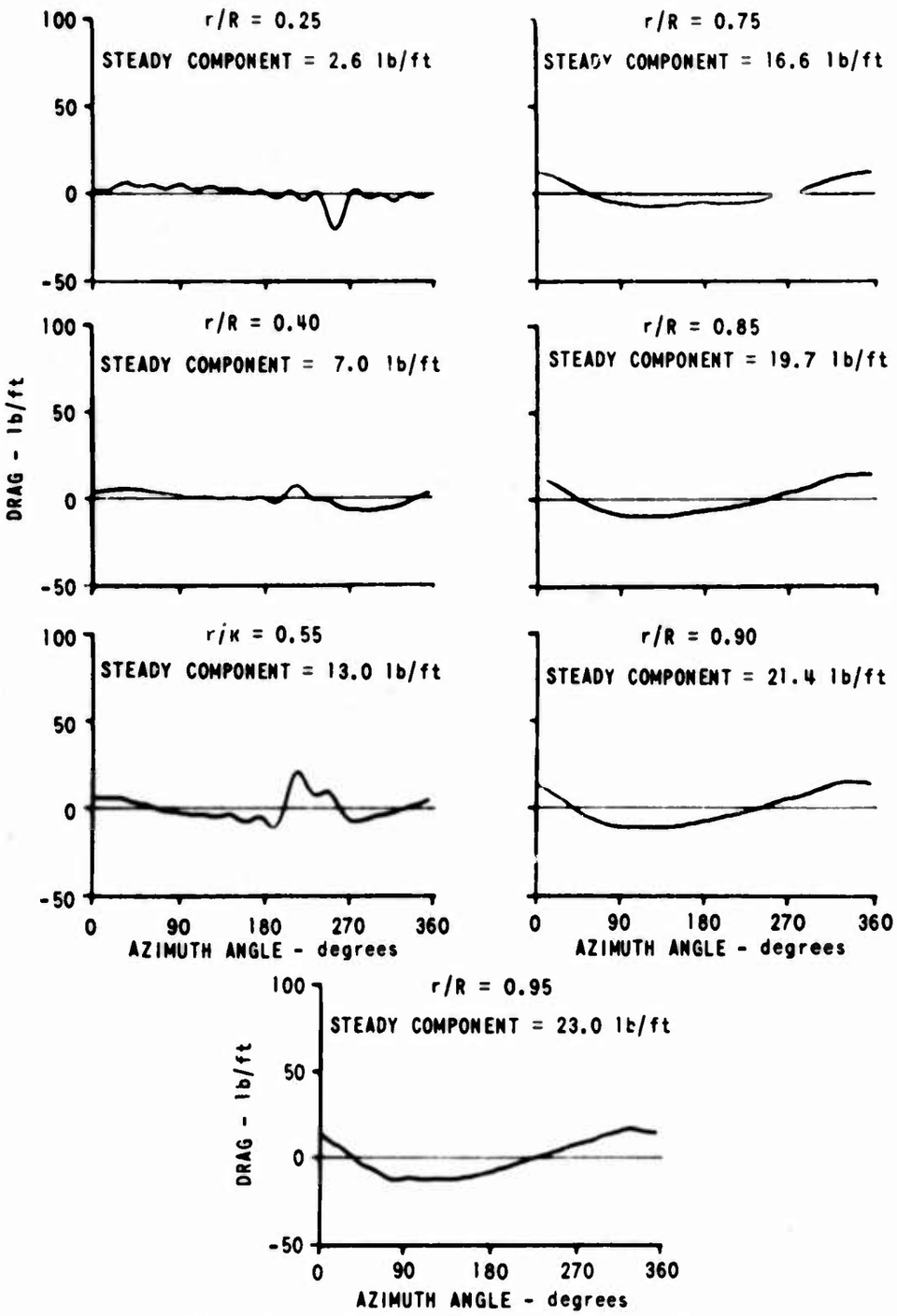

Figure 23. COMPUTED AZIMUTHAL VARIATIONS OF BLADE DRAG DISTRIBUTION; H-34 AT $\mu = 0.29$.

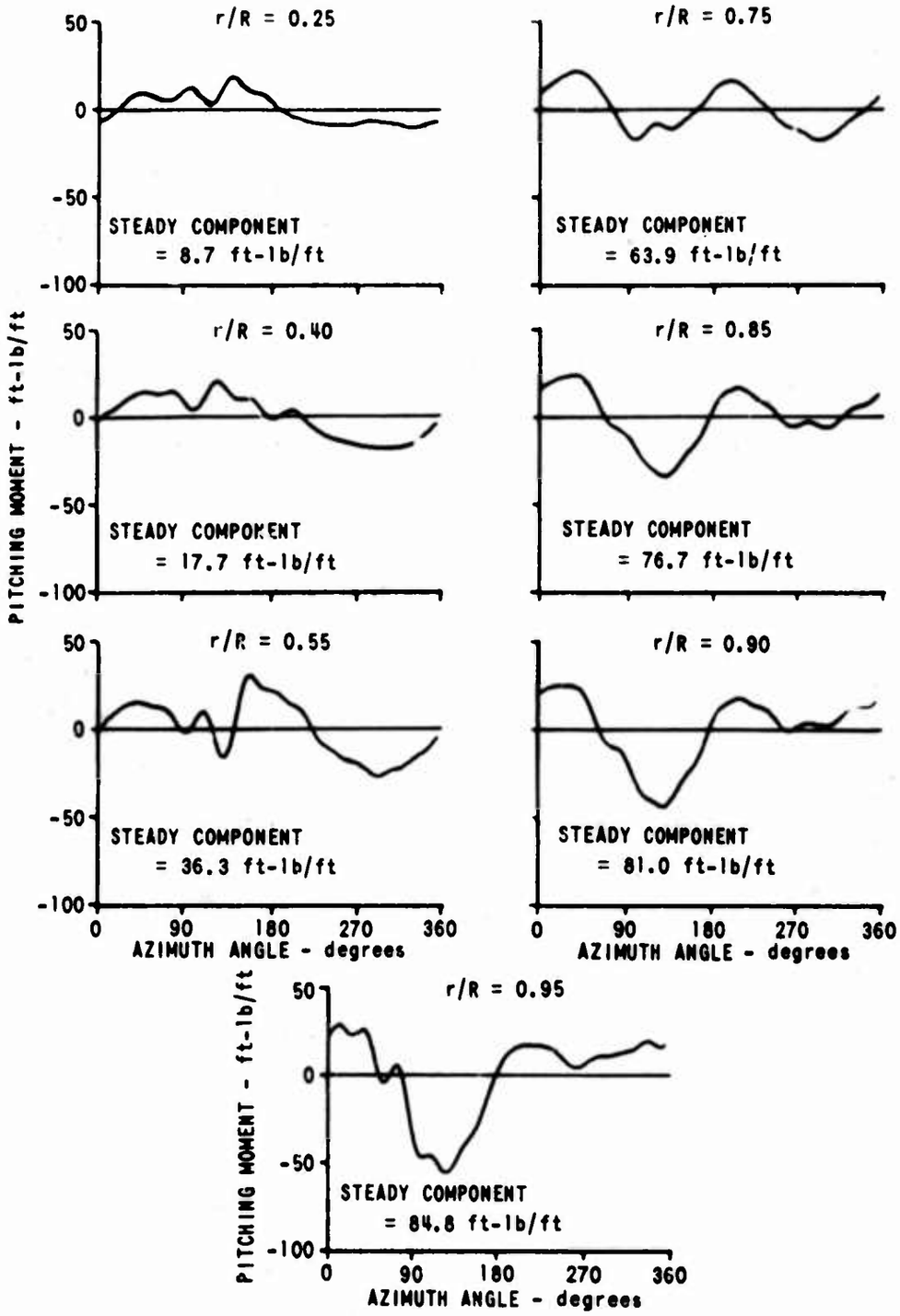

Figure 24. COMPUTED AZIMUTHAL VARIATIONS OF BLADE PITCHING MOMENT (ABOUT MIDCHORD) DISTRIBUTION; H-34 AT μ = 0.29.

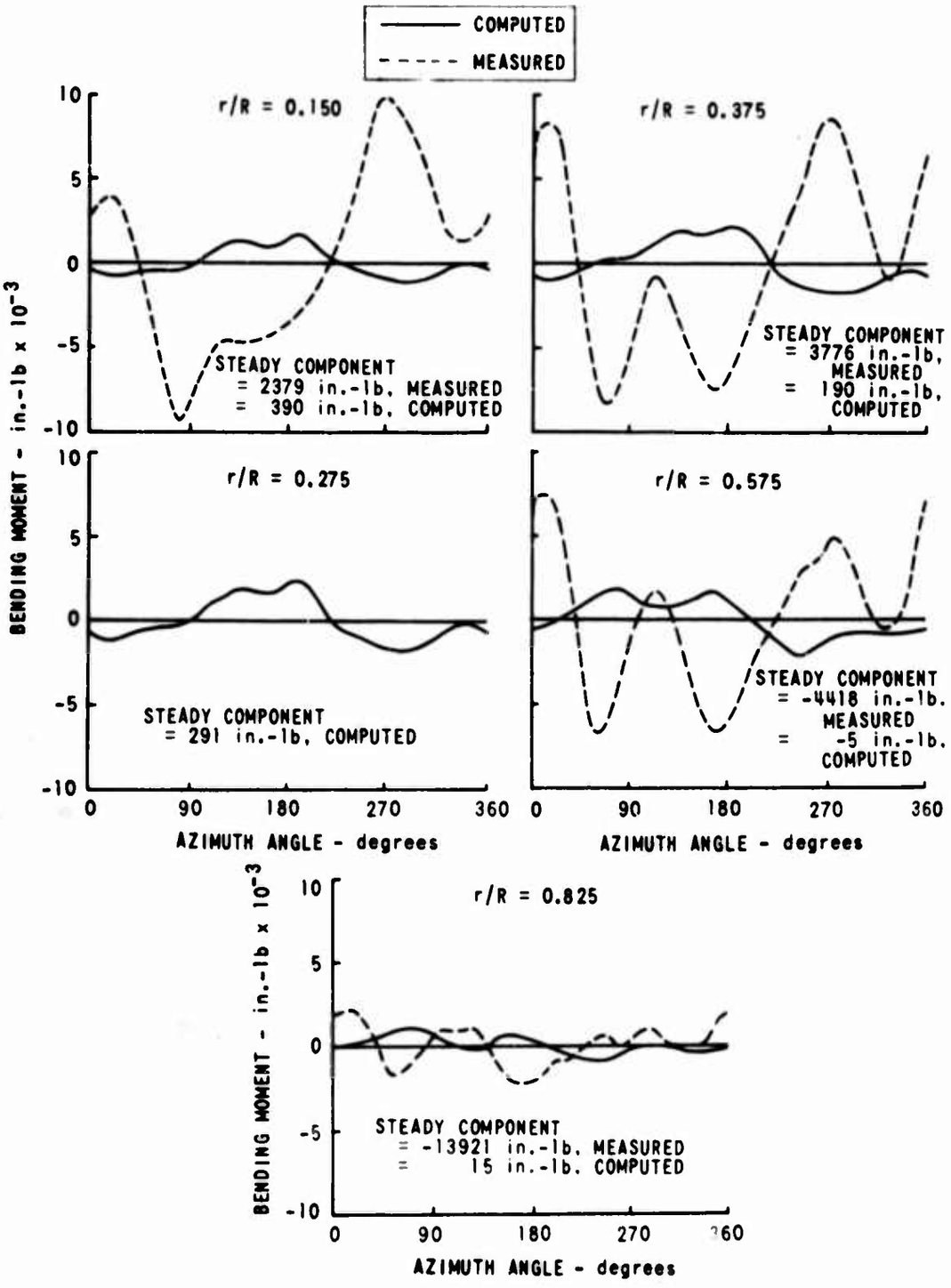

Figure 25. MEASURED AND COMPUTED AZIMUTHAL VARIATIONS OF BLADE CHORDWISE BENDING MOMENTS; H-34 AT μ = 0.29.

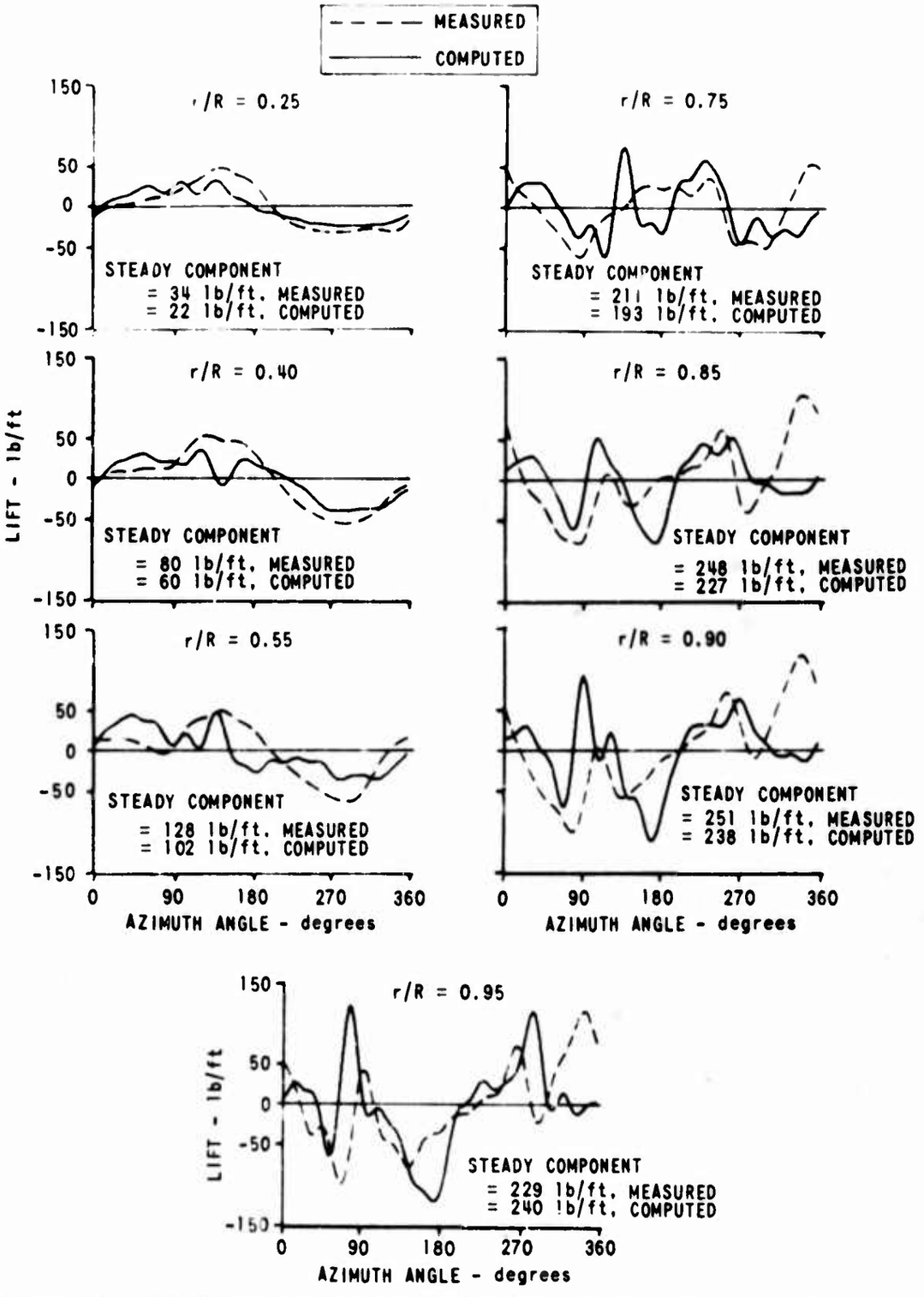

Figure 26. MEASURED AND COMPUTED AZIMUTHAL VARIATIONS OF BLADE LIFT DISTRIBUTION; H-34 at μ = 0.18.

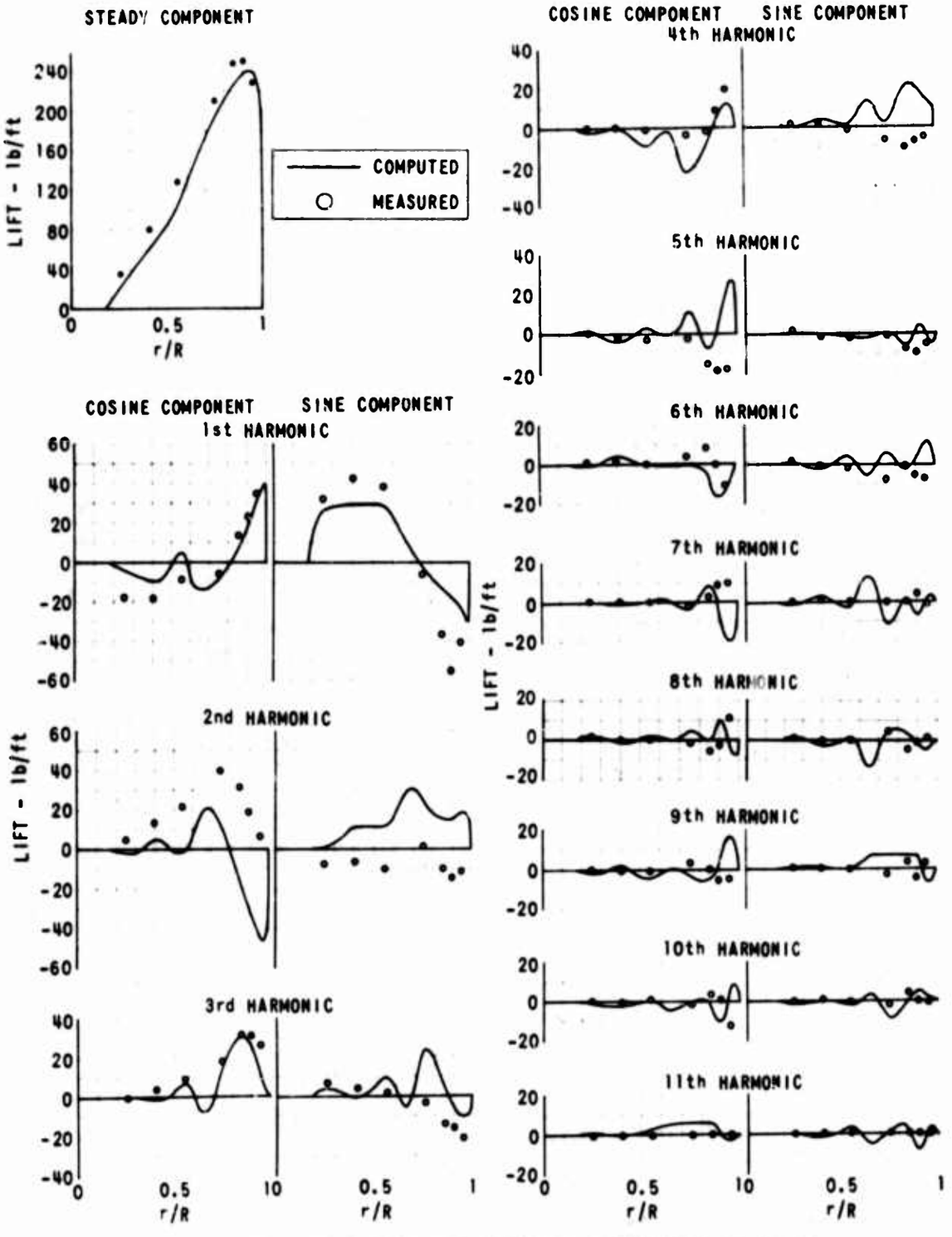

Figure 27. MEASURED AND COMPUTED HARMONICS OF BLADE LIFT DISTRIBUTION; H-34 AT μ = 0.18.

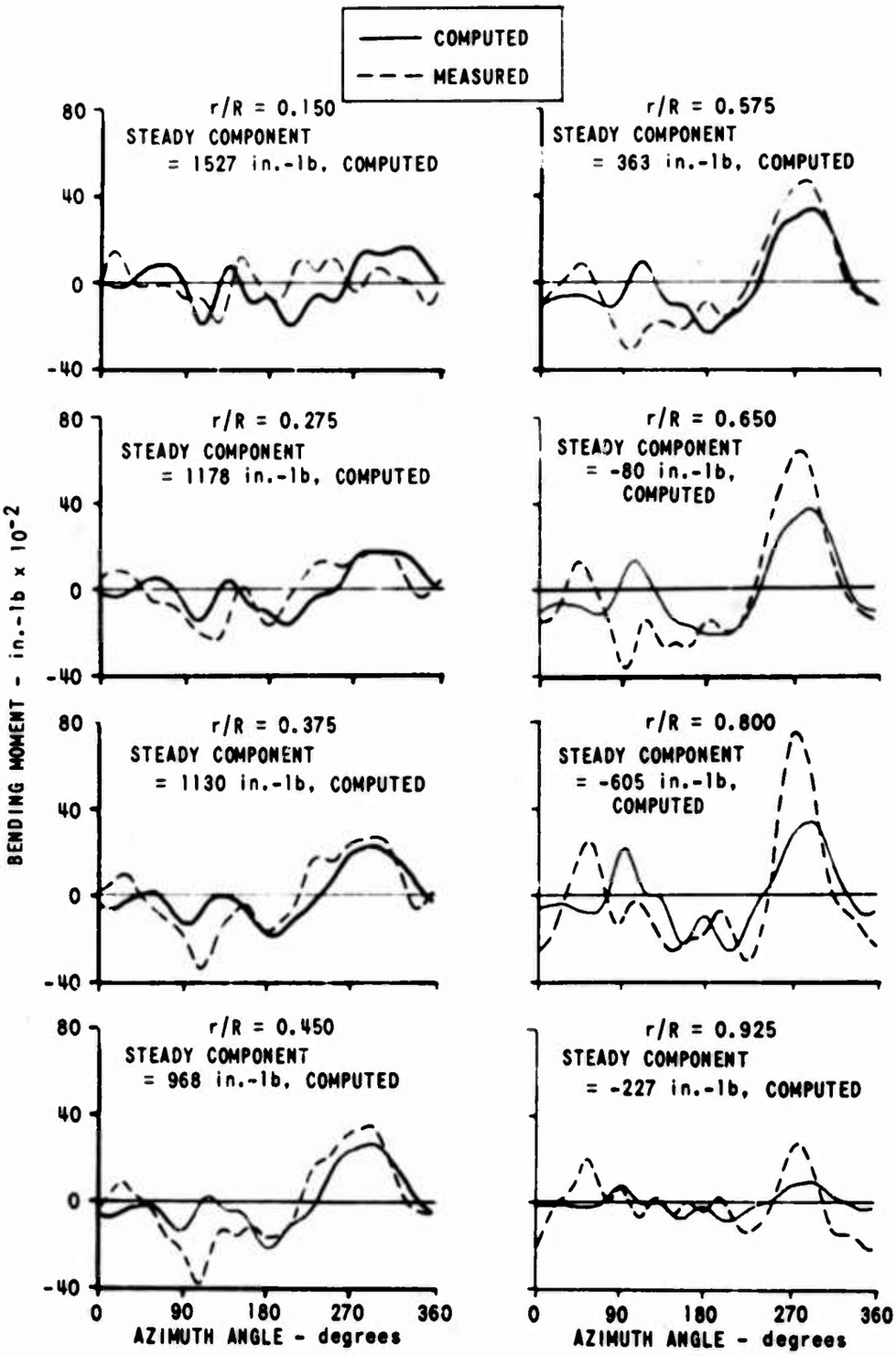

Figure 28. MEASURED AND COMPUTED AZIMUTHAL VARIATION OF BLADE FLATWISE BENDING MOMENTS; H-34 AT $\mu = 0.18$.

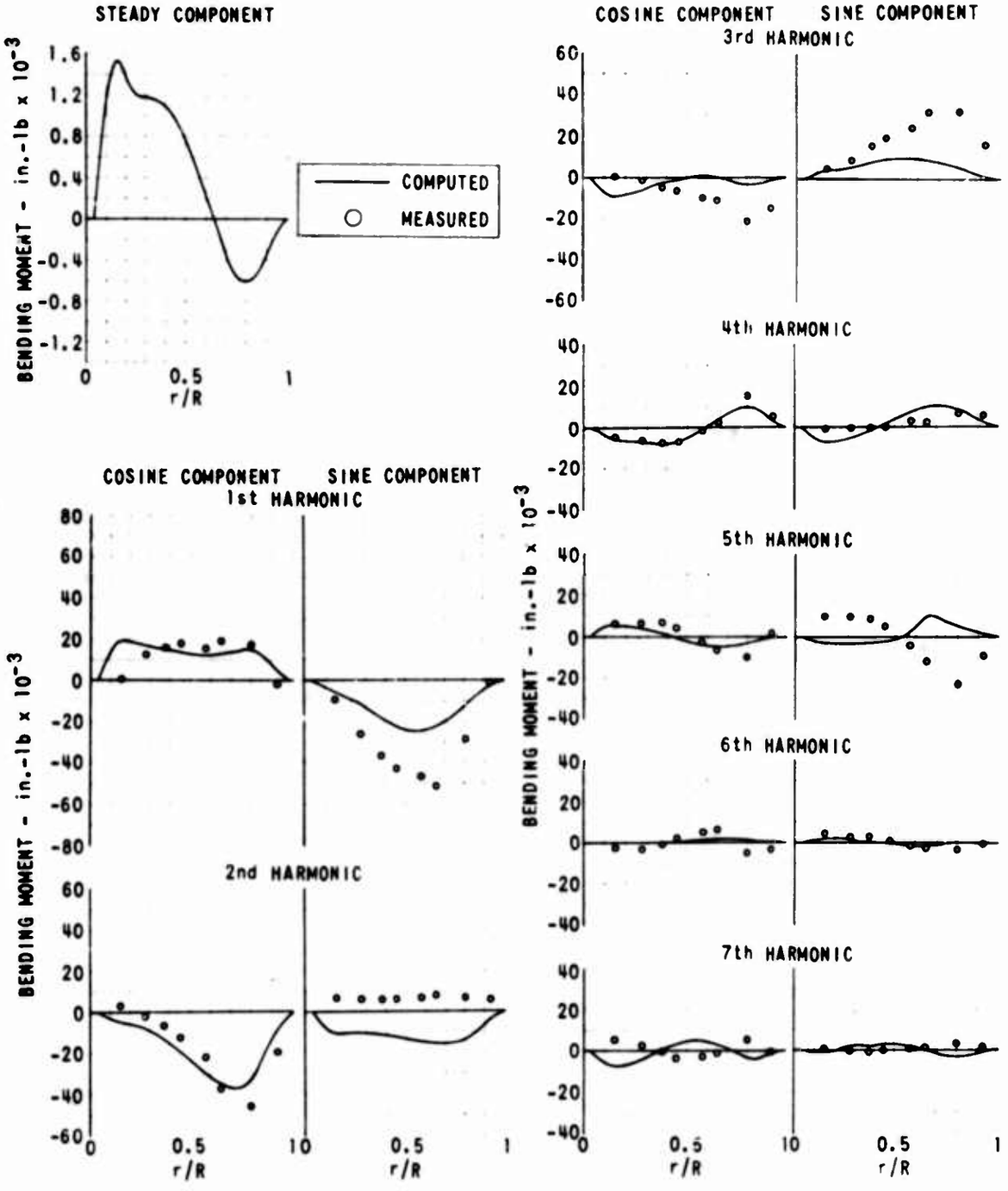

Figure 29. MEASURED AND COMPUTED HARMONICS OF BLADE FLATWISE BENDING MOMENT; H-34 AT μ = 0.18.

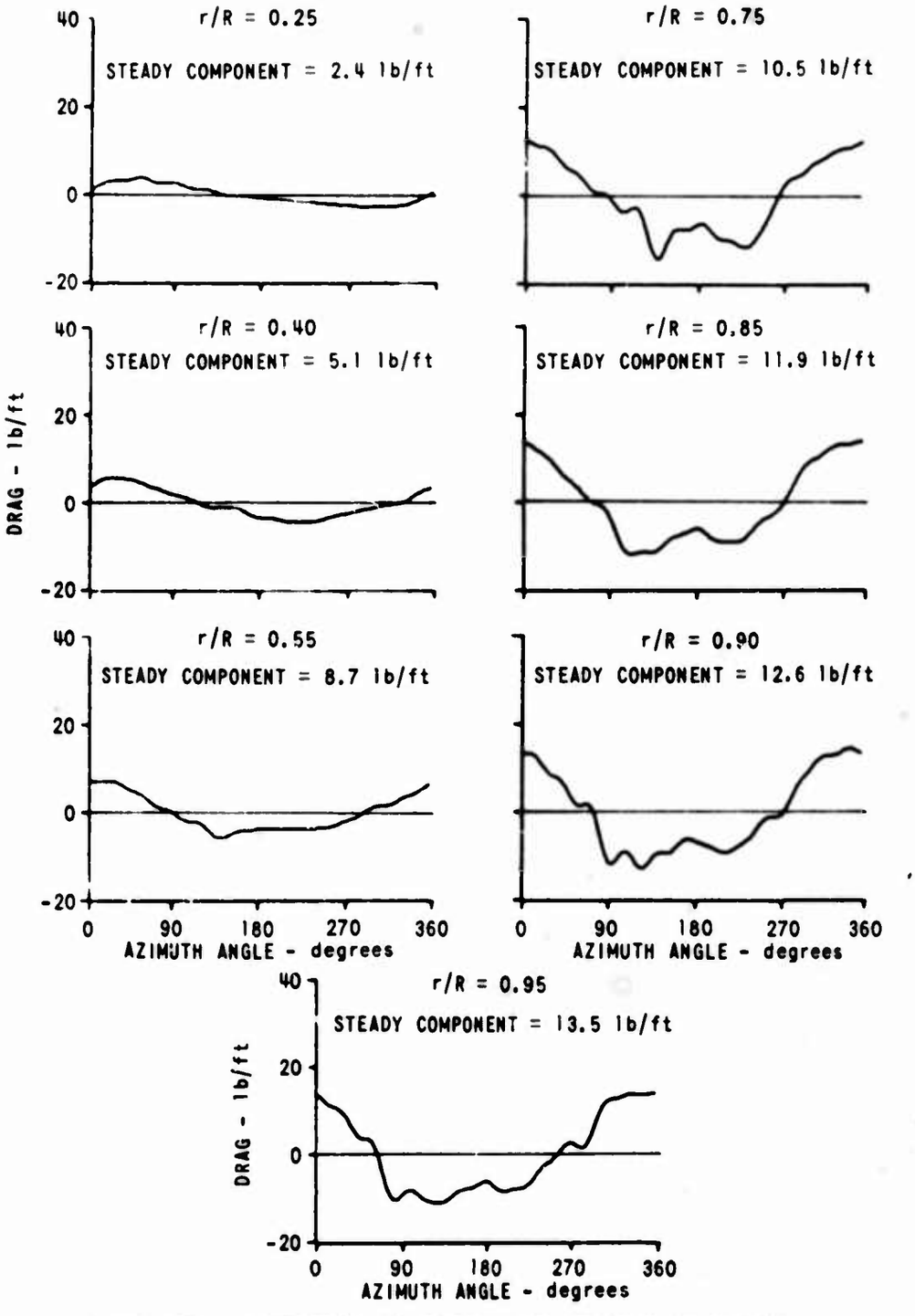

Figure 30. COMPUTED AZIMUTHAL VARIATIONS OF BLADE DRAG DISTRIBUTION; H-34 AT μ = 0.18.

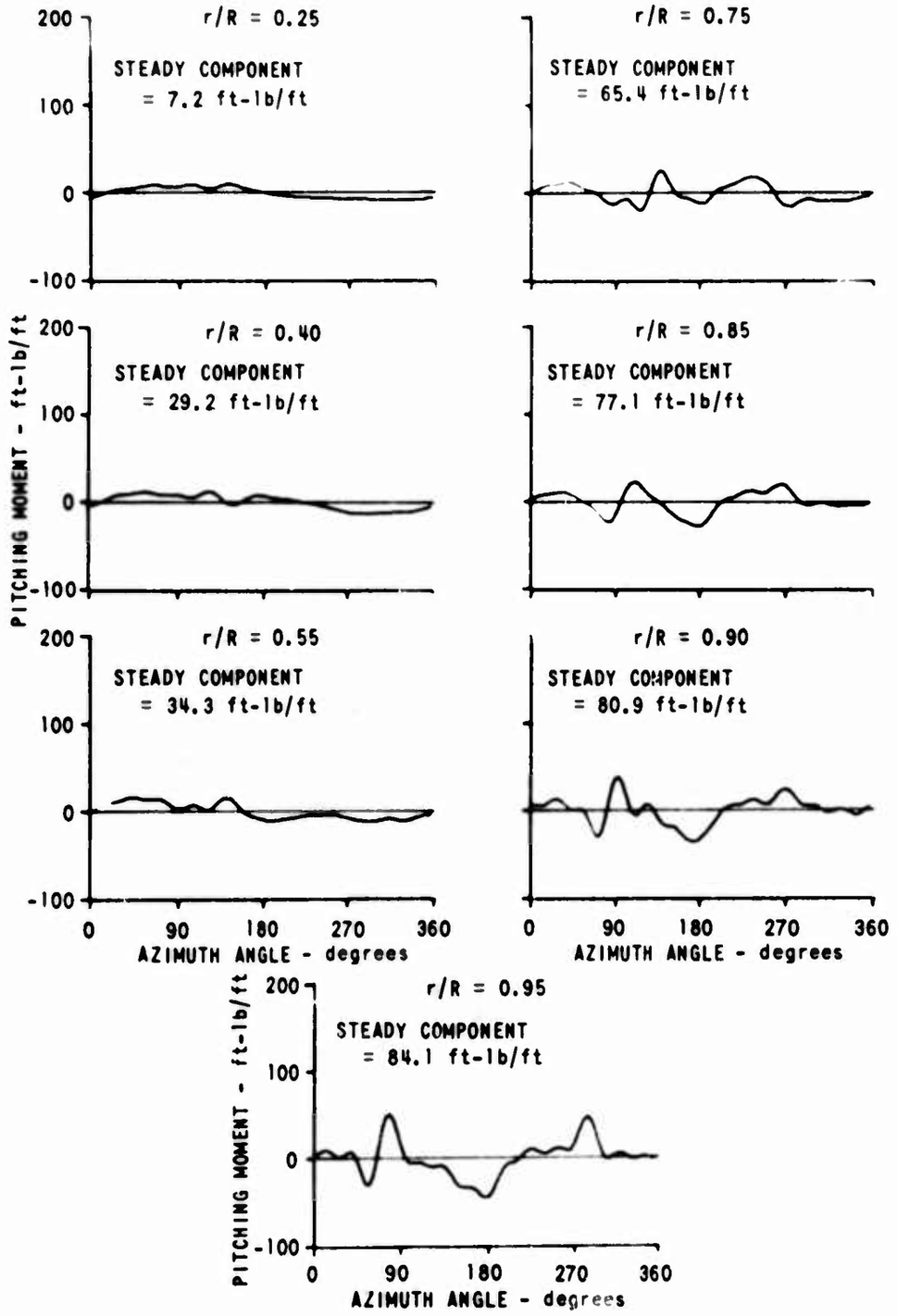

Figure 31. COMPUTED AZIMUTHAL VARIATIONS OF BLADE PITCHING MOMENT (ABOUT MIDCHORD) DISTRIBUTION; H-34 AT μ = 0.18.

REFERENCES

1. Piziali, R. A., Cornell Aeronautical Laboratory, Inc., A Method for Predicting the Aerodynamic Loads and Dynamic Response of Rotor Blades, U. S. Army Aviation Materiel Laboratories, Fort Eustis, Virginia, USAAVLABS TR 65-74, January 1966.

2. Daughaday, H., DuWaldt, F. A., and Gates, C. A., Investigation of Helicopter Rotor Flutter and Load Amplification Problems, Cornell Aeronautical Laboratory, Inc., Buffalo, New York, CAL Report SB-862-S-4, August 1956.

3. Chang, T. T., A Flutter Theory for a Flexible Helicopter Rotor Blade in Vertical Flight, Cornell Aeronautical Laboratory, Inc., Buffalo, New York, CAL Report SB-862-S-1, July 1954.

4. Targoff, W. P., The Bending Vibrations of a Twisted Rotating Beam, Proceedings from Third Midwestern Conference on Solid Mechanics, Ann Arbor, Michigan, 1957, pp. 177-194.

5. von Karman, T., and Sears, W. R., "Airfoil Theory for Non-Uniform Motion", Journal of the Aeronautical Sciences, Volume 5, No. 10, August 1938.

6. Di Prima, R. C., and Handelman, G. H., "Vibrations of Twisted Beams", Quarterly Applied Mathematics, Volume XII, No. 3, October 1954, pp. 241-259.

7. Bell Helicopter Company, Measurement of Dynamic Airloads on a Full-Scale Semirigid Rotor, U. S. Army Aviation Materiel Laboratories, Fort Eustis, Virginia, TCREC TR 62-42, December 1962.

8. Scheiman, J., A Tabulation of Helicopter Rotor-Blade Differential Pressures, Stresses, and Motions as Measured in Flight, National Aeronautics and Space Administration, Langley Field, Virginia, NASA TM X-952, March 1964.

9. Graham, D. J., Nitzberg, G. E., and Olson, R. N., A Systematic Investigation of Pressure Distributions at High Speeds Over Five Representative NACA Low-Drag and Conventional Airfoil Sections, National Advisory Committee for Aeronautics, Moffett Field, California, NACA TR 832, 1945. (See Figure 19.)

10. Lizak, A. A., Two-Dimensional Wind-Tunnel Tests of an H-34 Main Rotor Airfoil Section, U.S. Army Aviation Materiel Laboratories, Fort Eustis, Virginia, TREC TR 60-53, September 1960.

11. McCloud, J. L., Biggers, J. C., and Maki, R. L., Full-Scale Wind-Tunnel Tests of a Medium Weight Utility Helicopter at Forward Speeds, National Aeronautics and Space Administration, Moffett Field, California, NASA TN D-1887, May 1963.

12. Seckel, E., Stability and Control of Airplanes and Helicopters, Academic Press, New York, New York, 1964. (See Section 7 of Appendix I.)

13. Scheiman J., and Ludi, L. H., Qualitative Evaluation of Effect of Helicopter Rotor-Blade Tip Vortex on Blade Airloads, Langley Research Center, Langley Station, Hampton, Virginia, NASA TN D-1637, May 1963.

APPENDIX

ORTHOGONALITY RELATIONS OF BENDING VIBRATION MODES OF A TWISTED ROTATING BEAM

The bending deformation of a twisted (rotating or nonrotating) beam is generally not in one plane. For this reason, recent practice in load and deformation analysis of a twisted propeller or helicopter blade utilizes bending vibration modes of the twisted rotating blade with both flatwise and chordwise deflection components as generalized coordinates. Since these modes all satisfy the same two governing differential equations and the same root and tip conditions, they satisfy certain relations (usually called the orthogonality relations) among themselves. This note presents a self-contained derivation of the general equations from which the relations pertaining to blades with given root conditions can be obtained immediately upon using the root conditions. The relations are useful in detecting the accuracy of results obtained from vibration analysis and in simplifying the equations of blade motions in which certain bending vibration modes are used as a group of the generalized coordinates. A blade with flapping and lead-lag hinges is among those used in the examples.

Existing methods for bending vibration analysis of twisted rotating blades (such as Reference 4) assume that the undeformed blade elastic axis is a straight line which lies in the plane of rotation and intersects the axis of rotation. Furthermore, the c.g. and central polar axes are assumed to be coincident with the elastic axis, and the built-in twist is assumed to be about the elastic axis. All these assumptions will be made here. In blade load and deformation analysis, Lagrange's equations of blade motions take the actual axis offsets and built-in coning into account by having constant generalized force terms that depend on the offsets and built-in coning. (The offset

between the elastic and c.g. axes also causes coupling between bending and torsional modes.)

Consider a blade section at a distance r from the axis of rotation,

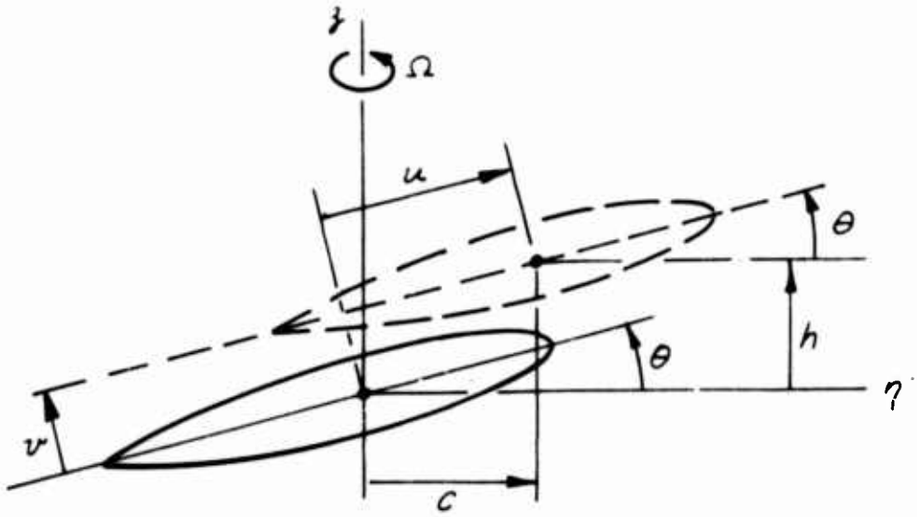

Figure 32. BLADE DEFLECTIONS DURING BENDING VIBRATION.

about which the blade (as well as the $r\eta\zeta$ system) is rotating in vacuum at a constant angular velocity Ω. With reference to Figure 32, the ζ-axis is the axis of rotation, the r-axis is perpendicular to the paper and pointing to the reader, and the η-axis is perpendicular to the ζr-plane. When the blade is undeformed, the section is shown by the solid line: its elastic center lies on the r-axis and its major principal central axis makes an angle $\theta(r)$, called the local blade angle, with the plane of rotation (i.e., the $r\eta$-plane). With the presence of bending deformation, the same section is shown by the

dotted line: its elastic center is displaced by (u , v) or (c , h) in a plane parallel to the $\eta\zeta$ -plane, while θ is assumed to remain unchanged. The deflection components $u(r)$ and $v(r)$ are called the chordwise and flatwise bending deflection components, respectively, while $c(r)$ and $h(r)$ are called the inplane and flapwise components, respectively. From Figure 32,

$$\left.\begin{aligned} h &= v\cos\theta + u\sin\theta \\ c &= u\cos\theta - v\sin\theta \end{aligned}\right\} \tag{87}$$

or

$$\left.\begin{aligned} v &= h\cos\theta - c\sin\theta \\ u &= c\cos\theta + h\sin\theta \end{aligned}\right\} . \tag{88}$$

Assuming that the blade sections remain plane during bending, the small deflection described above is the result of the small rotation of each blade section about an axis which lies in the plane of the section and intersects the elastic axis. The rotation has one component equal to $\frac{dh}{dr}$ radians in the negative η -direction and the other component equal to $\frac{dc}{dr}$ radians in the ζ -direction, according to the right-hand rule of representing rotations by vectors. The curvature of the projection of the deformed elastic axis on the ζr -plane or on the $r\eta$ -plane is equal to $\frac{d^2h}{dr^2}$ or $\frac{d^2c}{dr^2}$, respectively.

Let G or F be the curvature of the projection of the elastic axis on the plane that contains the local major principal central axis and the r -axis or on the plane that contains the local minor principal central axis and the r -axis, respectively. Also, let $\tilde{M}$ and $\tilde{\tilde{M}}$ be the flatwise (about the local major principal central axis) and chordwise (about the local minor principal central axis) bending moments acting on a blade section.* According to the engineering beam theory, which assumes that the beam cross sections remain plane during bending, the

* Positive $\tilde{M}$ and $\tilde{\tilde{M}}$ tend to compress the upper surface and leading edge, respectively.

following relations hold at any blade section:

$$\tilde{M} = BF \tag{89}$$

and

$$\tilde{\tilde{M}} = bG \tag{90}$$

where B and b, with $b > B$ usually, are the flatwise and chordwise flexural rigidities of the blade section.

On account of the blade's being twisted (namely, $\frac{d\theta}{dr} \neq 0$), the curvatures F and G (each belongs to the projection of the elastic axis on a plane that rotates, as r changes, about the r-axis with respect to a coordinate system fixed to the blade) are not given by

$$F = \frac{d^2v}{dr^2} \qquad \text{and} \qquad G = \frac{d^2u}{dr^2}$$

but are given by

$$\left.\begin{aligned} F &= \frac{d^2h}{dr^2}\cos\theta - \frac{d^2c}{dr^2}\sin\theta \\ G &= \frac{d^2c}{dr^2}\cos\theta + \frac{d^2h}{dr^2}\sin\theta \end{aligned}\right\} \tag{91}$$

or, by the use of (87),

$$\left.\begin{aligned} F &= \frac{d^2v}{dr^2} + 2\frac{d\theta}{dr}\frac{du}{dr} + \frac{d^2\theta}{dr^2}u - \left(\frac{d\theta}{dr}\right)^2 v \\ G &= \frac{d^2u}{dr^2} - 2\frac{d\theta}{dr}\frac{dv}{dr} - \frac{d^2\theta}{dr^2}v - \left(\frac{d\theta}{dr}\right)^2 u \end{aligned}\right\} . \tag{92}$$

Let $\tilde{M}$ and $\tilde{\tilde{M}}$ be the flapwise and inplane components of the bending moment acting on a blade section such that

$$\begin{aligned} \bar{M} &= \tilde{M}\cos\theta + \tilde{\tilde{M}}\sin\theta \\ &= BF\cos\theta + bG\sin\theta \\ &= B\left(\frac{d^2h}{dr^2}\cos\theta - \frac{d^2c}{dr^2}\sin\theta\right)\cos\theta \\ &\quad + b\left(\frac{d^2c}{dr^2}\cos\theta + \frac{d^2h}{dr^2}\sin\theta\right)\sin\theta \end{aligned} \tag{93}$$

and

$$\bar{M} = \tilde{\bar{M}}\cos\theta - \tilde{M}\sin\theta$$

$$= bG\cos\theta - BF\sin\theta$$

$$= b\left(\frac{d^2c}{dr^2}\cos\theta + \frac{d^2h}{dr^2}\sin\theta\right)\cos\theta$$

$$- B\left(\frac{d^2h}{dr^2}\cos\theta - \frac{d^2c}{dr^2}\sin\theta\right)\sin\theta . \tag{94}$$

Let $\bar{\rho}$ and $\bar{p}$ be the components of loading, perpendicular to the deformed elastic axis, per unit length of blade in the ζ- and η-directions, respectively. Then, for a rotating blade in free bending oscillations at a natural frequency of ω radians/second, the loading component $\bar{p}$ is given by *

$$\bar{p} = \mu\omega^2 h + \frac{d}{dr}\left(X\frac{dh}{dr}\right) \tag{95}$$

where μ is the mass per unit length of blade and, with R being the blade tip radius,

$$X = \Omega^2\int_r^R \mu r\,dr \tag{96}$$

is the centrifugal force acting on a blade section at any r. Since the centrifugal force has a shear component equal to

$$X\frac{dh}{dr}$$

the upward component of transverse loading, or the contribution to $\bar{p}$, due to Ω is equal to the last term of (95). Carrying out the

---

* The Coriolis force, which has the effect of increasing X by

$$\Delta X = 2\Omega\int_r^R \dot{c}\,\mu\,dr,$$

is neglected in vibration analysis.

differentiation, (95) becomes

$$\bar{p} = \mu\omega^2 h + X\frac{d^2h}{dr^2} - \mu\Omega^2 r\frac{dh}{dr}. \tag{97}$$

Similarly, the corresponding $\bar{\bar{p}}$ can be expressed as

$$\bar{\bar{p}} = \mu\omega^2 c + X\frac{d^2c}{dr^2} - \mu\Omega^2 r\frac{dc}{dr} + \mu\Omega^2 c. \tag{98}$$

The last term of (98) is due to the fact that when the c. g. of a mass is off from the r -axis in the η -direction, there is a centrifugal force component in the η -direction acting on the mass. The governing equations for free vibrations are

$$\frac{d^2\bar{M}}{dr^2} = \bar{p} \tag{99}$$

and

$$\frac{d^2\bar{\bar{M}}}{dr^2} = \bar{\bar{p}} \tag{100}$$

with $\bar{M}$, $\bar{\bar{M}}$, $\bar{p}$ and $\bar{\bar{p}}$ as given by (93), (94), (97), and (98), respectively. * When any particular i^{th} or j^{th} mode is under consideration, the subscript i or j will be added to ω, h, c, $\bar{p}$, $\bar{\bar{p}}$, $\bar{M}$, $\bar{\bar{M}}$, F and G.

The four boundary conditions at the blade tip, where $r = R$,

*(99) and (100) are in agreement with Reference 6, since the two scalar equations below (4.8) of Reference 6 are the following two combinations of (99) and (100):

$$(99)\cos\theta - (100)\sin\theta$$

and

$$(100)\cos\theta + (99)\sin\theta .$$

may be written as

$$(\bar{M})_{r=R} = \left(\frac{d\bar{M}}{dr}\right)_{r=R} = (\bar{\bar{M}})_{r=R} = \left(\frac{d\bar{\bar{M}}}{dr}\right)_{r=R} = 0. \tag{101}$$

Since (99) and (100) are a pair of fourth-order differential equations in h and c, four more boundary conditions are required for each actual case. These additional boundary conditions are the "root" conditions which, for the present analysis, are assumed to be specified at $r = r_0$.

By first multiplying (99) and (100) for any i^{th} mode by h and c of any j^{th} mode, respectively, then adding them together, and finally integrating over r from r_0 to R,

$$\int_{r_0}^{R}\left(\frac{d\bar{M}_i}{dr} h_j + \frac{d\bar{\bar{M}}_i}{dr} c_j\right) dr = \int_{r_0}^{R}\left(\bar{p}_i h_j + \bar{\bar{p}}_i c_j\right) dr. \tag{102}$$

By integrating by parts twice, using (101), the left-hand side of (102) may be expressed as

$$\int_{r_0}^{R}\left(\frac{d^2\bar{M}_i}{dr^2} h_j + \frac{d^2\bar{\bar{M}}_i}{dr^2} c_j\right) dr = \left(\bar{M}_i \frac{dh_j}{dr} - \frac{d\bar{M}_i}{dr} h_j + \bar{\bar{M}}_i \frac{dc_j}{dr} - \frac{d\bar{\bar{M}}_i}{dr} c_j\right)_{r=r_0} + \int_{r_0}^{R}\left(\bar{M}_i \frac{d^2 h_j}{dr^2} + \bar{\bar{M}}_i \frac{d^2 c_j}{dr^2}\right) dr. \tag{103}$$

By the use of (96) through (98),

$$\int_{r_0}^{R}\left(\bar{p}_i h_j + \bar{\bar{p}}_i c_j\right) dr = \omega_i^2 \int_{r_0}^{R} \mu (h_i h_j + c_i c_j) dr + \int_{r_0}^{R}\left\{\frac{d}{dr}\left(\chi \frac{dh_i}{dr}\right) h_j + \frac{d}{dr}\left(\chi \frac{dc_i}{dr}\right) c_j\right\} dr + \Omega^2 \int_{r_0}^{R} \mu c_i c_j \, dr,$$

which, by applying integration by parts to the integral that contains χ and subsequently using (96), may be written

$$\int_{r_0}^{R}(\bar{p}_i h_j + \bar{\bar{p}}_i c_j)\,dr$$

$$= \omega_i^2\int_{r_0}^{R}\mu(h_i h_j + c_i c_j)\,dr + \Omega^2\left\{\int_{r_0}^{R}\mu c_i c_j\,dr\right.$$

$$\left. - \int_{r_0}^{R}\left(\int_r^R \mu r\,dr\right)\left(\frac{dh_i}{dr}\frac{dh_j}{dr} + \frac{dc_i}{dr}\frac{dc_j}{dr}\right)dr - \left(\frac{dh_i}{dr}h_j + \frac{dc_i}{dr}c_j\right)_{r=r_0}\int_{r_0}^{R}\mu r\,dr\right\} \quad (104)$$

Now, substitution of (103) and (104) into (102) yields

$$K_{ij} - \Omega^2\left(\hat{T}_{ij} - A_{ij}\int_{r_0}^{R}\mu r\,dr\right) + B_{ij} = \omega_i^2\hat{M}_{ij} \quad (105)$$

where

$$K_{ij} \equiv \int_{r_0}^{R}\left(\bar{M}_i\frac{d^2h_j}{dr^2} + \bar{\bar{M}}_j\frac{d^2c_j}{dr^2}\right)dr$$

$$= \int_{r_0}^{R}\left(\tilde{M}_i F_j + \tilde{\tilde{M}}_i G_j\right)dr = \int_{r_0}^{R}\left(\frac{1}{B}\tilde{M}_i\tilde{M}_j + \frac{1}{b}\tilde{\tilde{M}}_i\tilde{\tilde{M}}_j\right)dr \quad (106)$$

$$\hat{T}_{ij} \equiv \int_{r_0}^{R}\mu c_i c_j\,dr$$

$$- \int_{r_0}^{R}\left(\int_r^R \mu r\,dr\right)\left(\frac{dh_i}{dr}\frac{dh_j}{dr} + \frac{dc_i}{dr}\frac{dc_j}{dr}\right)dr \quad (107)$$

$$\hat{M}_{ij} \equiv \int_{r_0}^{R}\mu(h_i h_j + c_i c_j)\,dr = \int_{r_0}^{R}\mu(v_i v_j + u_i u_j)\,dr \quad (108)$$

$$A_{ij} \equiv \left(\frac{dh_i}{dr}h_j + \frac{dc_i}{dr}c_j\right)_{r=r_0} \quad (109)$$

$$B_{ij} \equiv \left(\bar{M}_i\frac{dh_j}{dr} - \frac{d\bar{M}_i}{dr}h_j + \bar{\bar{M}}_i\frac{dc_j}{dr} - \frac{d\bar{\bar{M}}_i}{dr}c_j\right)_{r=r_0} \quad (110)$$

Since (102) and, hence, (105) hold when i and j are interchanged and since

$$K_{ji} = K_{ij}\,, \qquad \hat{T}_{ji} = \hat{T}_{ij} \qquad \text{and} \qquad \hat{M}_{ji} = \hat{M}_{ij}\,,$$

it is clear that

$$K_{ij} - \Omega^2 \left(\hat{I}_{ij} - A_{ji} \int_{r_0}^{R} \mu r \, dr \right) + B_{ji} = \omega_j^2 \hat{M}_{ij} \, . \qquad (111)$$

Subtracting (111) from (105),

$$(\omega_i^2 - \omega_j^2) \hat{M}_{ij} - (B_{ij} - B_{ji}) - \Omega^2 (A_{ij} - A_{ji}) \int_{r_0}^{R} \mu r \, dr = 0 \, . \qquad (112)$$

Equations (112) and (105) are the desired equations. Some root constraints of practical interest will be dealt with in the examples that follow. As the examples show, (111) yields a relation stating that there is no inertial coupling between any two different modes. Consequently, (105) yields one relation stating that the elastic and centrifugal couplings between any two different modes cancel each other, and another relation stating that for each mode, the strain energy at either extreme configuration minus the work done by the centrifugal loading during the change of configuration from the neutral one to either extreme one is equal to the kinetic energy at the neutral configuration. (The absence of inertial coupling and the cancellation between the elastic and centrifugal couplings mean that there is, in effect, no coupling when the blade is in vacuum.)

As an example, consider the case with the following root conditions:

$$\left.\begin{aligned} \bar{M} &= k_F \frac{dh}{dr} \\ \bar{M} &= k_D \frac{dc}{dr} \\ h &= c = 0 \end{aligned}\right\} \qquad r = r_0$$

where k_F and k_D are given torsional elastic constants. For this case, (109) and (110) yield

$$A_{ij} = A_{ji} = 0$$

and

$$B_{ij} = B_{ji} = k_F \left(\frac{dn_i}{dr} \frac{dn_j}{dr} \right)_{r=r_0} + k_D \left(\frac{dc_i}{dr} \frac{dc_j}{dr} \right)_{r=r_0}$$

and, hence, (112) yields

$$\hat{M}_{ij} = \int \mu (h_i h_j + c_i c_j)\, dr = 0, \qquad j \neq i . \tag{113}$$

Consequently, (105) yields

$$K_{ij} + k_F \left(\frac{dh_i}{dr}\frac{dh_j}{dr}\right)_{r=r_o} + k_D \left(\frac{dc_i}{dr}\frac{dc_j}{dr}\right)_{r=r_o} - \Omega^2 \hat{T}_{ij} = 0, \qquad j \neq i \tag{114}$$

and also

$$K_{ii} + k_F \left(\frac{dh_i}{dr}\right)^2_{r=r_o} + k_D \left(\frac{dc_i}{dr}\right)^2_{r=r_o} - \Omega^2 \hat{T}_{ii} = \omega_i^2 \hat{M}_{ii} . \tag{115}$$

For the two extreme cases where the blade is cantilevered at $r = r_o$ (namely, both k_F and k_D approach infinity, yet both $\bar{M}_{r=r_o}$ and $\bar{\bar{M}}_{r=r_o}$ are finite) and where the blade is fully articulate (namely, $k_F = k_D = 0$), the relations

$$k_F \left(\frac{dh_i}{dr}\frac{dh_j}{dr}\right)_{r=r_o} = k_D \left(\frac{dc_i}{dr}\frac{dc_j}{dr}\right)_{r=r_o} = 0$$

hold for $j \neq i$ or $j = i$, so that (114) and (115) reduce to

$$K_{ij} - \Omega^2 \hat{T}_{ij} = 0, \qquad j \neq i \tag{116}$$

and

$$K_{ii} - \Omega^2 \hat{T}_{ii} = \omega_i^2 \hat{M}_{ii} . \tag{117}$$

Results in agreement with (113) and (116) are obtained in Reference 6, which treats a blade cantilevered at $r = 0$.

As another example, consider a blade with flapping and lead-lag hinges. With reference to Figure 33, the flapping hinge is

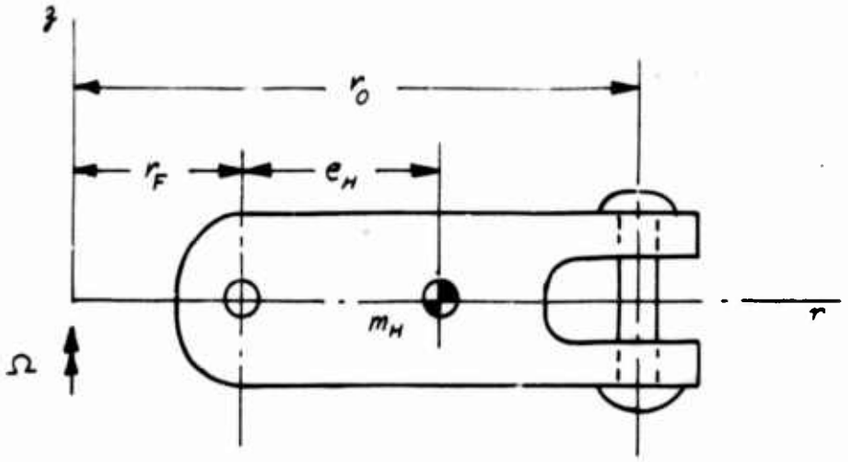

Figure 33. RIGID LINK CONNECTING FLAPPING AND LEAD-LAG HINGES.

located at $r = r_F$ and the lead-lag hinge at $r = r_0$. The link, shown in Figure 33, connecting the two hinges is assumed to be rigid, so that

$$(h)_{r=r_0} = (r_0 - r_F)\left(\frac{dh}{dr}\right)_{r=r_0} \tag{118}$$

and

$$(c)_{r \le r_0} = (\bar{M})_{r=r_0} = 0 \tag{119}$$

are three of the root conditions. The other root condition can be obtained from the requirement that the moment about the flapping axis must vanish; namely, $(\bar{M})_{r=r_F} = 0$. This moment may be expressed as

$$(\bar{M})_{r=r_F} = (\bar{M})_{r=r_0} - (r_0 - r_F)\left(\frac{d\bar{M}}{dr}\right)_{r=r_0} + \bar{M}_H$$

where $\bar{M}_H$ is the moment about the flapping hinge due to the inertia of the link. Letting J_H be the mass moment of inertia of the link about

the flapping hinge and dm be a mass element in the link,

$$\bar{M}_H = \omega^2 J_H \left(\frac{dh}{dr}\right)_{r=r_0} - \Omega^2 \left(\frac{dh}{dr}\right)_{r=r_0} \int \left\{ r(r - r_F) - z^2 \right\} dm$$

or, assuming the link to be symmetric with respect to the $r\eta$-plane so that $\int z f(r) dm = 0$,

$$\bar{M}_H = \omega^2 J_H \left(\frac{dh}{dr}\right)_{r=r_0} - \Omega^2 \left(\frac{dh}{dr}\right)_{r=r_0} \int \left\{ r(r - r_F) - z^2 \right\} dm$$

or, using $J_H = \int \left\{ (r - r_F)^2 + z^2 \right\} dm$ and $J_{Hz} = \int z^2 dm$,

$$\bar{M}_H = \left\{ \omega^2 J_H - \Omega^2 \left(J_H - 2 J_{Hz} + m_H r_F e_H \right) \right\} \left(\frac{dh}{dr}\right)_{r=r_0} \tag{120}$$

where m_H is the mass of the link and e_H is the distance (in the r-direction) from the flapping hinge to the c.g. of the link. Therefore, the fourth root condition is

$$\left\{ \bar{M} - (r_0 - r_F) \frac{d\bar{M}}{dr} \right\}_{r=r_0} = \left\{ -\omega^2 J_H + \Omega^2 \left(J_H - 2 J_{Hz} + m_H r_F e_H \right) \right\} \left(\frac{dh}{dr}\right)_{r=r_0}. \tag{121}$$

By the use of (118), (119) and (121), (109) and (110) yield

$$A_{ij} = (r_0 - r_F) \left(\frac{dh_i}{dr} \frac{dh_j}{dr} \right)_{r=r_0} = A_{ji}$$

and

$$B_{ij} = \left\{ -\omega_i^2 J_H + \Omega^2 \left(J_H - 2 J_{Hz} + m_H r_F e_H \right) \right\} \left(\frac{dh_i}{dr} \frac{dh_j}{dr} \right)_{r=r_0}$$

and, hence, (112) yields

$$M_{ij} \equiv \hat{M}_{ij} + J_H \left(\frac{dh_i}{dr} \frac{dh_j}{dr} \right)_{r=r_0} = 0, \qquad j \neq i. \tag{122}$$

Consequently, (105) yields

$$K_{ij} - \Omega^2 T_{ij} = 0, \qquad j \neq i \tag{123}$$

and

$$K_{ii} - \Omega^2 T_{ii} = \omega_i^2 M_{ii} \tag{124}$$

where

$$\bar{T}_{ij} \equiv \hat{T}_{ij} - \left\{(r_0 - r_F)\int_{r_0}^{R} \mu r\,dr + J_H - 2J_{H_z} + m_H r_F e_H\right\}\left(\frac{dh_i}{dr}\frac{dh_j}{dr}\right)_{r=r_0}. \quad (125)$$

Finally, some remarks on the teetering rotor (in which the two blades can flap only as a continuous beam and $r_F = 0$) will be made. The hub mechanism that flaps with the blades is usually treated as a rigid mass rigidly attached to the blades at $r = 0$. This rigid mass is symmetric with respect to the z-axis, just like the two blades. Suppose each blade has a lead-lag hinge at $r = r_0$ (the results below apply to the case without lead-lag hinges upon setting $r_0 = 0$). Assume that the portion of the blades between the two lead-lag hinges is rigid, and let $2J_H$ be the total moment of inertia about the flapping axis of the masses of the hub mechanism and the part of the blades between the lead-lag hinges, with $2J_{H_z}$ being contributed by the z-direction spread only. Using the superscripts [1] and [2] to indicate quantities belonging to the two different blades, the joining together of the two blades at $r = 0$ requires

$$\left(\frac{dh}{dr}\right)^{[2]}_{r=r_0} = -\left(\frac{dh}{dr}\right)^{[1]}_{r=r_0}.$$

Consequently, the two blades can have only two different types of free oscillations:

Type I:

$$h^{[2]} = -h^{[1]}; \qquad c^{[2]} = -c^{[1]};$$

$$\left(\bar{M} - r_0\frac{d\bar{M}}{dr}\right)^{[2]}_{r=r_0} = -\left(\bar{M} - r_0\frac{d\bar{M}}{dr}\right)^{[1]}_{r=r_0} = \bar{M}_H^{[1]}.$$

[$\bar{M}_H$ is given by (120) with $r_F = 0$.]

Type II:

$$h^{[2]} = h^{[1]}; \qquad c^{[2]} = c^{[1]};$$

$$\left(\frac{dh}{dr}\right)^{[2]}_{r=r_0} = \left(\frac{dh}{dr}\right)^{[1]}_{r=r_0} = 0.$$

The results turn out to be that, for both i and j belonging to either Type I or Type II, (122) through (124) are satisfied by either blade. Note that the last condition of Type II automatically reduces (122), (123) and (124) to (113), (116) and (117), respectively. If one of the i and j belongs to Type I and the other to Type II, then define

$$K_{ij} = K_{ij}^{[1]} + K_{ij}^{[2]}$$

$$\hat{T}_{ij} = \hat{T}_{ij}^{[1]} + \hat{T}_{ij}^{[2]}$$

$$\hat{M}_{ij} = \hat{M}_{ij}^{[1]} + \hat{M}_{ij}^{[2]}$$

for the two blades together and find

$$K_{ij} = \hat{T}_{ij} = \hat{M}_{ij} = \left(\frac{dh_i}{dr}\ \frac{dh_j}{dr}\right)_{r=r_0} = 0$$

so that (122) and (123) are satisfied by the two blades together.

Unclassified

Security Classification

DOCUMENT CONTROL DATA - R & D

(Security classification of title, body of abstract and indexing annotation must be entered when the overall report is classified)

1. ORIGINATING ACTIVITY (Corporate author) Cornell Aeronautical Laboratory, Inc. Buffalo, New York 14221	2a. REPORT SECURITY CLASSIFICATION Unclassified 2b. GROUP

3. REPORT TITLE

A Method for Predicting the Trim Constants and the Rotor-Blade Loadings and Responses of a Single-Rotor Helicopter

4. DESCRIPTIVE NOTES (Type of report and inclusive dates)

Final Report, February 1966 - July 1967

5. AUTHOR(S) (First name, middle initial, last name)

Chang, T. T.

6. REPORT DATE	7a. TOTAL NO. OF PAGES	7b. NO. OF REFS
November 1967	106	13

8a. CONTRACT OR GRANT NO.	9a. ORIGINATOR'S REPORT NUMBER(S)
DA 44-177-AMC-384(T) b. PROJECT NO. c. 1F125901A14604 d.	USAAVLABS Technical Report 67-71 9b. OTHER REPORT NO(S) (Any other numbers that may be assigned this report) CAL Report No. BB-2205-S-1

10. DISTRIBUTION STATEMENT

This document has been approved for public release and sale; its distribution is unlimited.

11. SUPPLEMENTARY NOTES	12. SPONSORING MILITARY ACTIVITY
	U. S. Army Aviation Materiel Laboratories Fort Eustis, Virginia 23604

13. ABSTRACT During a previous program, Cornell Aeronautical Laboratory, Inc., developed a method of computing rotor-blade loads and motions of a single-rotor helicopter in steady forward flight by assuming that the blade pitch-control settings (collective, longitudinal cyclic, and lateral cyclic) and the rotor-shaft tilt angle are known and that the blade motions are restricted to flapping and flapwise bending. The present effort was undertaken to extend the previously developed method by (1) including the blade inplane and torsional motions, and (2) treating the four trim constants (namely, the blade pitch-control settings and the rotor-shaft tilt angle) as unknowns. The trim constants are different for different flight conditions and are determined through the use of four appropriate, average equilibrium conditions of the helicopter. These equilibrium conditions are called the trim equations and are derived in this report, taking into account the inertial forces of the blades due to elastic deformations.

Lagrange's equations for the blade motions are given. The generalized coordinates employed in these equations to represent blade bending are those which have deflection components in two mutually perpendicular directions. Orthogonality relations of vibration modes of twisted, rotating blades are derived and are used in simplifying the equations of blade motion. A successive approximation procedure was developed which, upon incorporation with the previously developed iterative procedure, yields the aerodynamic loads, the blade responses, and the required trim constants. Computed results are obtained for the UH-1A rotor at advance ratios of 0.26 and 0.08 and for the H-34 rotor at advance ratios of 0.29 and 0.18. Comparisons of these results with available measured results are presented.

DD FORM 1 NOV 68 1473 REPLACES DD FORM 1473, 1 JAN 64, WHICH IS OBSOLETE FOR ARMY USE.

Unclassified

Security Classification

14. KEY WORDS	LINK A		LINK B		LINK C	
	ROLE	WT	ROLE	WT	ROLE	WT
Fluid Mechanics Helicopter Rotor Wake Helicopter Blade Loads						